

## 5. SITE 522<sup>1</sup>

### Shipboard Scientific Party<sup>2</sup>

#### HOLE 522

**Date occupied:** 1830, 6 May 1980  
**Date departed:** 1615, 9 May 1980  
**Time on hole:** 70 hr.  
**Position:** 26°6.843' S; 5°7.784' W  
**Water depth (sea level; corrected m; echo-sounding):** 4441.0  
**Water depth (rig floor; corrected m; echo-sounding):** 4451.0  
**Bottom felt (m, drill pipe):** 4456.6  
**Penetration (m):** 148.7  
**Number of cores:** 39  
**Total length of cored section (m):** 148.7  
**Total core recovery (m):** 137.7  
**Core recovery (%):** 92  
**Oldest sediment cored:**  
Depth sub-bottom (m): 148.7  
Nature: Nannofossil ooze  
Age: late Eocene  
**Principal results:** See discussion following Hole 522B data.

#### HOLE 522A

**Date occupied:** 1615, 9 May 1980  
**Date departed:** 1800, 12 May 1980  
**Time on hole:** 74 hr.  
**Position:** 26°6.843' S; 5°7.784' W  
**Water depth (sea level; corrected m; echo-sounding):** 4441.0  
**Water depth (rig floor; corrected m; echo-sounding):** 4451.0  
**Bottom felt (m, drill pipe):** 4456.6  
**Penetration (m):** 156.0

**Number of cores:** 31  
**Total length of cored section (m):** 106.0  
**Total core recovery (m):** 97.9  
**Core recovery (%):** 89.8  
**Oldest sediment cored:**  
Depth sub-bottom (m): 156.0  
Nature: Nannofossil ooze  
Age: late Eocene  
**Basement**  
Sub-bottom depth (m): 156.0  
**Principal results:** See discussion following Hole 522B data.

#### HOLE 522B

**Date occupied:** 1800, 12 May 1980  
**Date departed:** 1130, 14 May 1980  
**Time on hole:** 35 hr.  
**Position:** 26°6.843' S; 5°7.784' W  
**Water depth (sea level; corrected m; echo-sounding):** 4441.0  
**Water depth (rig floor; corrected m; echo-sounding):** 4451.0  
**Bottom felt (m, drill pipe):** 4456.6  
**Penetration (m):** 170.4  
**Number of cores:** 6  
**Total length of cored section (m):** 40.5  
**Total core recovery (m):** 25.3  
**Core recovery (%):** 62.6  
**Oldest sediment cored:**  
Depth sub-bottom (m): 154.0  
Nature: Nannofossil ooze  
Age: late Eocene  
**Basement:**  
Depth sub-bottom (m): 154.0  
Nature: Basalt  
**Principal results:** Holes 522, 522A, 522B—

1. Recovered a complete magnetostratigraphic record for the sedimentary sequence from Quaternary to upper Eocene, or Chron C-16-R, Nannofossil Zone 20, and Foraminifer Zone CP15b with the exception of the middle and late middle Miocene. The correlation between the magnetostratigraphy and seafloor anomalies is good for the Oligocene and upper Eocene section. The dissolution of the Paleogene fossils is moderate or slight. One of us (K.H.) believes the site should be recommended as a reference locality for the Oligocene magnetostratigraphy.

2. Established the highest and lowest occurrences of numerous key foraminifer and nannofossil species useful in the zonation of the Oligocene and upper Eocene sediments.

3. Obtained a magnetostratigraphic age of 37.1 m.y. for the nannofossil-dated Eocene/Oligocene boundary (on the basis of assuming a linear rate of seafloor spreading during the 66.5 m.y. of the Cenozoic).

4. Established a precisely dated record of increasing dissolution during the Oligocene and of intense dissolution during the Miocene.

<sup>1</sup> Hsü, K. J., LaBrecque, J. L., et al., *Init. Repts. DSDP*, 73: Washington (U.S. Govt. Printing Office).

<sup>2</sup> Ken J. Hsü (Co-Chief Scientist), Geologisches Institut, Eidgenössische Technische Hochschule, CH-8092 Zürich, Switzerland; John L. LaBrecque (Co-Chief Scientist), Lamont-Doherty Geological Observatory, Columbia University, Palisades, New York; Max F. Carman, Jr., Department of Geology, University of Houston, Houston, Texas; Andrew M. Gombos, Jr., Exxon Production Research Company, Houston, Texas; Anne-Marie Karpoff, Institut de Geologie, 67084 Strasbourg Cedex, France; Judith A. McKenzie, Geologisches Institut, Eidgenössische Technische Hochschule, CH-8092 Zürich, Switzerland; Stephen F. Percival, U.S. Geological Survey, Menlo Park, California; Nikolai P. Petersen, Institut für Geophysik, Universität Munich, D-8000 Munich, Federal Republic of Germany; Kenneth A. Pisciotta, Deep Sea Drilling Project, Scripps Institution of Oceanography, La Jolla, California (present address: Sohio Petroleum Company, 100 Pine Street, San Francisco, California); Richard Z. Poore, U.S. Geological Survey, Menlo Park, California (present address: U.S. Geological Survey, Reston, Virginia); Edward Schreiber, Department of Earth and Environmental Sciences, Queens College (CUNY), Flushing, New York; Lisa Tauxe, Department of Geological Sciences, Lamont-Doherty Geological Observatory, Columbia University, Palisades, New York (present address: Scripps Institution of Oceanography, La Jolla, California); Peter Tucker, Department of Geophysics, University of Edinburgh, Edinburgh, United Kingdom; Helmut J. Weissert, Department of Geological Sciences, University of Southern California, Los Angeles, California (present address: Eidgenössische Technische Hochschule, CH-8092 Zürich, Switzerland); and Ramil Wright, Department of Geology, Florida State University, Tallahassee, Florida (present address: Exxon Production Research Company, Houston, Texas).

5. Confirmed the occurrence of *Braarudosphaera* chalk along the 30°S parallel during the middle Oligocene (Chronos C-10-R and C-12-R), when oceanographic conditions may have been unusual.
6. Confirmed the near synchronicity of the sediment and basement magnetization to support the previous practice of dating basalt basement on the basis of the paleontology of the oldest sediment.
7. Sampled a 19-m sequence of fresh basalt for petrochemical studies.
8. Measured the magnetization of sediment and basalt. Basalt magnetization indicates little latitudinal displacement of the site since the beginning of the Eocene; however, sediment magnetization indicates significant latitudinal displacement.
9. Obtained two moderately good downhole temperature measurements and a low heat flow value (1.17 heat flow units) that suggests that ocean water is being drawn down into the topmost porous basalt basement.

## BACKGROUND AND OBJECTIVES

Isotopic analyses of planktonic and benthic foraminifer samples indicated a rapid reduction of 4 to 5°C of both the surface and the bottom temperatures of the world's oceans at the end of the Eocene (Douglas and Savin, 1975; Shackleton and Kennett, 1973). This drop in ocean temperature, which is also known as the terminal Eocene crisis, has been related to various other events that happened or have been theorized to have happened at about this time, such as the start of Antarctic glaciation, the beginning of Antarctic bottom currents, the opening of the Drake Passage, and the cratering of the Earth by a large extraterrestrial body. To sort out causes and effects, the precise timing of the various events must be known. Furthermore, it is necessary to clarify the timing and to define the duration of the terminal Eocene crisis itself to determine whether the temperature drop was the result of one event or the consequence of a series of oscillations during a time interval too brief and with a periodicity too short for the effects to be visible in available DSDP cores. The main objective of drilling this site, which was originally defined as Site IV-4, was, therefore, to sample the Oligocene and uppermost Eocene pelagic sequence for the study of the terminal Eocene crisis.

We chose a location where the crest was young and the paleodepth of the site was above the Oligocene carbonate lysocline so we could obtain calcareous fossils for paleoceanographic analysis. We also needed a location on a gentle submarine slope, where contamination by the redeposition of sediment would be absent (or minimal), and we wanted a location where the sedimentation rate had been nearly constant; under these conditions we could work out a precision stratigraphy through the correlation of biostratigraphy, magnetostratigraphy, and seafloor lineations. It could not be foreseen whether all these conditions could be met at one site. Site IV-4 was to be drilled first. If some objectives could not be met at this site, Site IV-5 would be drilled.

The original position for Site IV-4 was on Magnetic Anomaly 13, and the area surveyed in detail by the University of Texas Marine Science Institute (UTMSI) was centered on this anomaly. However, it was decided during the 1979 Barbados meeting of the Ocean Paleoenvironment Panel to shift the site eastward, to a position

over Anomaly 16; this location would permit us to penetrate the Oligocene/Eocene boundary and obtain enough upper Eocene sediment samples to study the terminal Eocene crisis. Again, as was done for the Miocene transect, two alternative locations were picked out, with Site IV-4A on a plateau and Site IV-4B in a basin. After drilling Sites 519, 520, and 521, we had no doubt that the site on the plateau would be more suited to the stated objectives.

The final choice of location was based upon a continuous seismic profiling (CSP) by UTMSI, which showed Site IV-4A to be on a small plateau covered by about 0.2 s of draped sediments. The seismic profiles obtained on the *Glomar Challenger* were excellent (after the profiling instruments were renovated), and the site was easy to find. The plateau is covered by a uniform blanket of draped sediments about 150 m thick. It seemed probable that the section could be penetrated by continuous drilling with the hydraulic piston corer (HPC). We planned therefore to drill with the HPC until the basement was reached and then to change the bit and drill an offset hole for engineering tests, heat flow measurements, and the acquisition of basement samples.

To recapitulate, the primary objective was to sample, by HPC, a continuous sequence of Oligocene and uppermost Eocene pelagic sediments. We wanted to sample sediments that had been deposited at nearly uniform rate, contained sufficient calcareous fossils for biostratigraphic, magnetostratigraphic, and paleoceanographic studies, and were free from contamination by resedimentation.

Additional objectives were (1) to study the symmetry (or the lack of it) of South Atlantic sedimentation, (2) to gather data contributing to an understanding of the Miocene calcite compensation depth (CCD) crisis, (3) to sample *Braarudosphaera* chalk for further analysis of a sediment consisting of monospecific nannofossil skeletons, (4) to date the seafloor lineations here (Anomaly 16) and to clarify their temporal relation to the Oligocene/Eocene boundary, (5) to obtain refined data on the history of South Atlantic seafloor spreading, (6) to sample basalts for age measurements, petrographic and chemical analyses, rock magnetic studies, and physical property measurements (e.g., seismic velocities), and (7) to obtain a reliable heat flow value for this part of the Mid-Atlantic Ridge.

After the first hole was drilled, we decided to drill a second HPC hole to continuously sample the basal Miocene to upper Eocene sequence instead of drilling Site IV-5. It was obvious that the sequence at Site IV-5 would be almost identical to that encountered at this site except that the basal sediments would be slightly older (~3 m.y. old). Besides, we expected greater dissolution in the targeted section (upper Eocene and Oligocene) at that site with its older crust. Finally, a double continuous coring at Site IV-4 might yield a perfect magnetostratigraphic section for the Oligocene, without gaps, deficiencies, or uncertainties. We were not sure we could core a new section at Site IV-5 as well as we could at Site IV-4. Everyone agreed that one perfect section would be preferable

to two incomplete sections. Therefore, the shipboard scientific staff unanimously decided to drill Hole 522A at the site of the first hole instead of at the proposed Site IV-5.

## OPERATIONS

### Site Approach

Site 522 was located by steaming along UTMSI Line 112 to the proposed Site IV-4A. Correlations between UTMSI magnetics and bathymetry and the observed *Glomar Challenger* data were checked to assure proper location.

Figure 1 displays the approach to Site 522. At 1445Z on 6 May 1980, the ship's course was set at  $77^\circ$  with a reduced speed of approximately 6 knots after a traverse from Site 521. By 1500Z, a strong correlation was recognized between the observed data and the UTMSI Line 112 data. At 1625Z the proposed Site IV-4A was recognized. Data over the proposed site indicated good coring potential to the co-chiefs, and at 1625Z a beacon was dropped. The vessel continued on to perform a short presite survey that terminated over the beacon. The beacon position was judged appropriate by the co-chiefs, geophysical measurements were terminated, and vessel positioning began.

### Coring Summary, Hole 522

Hole 522 was in auto on site at 1830Z on 6 May, and the rigging of the bottom hole assembly started. At

0400Z on 7 May, the drill string reached 4443 m below rig floor, 2 m above the water depth registered by a pinger attached to the HPC and 8 m above the precision depth recorder (PDR) register. The first two pistons were fired into water, and core barrels were recovered without having touched the bottom. After two failures, the operations manager and the drill crew were instructed to feel for bottom with the drill string before firing the HPC. The drill pipe touched bottom at about 4456 m, the HPC was fired from 4454 m, and the first core containing 2.9 m of sediments was hauled up at 0838Z (Table 1). The experience suggests that the first hydraulic piston core should be taken after the drill string has touched the bottom and that the operations manager should be informed whether the scientific objectives require the recovery of Holocene oozes, which are difficult to recover. Eventually it was discovered that the pinger was mislocated by one pipe joint, resulting in a 9.5-m error of measurement.

Coring operations proceeded smoothly until 0120Z on 8 May, when Core 13 was recovered and the barrel proved to be empty. As at previous sites, the missed core penetrated a red clay (or nannofossil clay) interval, and the flapper valve of the core catcher had probably failed to close. Measures should be taken to improve the functioning of the flapper valve during coring in sticky marl ooze and red clay. Coring operations in Oligocene nannofossil ooze ran smoothly until Core 23 was retrieved and the core barrel was empty. In a smear of nannofossil ooze stuck to the rim of the core catcher there was a

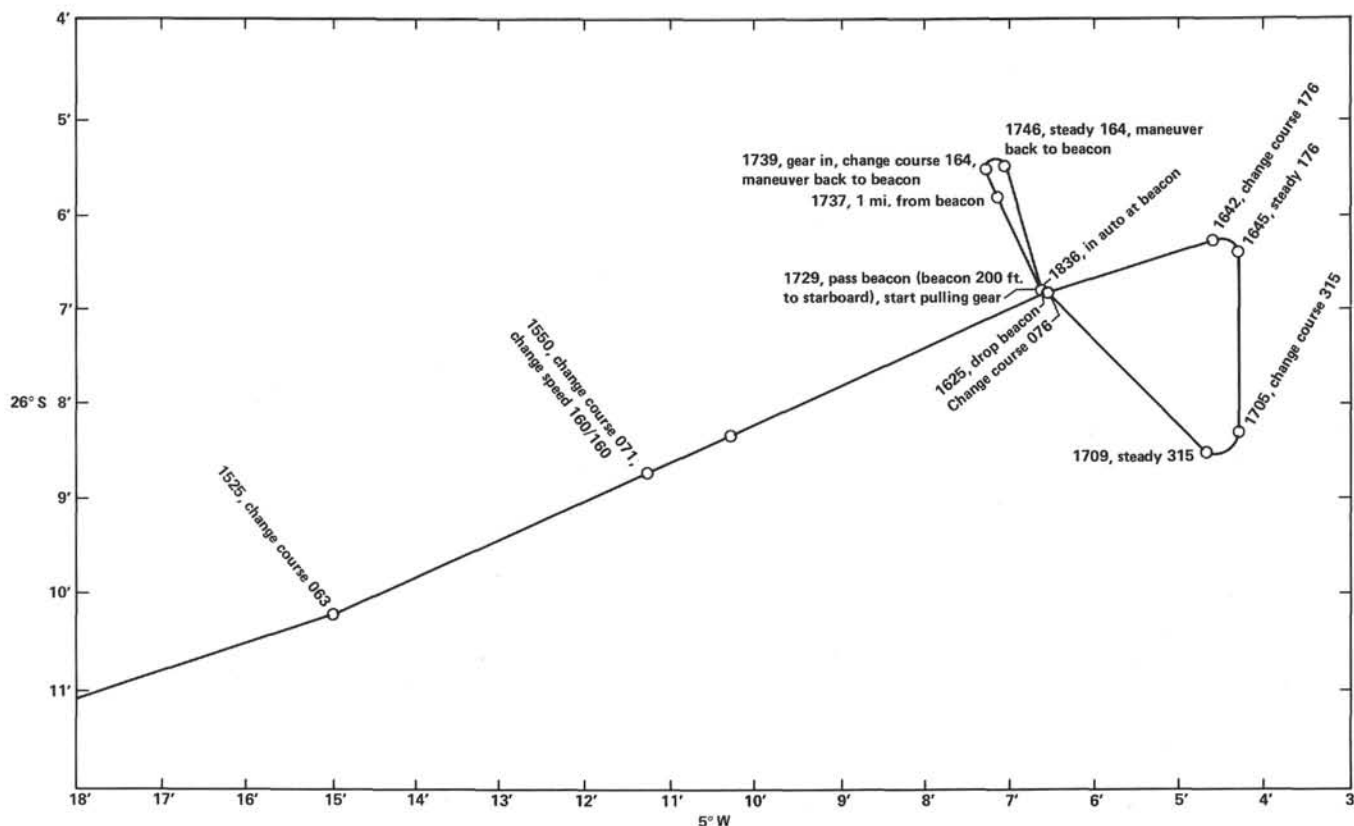


Figure 1. *Glomar Challenger* approach track, Site 522.

Table 1. Coring summary, Site 522.

Core	Date (May 1980)	Time (hr.)	Depth from drill floor (m)	Depth below seafloor (m)	Length cored (m)	Length recovered (m)	Recovery (%)
Hole 522							
1	7	0838	4456.6-4459.5	0-2.9	2.9	2.9	70
2	7	1021	4459.9-4463.9	2.9-7.3	4.4	4.1	93
3	7	1142	4463.9-4467.4	7.3-10.8	3.5	3.3	94
4	7	1300	4467.4-4471.8	10.8-15.2	4.4	4.3	97
5	7	1422	4471.8-4476.2	15.2-19.6	4.4	4.0	90
6	7	1522	4476.2-4480.6	19.6-24.0	4.4	3.4	77
7	7	1711	4480.6-4485.0	24.0-28.4	4.4	4.4	100
8	7	1825	4485.0-4489.4	28.4-32.8	4.4	3.7	84
9	7	1943	4489.4-4493.8	32.8-37.2	4.4	3.6	81
10	7	2105	4493.8-4497.8	37.2-41.2	4.0	3.9	97
11	7	2220	4497.8-4500.8	41.2-44.2	3.0	2.9	96
12	7	2350	4500.8-4504.8	44.2-48.2	4.0	3.7	92
13	8	0120	4504.8-4507.3	48.2-50.7	2.5	tr	0
14	8	0242	4507.3-4511.7	50.7-55.1	4.4	4.6	102
15	8	0410	4511.7-4516.1	55.1-59.5	4.4	4.4	100
16	8	0510	4516.1-4520.5	59.5-63.9	4.4	4.4	100
17	8	0700	4520.5-4524.9	63.9-68.3	4.4	4.6	104
18	8	0915	4524.9-4529.3	68.3-72.7	4.4	4.2	95
19	8	1040	4529.3-4533.7	72.7-77.3	4.4	4.3	97
20	8	1145	4533.7-4537.7	77.3-81.3	4.0	2.8	7
21	8	1515	4537.7-4542.1	81.3-85.7	4.4	4.3	97
22	8	1430	4542.1-4546.5	85.7-90.1	4.4	4.3	97
23	8	1540	4546.5-4548.0	90.1-91.6	1.5	tr	0
24	8	1714	4548.0-4548.0	91.6-91.6	0	tr	0
25	8	1845	4548.0-4552.0	91.6-95.6	4.0	4.0	100
26	8	2020	4552.0-4556.4	95.6-99.8	4.4	4.4	100
27	8	2138	4556.4-4560.8	99.8-104.2	4.4	4.6	104
28	8	2258	4560.8-4565.2	104.2-108.6	4.4	4.4	100
29	9	0005	4565.2-4569.6	108.6-113.0	4.4	4.3	97
30	9	0140	4569.6-4574.0	113.0-117.4	4.4	4.4	100
31	9	0300	4574.0-4578.4	117.4-121.8	4.4	4.2	95
32	9	0415	4578.4-4582.8	121.8-126.2	4.4	4.5	102
33	9	0550	4582.8-4586.3	126.2-129.7	3.5	3.4	97
34	9	0705	4586.3-4590.3	129.7-133.7	4.0	4.1	102
35	9	0825	4590.3-4592.8	133.7-136.2	2.5	2.5	100
36	9	0945	4592.8-4596.3	136.2-139.7	3.5	3.6	102
37	9	1140	4596.3-4600.3	139.7-143.7	4.0	3.9	97
38	9	1315	4600.3-4604.3	143.7-147.7	4.0	3.3	82
39	9	1446	4604.3-4605.3	147.7-148.7	1.0	tr	0
Hole 522A							
1	9	1800	4503.6-4508.1	47.0-51.5	4.5	4.5	100
2	9	1915	4508.1-4512.6	51.5-56.0	4.5	4.3	95
3	9	2050	4512.6-4517.1	56.0-60.5	4.5	4.3	95
4	9	2200	4517.1-4521.6	60.5-65.0	4.5	4.1	91
5	9	2336	4521.6-4526.1	65.0-69.5	4.5	4.2	93
6	10	0112	4526.1-4529.1	69.5-71.5	3.0	2.5	83
7	10	0245	4529.1-4533.6	71.5-77.0	4.5	4.3	95
8	10	0415	4533.6-4537.1	77.0-80.5	3.5	3.1	88
9	10	0534	4537.1-4540.6	80.5-84.0	3.3	3.5	106
10	10	0705	4540.6-4544.1	84.0-87.5	3.5	3.6	102
11	10	0824	4544.1-4546.1	87.5-89.5	2.0	2.0	100
12	10	0945	4546.1-4548.1	89.5-91.5	2.0	1.6	8
13	10	1110	4548.1-4552.1	91.5-95.5	4.0	3.9	97
14	10	1225	4552.1-4556.6	95.5-100.0	4.5	4.1	91
15	10	1350	4556.6-4561.1	100.0-104.5	4.5	2.3	51
16	10	1530	4561.1-4564.1	104.5-107.5	3.0	1.7	56
17	10	1720	4564.1-4568.6	107.5-112.0	4.5	2.9	64
18	10	1900	4568.6-4573.1	112.0-116.5	4.5	2.6	57
19	10	2120	4573.1-4577.1	116.5-120.5	4.0	3.9	97
20	10	2300	4577.1-4578.1	120.5-121.5	1.0	1.5	100
21	11	0024	4578.1-4578.1	121.5-121.5	0	0	—
22	11	0215	4578.1-4582.1	121.5-125.5	4.0	3.9	97
23	11	0333	4582.1-4585.6	125.5-129.0	3.5	3.8	108
24	11	0452	4585.6-4588.1	129.1-131.5	2.5	2.5	100
25	11	0623	4588.1-4592.1	131.5-135.5	4.0	4.1	102
26	11	0755	4592.1-4596.1	135.5-139.5	4.0	4.1	102
27	11	0925	4596.1-4600.1	139.5-143.5	4.0	3.4	85
28	11	1055	4600.1-4604.1	143.5-147.5	4.0	4.0	100
29	11	1210	4604.1-4608.1	147.5-151.5	4.0	3.9	97
30	11	1340	4608.1-4611.1	151.5-154.5	3.0	2.3	76
31	11	1455	4611.1-4612.6	154.5-156.0	1.5	1.0	66
Total					109	97.9	89.8
Hole 522B							
	12	1530	Heat Flow Test 1				
	12	1705	Heat Flow Test 2				
1	12	2105	4574.0-4583.5	117.4-126.9	9.5	9.4	98
2	12	2330	4596.0-4605.5	139.4-148.9	9.5	5.3	55
	13	0200	Heat Flow Test 3				
3	13	0826	4605.5-4613.5	148.9-156.9	8.0	4.5	56
4	13	1530	4613.5-4617.5	156.9-160.4	3.5	2.3	65
5	13	2359	4617.0-4624.0	160.4-167.4	7.0	3.1	44
6	14	1105	4624.0-4627.0	167.4-170.4	3.0	0.7	23
Total					40.5	25.3	62.5

1-mm speck of white chalk. A smear slide of the sample confirmed the suspicion that the middle Oligocene *Braarudosphaera* chalk had obstructed the HPC. In the meantime, after washing the drill string down 1.5 m, Core 24 was hauled up and the core barrel was again found to be empty. The drill crew was instructed to change from two small shear pins to three big shear pins. The drill string did not wash down. The HPC seemed to have achieved full stroke, even though pressure failed to build up. When Core 25 was hauled up recovery was found to be normal, and this core contained a 25-cm-thick *Braarudosphaera* ooze. The coring of nannofossil ooze continued without difficulty until 0530Z on 9 May, when the HPC seemed to have hit a hard layer, probably basement, although the sediment was younger than the predicted age of the oldest sediment. A staff meeting was called to discuss alternatives. All agreed that a duplicate HPC sequence from basal Miocene down was essential, but some questioned whether we should drill for basement samples here or at Site IV-5. The disagreement proved to be unnecessary, however, because the next core (Core 34) came up with a full recovery of oozes. After a late Eocene foraminifer assemblage was found in Sample 522-36, CC, we all agreed to get a duplicate sequence of hydraulic piston cores and then to drill for basement samples here. Coring continued until the HPC seemed to have hit a hard layer again; this happened when the HPC was fired from 146 m sub-bottom, when Core 39 was taken. It was decided not to risk jamming the HPC in the drill pipe, which would have necessitated tripping the string to the rig floor for the second HPC hole. The hole was terminated at 148.7 m in upper Eocene sediments (Magnetic Chron C-13).

### Coring Summary, Hole 522A

The drill string cleared the mudline at 1600Z on 9 May, and Hole 522A was spudded in at 1615Z on 9 May without an offset in the vessel's position (Table 1). Continuous coring continued and cores came up more or less regularly at 1.5-hr. intervals. It was anticipated that we would hit the top of *Braarudosphaera* chalk at about 90 m sub-bottom. The chief scientists advised the use of three shear pins but were overruled by the operations manager, who preferred two shear pins. Core 11 failed to achieve full stroke and bottomed in chalk, with 2.0 m of recovery. Core 12 again failed to achieve full stroke; only 1.6 m of sediments were recovered, but the core did penetrate the first bed of *Braarudosphaera* chalk. Core 13 achieved full stroke, and the second bed of *Braarudosphaera* chalk (30 cm thick) was recovered with little disturbance. Coring continued with frequent liner failures and poor recoveries until Core 21 was fired, when, at 121.5 m sub-bottom, the HPC again seemed to hit a hard layer. However, Core 22 achieved full stroke and resulted in nearly full recovery. Coring then continued without difficulty until the basement was reached. The HPC failed to achieve full stroke while Cores 30 and 31 were being taken. Later, at 156.0 m sub-bottom, while the drill string was being washed down for Core 32, the drill string hit hard basement and the HPC was not fired. At 1600Z on 11 May, the drill crew was given the

order to start pulling out of the hole. The drill string cleared the mudline at 1800Z and the bit was on deck at 0106Z on 12 May.

### Coring Summary, Hole 522B

Hole 522B was offset 100 ft. northeast of the original hole. The drill crew changed the drill bit and ran the pipe down until 0930Z on 12 May, when the Bowen sub-assembly was picked up. Between 1000Z and 1115Z the first test of heave-sensing tools was carried out. At 1127Z Hole 522B was spudded in at a water depth of 4456.6 m. After 1315Z the instrument barrel was retrieved, but the data were lost because of battery failure. Meanwhile, the first heat flow (HF) probe was pumped down, and the first HF measurement and water samples were taken at 33 m sub-bottom. At 1530, the probe was retrieved, but the run was a double failure because of a bad connector between the temperature and water-sample modules. The drill string was then washed down to 62 m, and the barrel was retrieved to be replaced by the HF probe at 1700Z. The latter was retrieved at 1930Z, and the second HF test proved to be successful.

Core 1 was cut at the interval from 117.4 to 126.9 m to find out why we had had difficulty in achieving full stroke with the HPC in this interval on two previous occasions (Table 1). The rotary core had full recovery; a thin layer of *Braarudosphaera* chalk was present. The layer hardly seemed likely to obstruct the HPC, but there seemed to be no other candidate. Core 2 was taken be-

cause the core barrel had to be retrieved for the third HF test, which was a qualified success. When retrieval of the HF package was attempted, it was found to be lodged in the bottom of the hole. HF data indicated the possibility of intermittent contact between sediment and the probe. The returned probe was found to be bent.

After the completion of HF measurements at 0200Z on 13 May, we started to core the basalt basement. Drilling was slow after basement was reached at 154.0 m sub-bottom, but the recovered cores contained very fresh basalt samples. In 26 hr., 16.4 m of basalt were drilled; less than 8 m were recovered. The time expended was equivalent to that needed to acquire a continuous 100-m-plus HPC section. With the consent of the shipboard petrologist, the hole was terminated at 0400Z on 14 May at 170.4 m sub-bottom. The crew then started to pull out of the hole. The drill string cleared the mudline at 0500Z, and the bit was on deck at 1110Z. After the rig floor was secure, the vessel departed at 1136Z on 14 May for Site 523.

## LITHOLOGY

### Sediments

We divided the pelagic sequence at Site 522 into five lithologic units on the basis of color, percent calcium carbonate, and fossil and mineralogical content (Fig. 2). Two correlative marker beds of Oligocene *Braarudosphaera* chalk were noted between 90 and 94 m sub-bot-

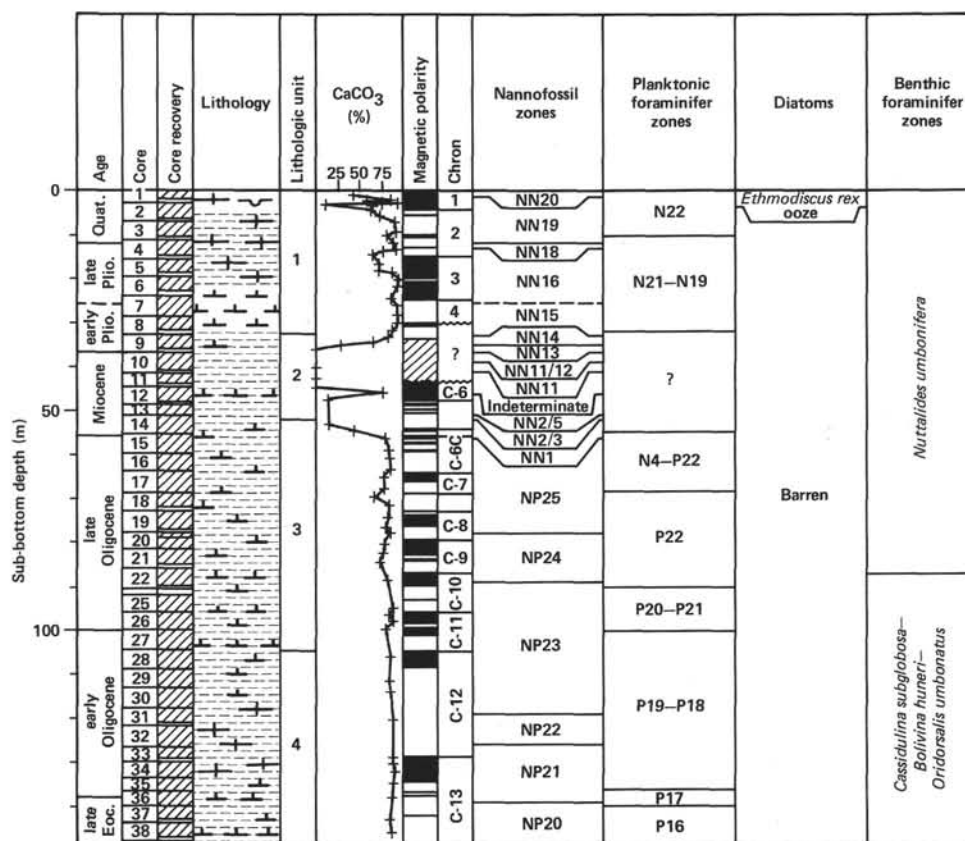


Figure 2. Stratigraphic summary, Hole 522. Lithology is defined in Hsü, LaBrecque, et al. (this vol.).

tom in Holes 522 and 522A. A third layer was found at 119.2 m sub-bottom in Hole 522B. In addition, the light to dark reddish brown sediments of the Miocene dissolution facies provided a significant, correlatable interval.

Unit 1 (Hole 522, Cores 1–8, 0–32.8 m sub-bottom) is made up of minor, decimeter-thick horizons of lighter (very pale brown, pale brown, and light yellowish brown) foraminifer–nannofossil ooze alternating with darker (light yellowish brown and yellowish brown) marly nannofossil ooze. The darker layers are distinguished by fewer foraminifers and a lower calcium carbonate content (Fig. 2). Between 1.72 and 1.85 m sub-bottom a white nannofossil diatom ooze was recovered.

Unit 2 (Hole 522, Cores 9–14, 32.8–55.1 m sub-bottom; Hole 522A, Core 1, 47.0–52.5 m sub-bottom) includes two dissolution intervals (32.8–45.5 and 45.5–55.1 m sub-bottom) of yellowish brown marly nannofossil ooze, overlying dark yellowish brown nannofossil clay, and dark reddish brown to dark brown iron-rich clay. The change from marly nannofossil ooze to nannofossil clay to iron-rich clay corresponds to a decrease in calcium carbonate content (Fig. 2). At the base of Unit 2, a brown, iron-rich, calcareous clay with 44% calcium carbonate marks the transition into a less dissolved facies.

The marly nannofossil ooze of Unit 3 (Hole 522, Cores 15–27, 55.1–104.2 m sub-bottom; Hole 522A, Cores 2–15, 52.5–104.5 m sub-bottom) ranges in color from very pale brown to light brown to light yellowish brown to yellowish brown and brown. Increased calcium carbonate contents in this unit vary between 69 and 90%. This range appears to be the result of smaller scale dissolution cycles than those of Unit 2 (Fig. 2). Between 90.0 and 94 m sub-bottom, two layers of pure *Braarudosphaera* chalk, separated by approximately 2.5 m of marly nannofossil ooze, were found. The layers are between 25 and 50 cm thick.

In terms of lithology the sediments of Unit 4 (Hole 522, Cores 28–39, 104.2–148.7 m sub-bottom; Hole 522A, Cores 16–Core 29, Section 1, 104.5–149.0 m sub-bottom; Hole 522B, Cores 1–2, 117.4–148.9 m sub-bottom) are classified as a nannofossil ooze to foraminifer–nannofossil ooze. The sediments are very pale and yellowish brown, and calcium carbonate content is relatively constant, with values between 86 and 92%. The small scale dissolution cycles noted in Unit 3 are not present. At 119.2 m in Hole 522B a 3-cm-thick layer of *Braarudosphaera* chalk similar to the layers in Unit 3 (Holes 522 and 522A) was recovered. This layer occurs about 20 m deeper than in the other two holes.

Unit 5 (Hole 522, not cored; Hole 522A, Core 29, Section 2–Core 31, 149.0–156 m sub-bottom; Hole 522B, Core 3, 148.9–156 m sub-bottom) is a dark yellow brown to brown and dark brown marly nannofossil ooze rich in volcanic glass and palagonite fragments. The calcium carbonate content averages about 85%. At 153.4 m sub-bottom, a greenish layer of nannofossil ooze containing altered volcanic fragments was recognized. A 3-cm fragment of white nannofossil limestone was found in the ooze directly above basalt in Hole 522B.

Variations in the Eocene to Quaternary pelagic sediments at Site 522 reflect changes in paleodepth and fluctuations of the CCD. The upper Eocene marly ooze of Unit 5 was deposited well above the CCD. The enrichment of iron oxides and clay minerals is probably due to diagenetic alteration of material close to the sediment/basalt contact. A thin ash layer near the base of this unit may indicate volcanic activity associated with the oceanic rifting. The decrease in the carbonate content between Unit 4 and Unit 3 can be explained by the gradual subsidence of the cooling oceanic crust. Miocene clay of Unit 2 indicates a drastic rise in the CCD. The carbonate-rich sediments of Unit 1 indicate a deepening of the Pliocene and Quaternary CCD. Fluctuations in the carbonate content in the upper Pliocene and Quaternary sediments may reflect the glacial–interglacial cycles of this period.

### Igneous Rocks

In total, 19 m of basalt were cored and 8.1 m (43%) were recovered in Hole 522B. Figure 3 summarizes the details of core and section number, lithology, and cooling unit designations. The entire sequence consists of 13 cooling units of olivine basalt, which are interpreted as both pillows and flows.

Units 1 to 4, 8, and 9 are designated as probable pillows because of the thinness of the units, the amount and orientation of the glassy margins, and the prevalence of quench textures in the internal parts of the units. Each of the pillow units is 1 m or less thick and has a thick (1-cm) glassy rind, and the textures of all samples studied from them are coarse quench or finer. All of these units have glassy rinds that make steep to nearly vertical angles with the core axis, suggesting that the units are lensoidal.

Most of the rest of the units (5, 6, and 10–13) are thicker, seem to have horizontal boundaries with thinner glass rinds, and show coarser (subophitic) textures that develop closer to glassy margins than in the units that are believed to be pillows. Unit 11 is thin (10 cm), has no glassy rind, is very fine- to medium coarse-grained, and appears to have this texture against the very fine-grained glassless top of Unit 12. These facts suggest that this unit may be a sill, but no direct evidence, such as an intrusive protrusion into Unit 10, is available to resolve the question.

The approximate thicknesses of units are 1 m for Unit 1, 0.33 m for Unit 2, 0.33 m for Unit 3, 0.5 m for Unit 4, 1 m for Unit 5, 1 m for Unit 6, 0.5 m for Unit 7, 1 m for Unit 8, 0.33 m for Unit 9, 1.33 m for Unit 10, 10 cm for Unit 11, 1 m for Unit 12, and 0.5 m for Unit 13.

The internal structures of these units are quite similar to those described for Hole 519A. Fracture sets and irregular fractures and veins are common throughout, although they are more concentrated in the pillow units. Conjugate fracture sets (30° + 45° to axis of core) are rather well developed in Units 5, 6, and 7 (flows), although they are more widely spaced than the fractures in the other units. Smectite and calcite linings and fill-

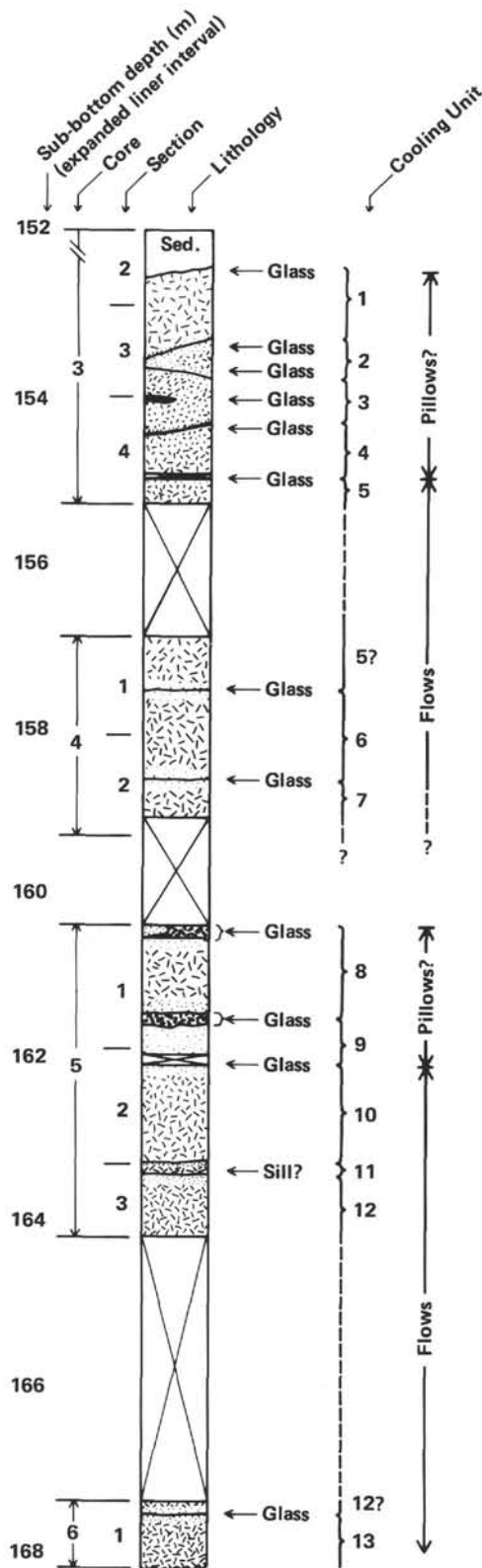


Figure 3. Summary of igneous rocks, Hole 522B.

ings are similar to those of Hole 519A. However, a few fractures in the center of Unit 6 (flow) are coated with amorphous, turquoise-colored and black sooty materials, suggesting Cu and Mn mineralization, although Cu and Mn concentrations are low in the fresh rocks. Other

evidence for low-temperature mineralization is found in the lower part of Unit 13, where vesicles are filled, or partly filled, with pyrite.

All rocks are slightly to moderately vesicular, consistently more so than those of Hole 519A. Vesicularity ranges from 1 to 5%, with the higher values in thin zones (1–2 cm thick) at unit boundaries and near the middles of Flow Units 5 and 6. Except for one thin zone in Unit 13 the vesicles are always less than 1.5 mm in diameter. One piece of Unit 13 is unique in having a 2-cm zone with highly irregular vesicles that range up to 5 mm long and interconnect to make the rock quite porous. In some of these vesicles there are euhedral clusters of pyrite. Most vesicles, however, are lined or filled with smectite of various shades of green, blue green, or brown or have a filling of calcite or white to clear amorphous material that has high relief and appears to be isotropic in the microscope.

In all rocks except those within about 5 cm of glassy margins, there occur small (0.05–1.2 mm) segregation vesicles (Pl. 1, Figs. 1 and 2). These are spherical features that are bounded by tangentially arranged plagioclase microlites and filled with a mixture of ultra fine-grained (mostly 0.01 mm) material. The phases identified are as follows: opaque minerals (often 25–50 vol. %), dendritic clinopyroxene and smectite, with rare plagioclase grains or very fine spherulites (Pl. 1, Figs. 3 and 4).

Chemically, the rocks are typical ocean floor plagioclase tholeiites (Dietrich et al., this vol.), with a maximum of 3% olivine in the norm. They are more evolved than those in Hole 519A (e.g., lower Mg numbers [0.58–0.64], higher TiO<sub>2</sub>, Y, Zr, Ba, Sr, and Rb, and lower Cr and Ni) except for the lowest unit, which seems to be closer to the Hole 519A basalts.

### Petrography

All units are aphyric (actually rather sparsely microphyric) basalts composed of approximately equal parts calcic plagioclase and normal augite (colorless, 2V<sub>Z</sub> 60°), with accessory forsteritic olivine, titanomagnetite, ilmenite, and rare chrome spinel. As such they are petrographically almost indistinguishable from the rocks of Hole 519A, and the textural and composition features outlined there apply equally here (Pl. 2). The occurrence of completely altered olivine in holocrystalline phases and the aforementioned more distinct vesicularity, including the presence of segregation vesicles, are the chief microscopic distinctions of these (Hole 522B) rocks.

The units designated as pillows in Figure 3 are characterized by glassy rims that grade into coarse quench textures (Zones 1 through 6) in their innermost portions. They lack the coarser subophitic and ophitic intersertal textures that occur throughout most of the units designated as flows.

The properties of the plagioclase microphenocrysts are the same as those described in the chapter for Hole 519A. Groundmass grains also have the same types, size ranges, morphology, and composition as those in Hole 519A. Likewise, the olivine (Pl. 1, Fig. 5), pyroxene, and opaque minerals occur in the same way and with the same textures and compositions as those found in the rocks of the earlier hole.

Alteration products have not been studied in detail, but in general there is a wider range of materials in the fractures, veins, and vesicles of these rocks than in the basalts from Hole 519A. Smectites of various morphologies (finely to more coarsely fibrous to extremely fine-grained massive) and colors (bright green, blue green, yellow green, yellow, orange, greenish brown, and pale brown) fill interstices, vesicles, and veins or coat vesicles and fractures. The orange to brown colors appear to be a function of a more altered (oxidized) state of the rock, and in some instances the alteration has caused almost hematite red discoloration of vesicle fillings.

### Conclusion

As in Holes 519A and 520, the similarity of the mineralogy and textures of the basaltic rocks in Hole 522B indicates that they have come from a single source, from common tholeiitic magma batch. Most were probably erupted over a relatively short period of time. However, the lowest unit (Unit 13) displays a magnetic reversal relative to all higher ones and thus should be at least 10,000 yr. older. It is petrographically indistinguishable from the others, but, as noted earlier, its chemistry is distinctive in that it appears to be slightly less evolved than rocks of the higher units, and in this regard Unit 13 is closer to the rocks of Hole 519A.

## BIOSTRATIGRAPHY

### Summary

A Quaternary through upper Eocene sedimentary section was recovered at Site 522 (Fig. 2). Hole 522 was continuously cored (with the HPC) almost to basement, Hole 522A was continuously cored (with the HPC) from 51.5 m sub-bottom to basement, and Hole 522B was discontinuously cored into basement. Calcareous microfossils are abundant and well preserved in the Quaternary but show increasing effects of dissolution downsection into the early Pliocene. The Miocene sediments show the effects of intense dissolution. The preservation of calcareous microfossils improves in the lowest Miocene to uppermost Oligocene; the lower Oligocene to upper Eocene assemblages are generally moderately well preserved.

### Hole 522

A summary of significant biostratigraphic data is given in Figure 4. The presence of a biostratigraphically mixed interval in Cores 3 and 4 obscures the location of the Quaternary/Pliocene boundary. Cores 4 through 8 contain Pliocene assemblages. The Pliocene/Miocene boundary probably occurs within the upper part of Core 10. Cores 10 through 14 are assigned to the Miocene. The upper/middle Miocene contact occurs in an interval with intensely dissolved carbonate. Consequently, the boundary cannot be located. A slight decrease in the intensity of carbonate dissolution in Core 12 results in the preservation of enough calcareous nannofossils to locate the middle/lower Miocene boundary within Core 12 or 13.

The Miocene/Oligocene boundary is placed in the upper part of Core 15 on the basis of both nannofossils and foraminifers. A complete Oligocene section was recovered in this hole. The position of the upper/lower Oligocene boundary is equivocal (see the section on planktonic foraminifers). The Oligocene/Eocene boundary is placed near the top of Core 36. The oldest sediments recovered in this Hole are late Eocene (NP20 and *Globorotalia cerroazulensis* Zone).

### Hole 522A

Hole 522A was cored to duplicate the Oligocene through Eocene section obtained in Hole 522 and to recover sediment down to basement. Nannofossils were examined from most core-catcher samples, and foraminifers were examined from late Eocene core-catcher samples. The results from Hole 522A compare well with those of Hole 522. The oldest sediments recovered in Hole 522A are referable to Nannofossil Zone NP20 and to Planktonic Foraminifer Zones P15-16.

### Hole 522B

Hole 522B was discontinuously cored. The sediment/basalt contact was recovered in Core 3. The nannofossils from just above basalt are referable to Zone NP20, and the planktonic foraminifers are tentatively assigned to Zone P15-16.

## Calcareous Nannoplanktons

### Hole 522

Sample 522-1-1, 108-109 cm is Quaternary NN20 in age, as indicated by the presence of *Gephyrocapsa oceanica* (Kamptner) and the absence of *Pseudoemiliana lacunosa* Gartner. The remainder of Core 1 through Sample 522-3, CC is considered Quaternary NN19 in age because of the presence of *P. lacunosa* Gartner. Within the above interval several horizons contain *Discoaster brouweri* Tan Sin Hok, a species that indicates NN18. These strata are probably slumped.

The flora in Sample 522-4-1, 78-79 cm is considered late Pliocene NN18 in age because of the presence of *D. brouweri* Tan Sin Hok. From Sample 522-4-3, 67-69 cm to Sample 522-6, CC a late Pliocene NN16 age is assigned because of the presence of *D. surculus* Martini and Bramlette. The occurrence of *Reticulofenestra pseudo-umbilicia* Gartner in Sample 522-7-2, 67-68 cm to Sample 522-8, CC indicates an early Pliocene NN15 age. Sample 522-9-1, 86-87 cm is considered early Pliocene NN14 because of the occurrence of *Amaurolithus tricorniculatus* (Gartner). The interval from Sample 522-9-2, 102-103 cm to 522-9-3, 41-42 cm is assigned to NN13 because of the presence of *Ceratolithus rugosus* Bukry and Bramlette without *D. asymmetricus* Gartner.

The sediments in Sample 522-9, CC and Sample 522-10-1, 119-120 cm are considered late Miocene NN11/12 because of the occurrence of *Amaurolithus* spp. From Core 10 through Core 14, age is difficult to determine. Sample 522-10-3, 25-26 cm is considered NN11 late Miocene because of the continued occurrence of *D. sur-*

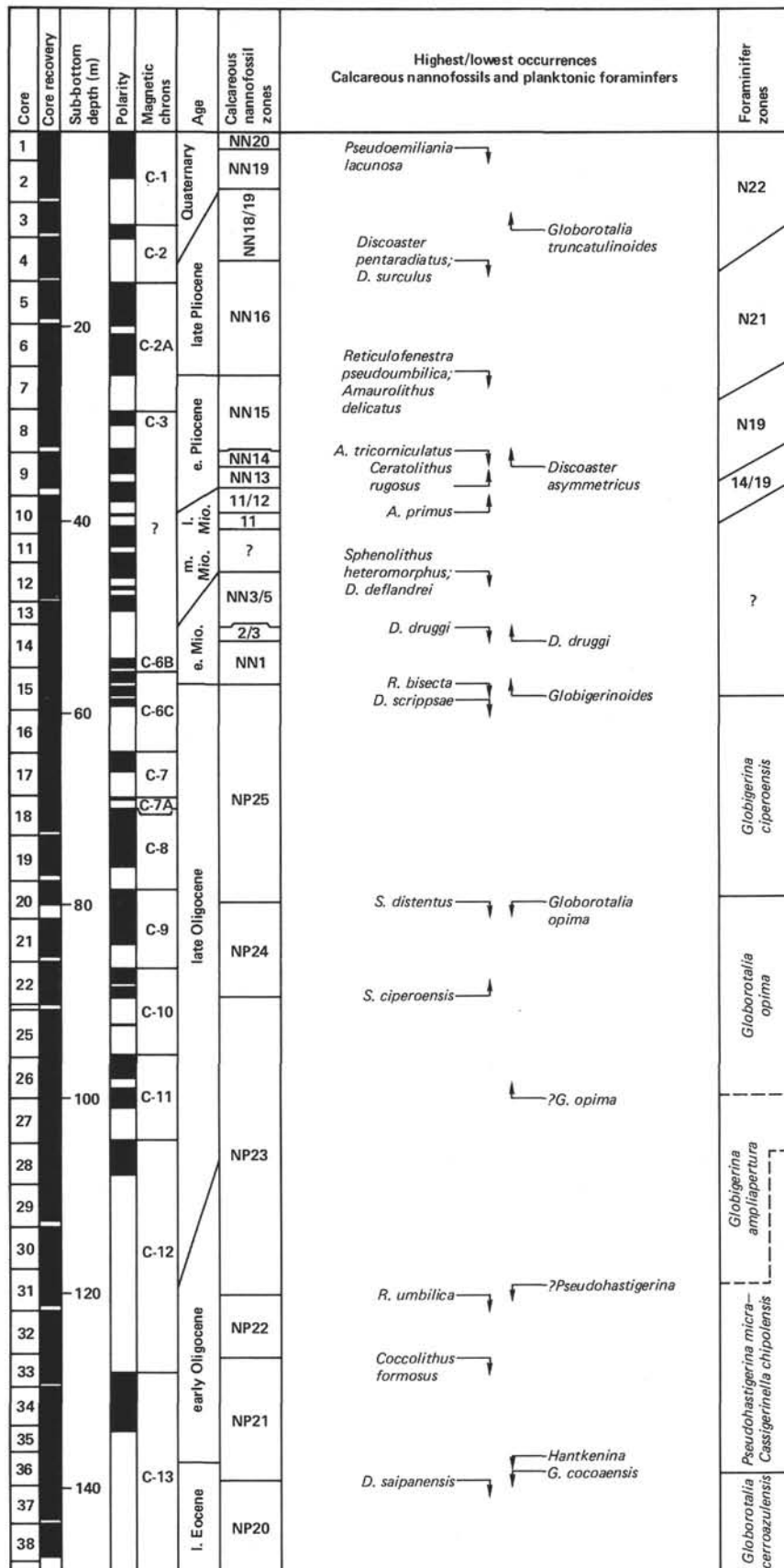


Figure 4. Biostratigraphic summary of significant calcareous planktonic microfossils, Hole 522. Solid blocks denote intervals of normal polarity.

*culus* Martini and Bramlette. Core 11 is barren. In Sample 522-12-2, 29–30 cm, *Sphenolithus heteromorphus* Bramlette and Wilcoxon is present, a species that indicates an age of NN3/5 middle Miocene. Sample 522-13, CC belongs to NN3/5 for similar reasons. Sample 522-14-1, 101–102 cm is considered NN2/3 early Miocene because of *D. druggii* Bramlette and Wilcoxon. The interval from Sample 522-14-2, 101–102 cm to 522-15-1, 100–102 cm is assigned to NN1 early Miocene because of the presence of *Coccolithus eopelagicus* Bramlette and Riedel.

The first Oligocene NP25 species assemblage is found in Sample 522-15-2, 100–102 cm, which contains *R. bisecta* (Hay, Mohler, and Wade) and *Dictyococcites scrippsae* Bukry and Percival. The interval from Sample 522-15-2, 100–102 cm to Sample 522-21-2, 60–62 cm is considered NP25 because of the absence of *S. distentus* Bramlette and Wilcoxon and *S. predistentus* Bramlette and Wilcoxon. The first appearance (downhole) of *S. ciproensis* Bramlette and Wilcoxon occurs in Sample 522-17, CC. The base of NP24 is placed at Sample 522-2-3, 32–34 cm because of the last occurrence (downhole) of *S. ciproensis* Bramlette and Wilcoxon. Therefore, NP24 is present from Sample 522-17-1, 70–72 cm to Sample 522-22-3, 32–34 cm. The interval from Sample 522-22, CC to Sample 522-31-2, 49–51 cm is assigned to NP23 because of the occurrence of *S. distentus* Bramlette and Wilcoxon and *S. predistentus* Bramlette and Wilcoxon without *S. ciproensis* Bramlette and Wilcoxon and *R. umbilica* (Levin). In Sample 522-25-2, 92–93 cm *Braarudosphaera* chalk is found. Specimens of *R. umbilica* (Levin), the marker for NP22, are frequent from Sample 522-32, CC to Sample 522-32-3, 49–57 cm. In Sample 522-33-1 (61–62 cm), *Cyclococcolithina formosa* (Kamptner) is found, which is the NP21 marker. This early Oligocene zone continues to Sample 522-36-3, 30–31 cm.

The Eocene/Oligocene boundary (NP20/21) is believed to occur above Sample 522-36, CC because of the first occurrence of *D. saipanensis* Bramlette and Riedel. The remaining three cores (Cores 37–39) are late Eocene NP20.

#### Hole 522A

Sample 522A-1, CC is indeterminate. Sample 522A-2, CC is considered early Miocene NN1 because of the occurrence of *Coccolithus eopelagicus* Bramlette and Riedel.

The interval from Sample 522A-3-1, 20 cm to 522A-4, CC is considered late Oligocene NP25 because of the occurrence of *Reticulofenestra bisecta* (Hay, Mohler, and Wade) and *Dictyococcites scrippsae* Bukry and Percival. Samples 522A-5, CC through 522-9, CC are NP24 in age because of the co-occurrence of *Sphenolithus distentus* Bramlette and Wilcoxon, *S. predistentus* Bramlette and Wilcoxon, and *S. ciproensis* Bramlette and Wilcoxon. The NP23/24 boundary is placed in Core 10 because of the last occurrence downhole of *S. ciproensis* Bramlette and Wilcoxon. Samples 522A-10, CC through 522A-18, CC are considered NP23 because of the absence of *R. umbilica* (Levin). The *Braa-*

*rudospaera* chalk is present in Sample 522A-11, CC. Samples 522A-19, CC and 522A-20, CC are considered NP22 early Oligocene because of the first downhole occurrence of *R. umbilica* (Levin). Samples 522A-22, CC through 522A-27, CC are NP21, as indicated by the presence of *Cyclococcolithina formosa* (Kamptner).

The Eocene/Oligocene boundary, NP20/21, is placed at Sample 522A-28-1, 90–91 cm, where *Discoaster saipanensis* Bramlette and Riedel first appears (downhole). From Sample 522A-28-1, 90–91 cm to Sample 522A-31, CC the samples are late Eocene NP20.

#### Hole 522B

Samples from the core catcher for Core 1 are considered early Oligocene (NP22) because of the occurrence of *Reticulofenestra umbilica* (Levin). Below this core catcher, *Discoaster barbadiensis* Bramlette and Riedel and *D. saipanensis* Bramlette and Riedel are found.

#### Planktonic Foraminifers

##### Hole 522

Late Eocene through Quaternary planktonic foraminifers were recovered in Hole 522. Cores 1 through 3 contain diverse, moderately well preserved Quaternary assemblages. *Globorotalia truncatulinoides* is consistently present, and the Pliocene/Quaternary boundary is placed between the core-catcher samples for Cores 3 and 4 because of the lowest occurrence of *G. truncatulinoides* in Sample 522-3, CC.

Samples 522-4, CC through 522-8, CC are Pliocene. *Globorotalia crassaformis*, *G. inflata* or *G. puncticulata*, *Orbulina universa*, *Globigerinoides obliquus*, and *G. conglobatus* are consistent components of these Pliocene assemblages. The increasing intensity of dissolution from Core 4 to Core 8 is indicated by the increasing fragmentation of the foraminifer assemblages downsection. Samples 522-9, CC through 522-14, CC are intensely dissolved, and planktonic foraminifers are extremely sparse and poorly preserved in this interval. The few species identified from Samples 522-9, CC through 522-13, CC are not particularly age diagnostic.

The preservation of planktonic foraminifers begins to improve in Sample 522-15, CC. The occurrence of a *Globigerinoides* sp. in Sample 522-14, CC and *Globorotalia kugleri* (s.l.) in Cores 14 through 17 suggests the base of the *G. kugleri* Zone, and the Oligocene/Miocene boundary is within Core 15. Typical *G. opima* ranges from Sample 522-21, CC down through Sample 522-26, CC. Thus, Samples 522-15, CC through 522-20, CC are assigned to the *Globigerina ciproensis* Zone, and Samples 522-21, CC through 522-26, CC are assigned to the *Globorotalia opima* Zone.

The first consistent occurrence (downsection) of *Pseudohastigerina* in Sample 522-31, CC marks the top of the *Pseudohastigerina micra*–*Cassigerinella chipolensis* Zone. Samples 522-27, CC through 522-30, CC are thus assigned to the *Globigerina ampliapertura* Zone. Samples 522-31, CC through 522-35, CC contain *Pseudohastigerina* spp., *Chiloguembelina cubensis* and, usually, *G. ampliapertura* without *Globorotalia cerroazu-*

*lensis* (s.l.) or *Hantkenina*. This interval is referable to the *P. mica*-*Cassigerinella chipolensis* Zone. The presence of *Hantkenina* and *G. cerroazulensis* in Sample 522-36,CC marks the top of the *G. cerroazulensis* Zone, and the Eocene/Oligocene boundary is placed between Samples 522-36,CC and 522-35,CC. Samples below Core 36 are also indicative of the *G. cerroazulensis* Zone.

The preservation of planktonic foraminifers in Samples 522-28,CC through 522-38,CC is fair to good. Changes in dissolution intensity are evident from sample to sample, however, suggesting that relatively short wavelength dissolution cycles occur in the late Eocene to early Oligocene.

#### Hole 522A

Core-catcher samples were examined from the lowest six cores in Hole 522A (Cores 26 through 31). Cores 26 through 28 duplicate the section and types of faunas recovered in Cores 36 through 38 of Hole 522. Sample 522A-29,CC (151.5 m sub-bottom) contains a P16 assemblage, but typical specimens of *Pseudohastigerina barbadoensis* were not found in Samples 522A-30,CC or 522A-31,CC. In addition, the presence of Sample 522A-31,CC of forms transitional between *Hantkenina alabamensis* and *Cribohantkenina inflata* suggests that this sample could be near the base of the *Globorotalia cerroazulensis* Zone.

#### Hole 522B

In Hole 522B, the sediment/basalt contact was recovered in Core 3, Section 2. The planktonic foraminifers from just above the contact are referable to the *Globorotalia cerroazulensis* Zone.

#### Diatoms

Pure *Ethmodiscus rex* ooze occurs at the bottom of Core 1 in Hole 522. All the samples from other holes at this site are barren of diatoms.

#### Benthic Foraminifers

Hole 522 contains a diverse bathyal to abyssal benthic foraminifer fauna. The late Miocene to Quaternary specimens are common and well preserved, whereas those of the late Eocene to middle Miocene are moderately abundant and moderately well preserved. Both frequency and preservation are strongly correlated with the degree of dissolution.

The late Miocene to Quaternary fauna is typical of the Antarctic Bottom Water (AABW); it is dominated by *Nuttallides umbonifera*, with subordinate amounts of *Oridorsalis umbonatus*, *Globocassidulina subglobosa*, *Epistominella exigua*, *Planulina wuellerstorfi*, and *Pullenia* spp.

Dissolution at this site was so intense during most of the middle and late Miocene that few benthic foraminifers are preserved. A 1- to 2-m sequence near 46 m sub-bottom (Section 522-29-2) contains a benthic foraminifer assemblage that differs from that of the late Miocene to Quaternary fauna by the absence of *N. umbonifera*. The dominant elements in the fauna are *O. umbonatus*, *G. subglobosa*, and *Cibicides kullenbergi*. If found

today, this assemblage would suggest the presence of a warmer, more saline, and more oxygen-enriched water mass than the AABW. Unfortunately, there are few samples in this interval, so biostratigraphic control is poor. The best calcareous nannofossil resolution that can be obtained in this interval is NN3/5, which spans a long interval across the early to middle Miocene boundary.

The early Miocene fauna is, like that of the upper part of Hole 522, dominated by *N. umbonifera*, with subordinate but significant amounts of *O. umbonatus*, *G. subglobosa*, *Pullenia* spp., and *Eponides* sp.

The late Oligocene fauna differs from that of the early Miocene only in the addition of *Bolivina huneri* and *Gyroidinoides girardensis* to the abundant elements. In the lower part of the upper Oligocene, below 87 m sub-bottom (Section 522-22-1), the proportion of *N. umbonifera* declines in the benthic foraminifer assemblage. This transition from a fauna depleted in *N. umbonifera* to one rich in the species occurred between 30.3 and 31.5 Ma. The water depth during this interval as determined from the subsidence curve (Fig. 5) was approximately 3300 m. If analogs with modern foraminifer distributions with respect to water masses are valid in the Oligocene, this water depth appears to be the boundary between a deep, cold, low-salinity, oxygen-depleted water mass and an overlying warmer, more saline and more oxygen-enriched water mass.

#### Dissolution

Figure 6 shows the downcore distribution of two measures of dissolution, the ratio of the benthic to planktonic foraminifers and the degree of fragmentation among planktonic foraminifer tests. The curves behave sympathetically, with the percentage of fragments being a more sensitive measure of dissolution during episodes of low to moderate dissolution and the percentage of benthic foraminifers more sensitive during episodes of moderate to intense dissolution.

Episodes of moderate dissolution, which correspond to Pleistocene glacial epochs, are sporadically recorded

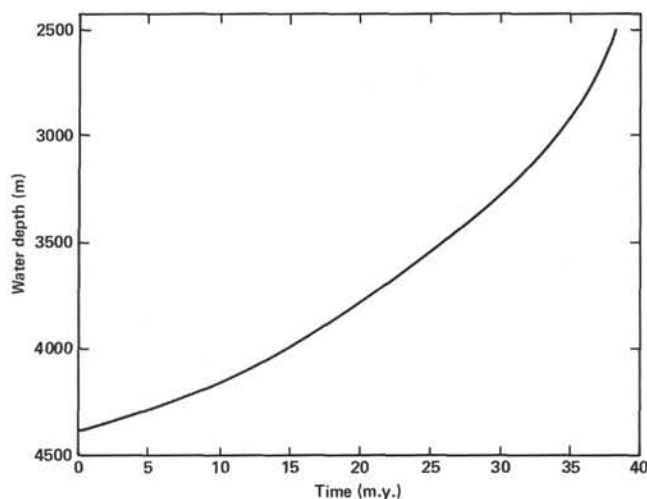


Figure 5. Bathymetry of Site 522 based on subsidence curves corrected for sediment load (Berger and von Rad, 1972).

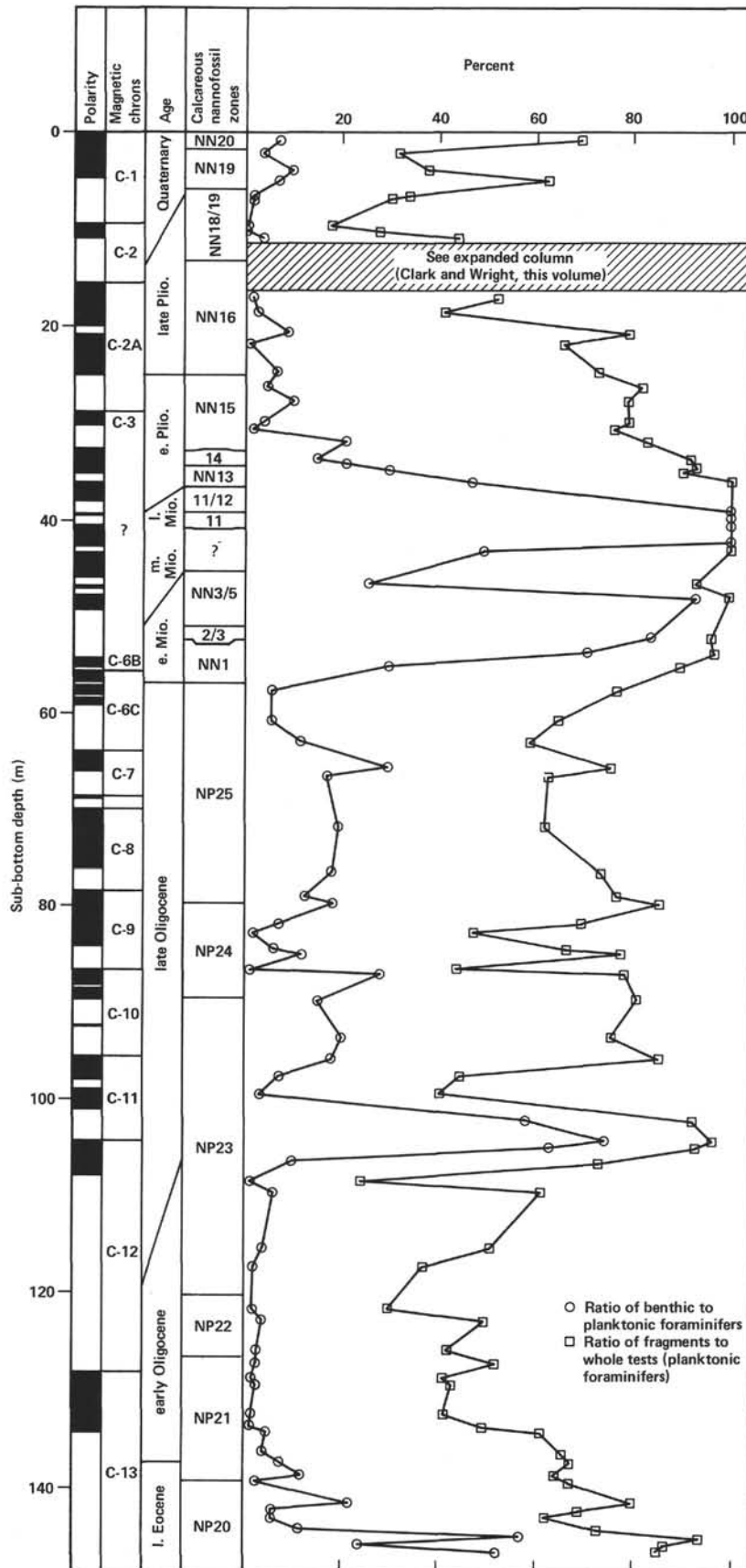


Figure 6. Dissolution indices, Hole 522. See text for discussion. Polarity as in Fig. 4.

in the upper part of the core. The dissolution indices correspond nicely to the isotopic and sedimentological record of the late Pliocene (see Clark and Wright; Weisert et al., this vol.).

The major dissolution events of the late and middle Miocene are merged in a condensed section centered about 40 m sub-bottom. A major event in the early Miocene is recorded by the indices at 50 to 58 m sub-bottom. Both of these events are also documented by the bulk carbonate curve (Fig. 2).

Dissolution is moderate to low throughout most of the late Oligocene, with one sharp intense peak occurring at 98 to 106 m sub-bottom, just above the top of Chron C-12. This event is recorded in the bulk carbonate curve (Fig. 2) by a minor decrease in carbonate content.

There is a significant increase in dissolution near the bottom of Hole 522 in upper Eocene sediments (145–146 m sub-bottom; Chron C-13-R).

### Sedimentation Rates

Excellent sediment recovery and good paleomagnetic data in Hole 522 provide numerous points for the calculation of sedimentation rates (Fig. 7). The chronology of the paleomagnetic datums is essentially that of LaBrecque et al. (1977) as modified by Mankinen and Dalrymple (1979) using the new decay and abundance constants recommended by the International Union of Geological Sciences Subcommittee on Geochronology.

Several episodes of strong dissolution during the Miocene account for the low accumulation rates between 34 and 58 m sub-bottom. The rate of 1 m/m.y. calculated here for the Miocene is an average figure.

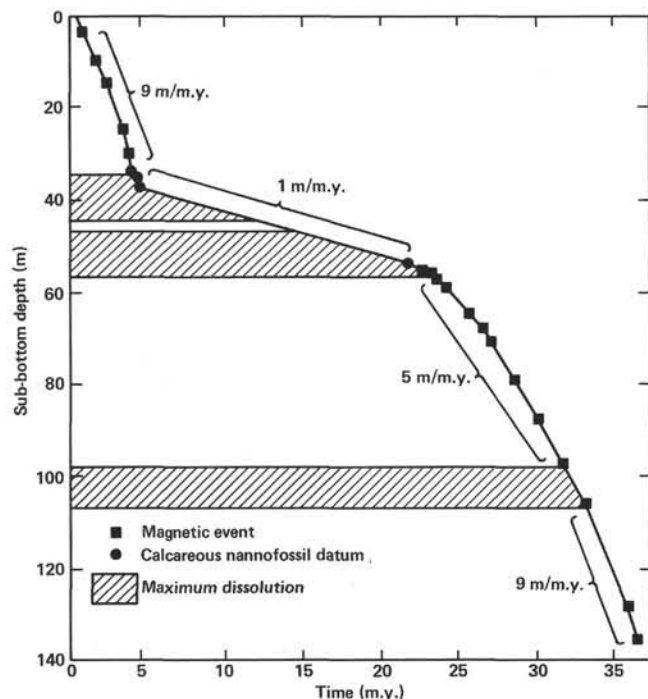


Figure 7. Sedimentation rates, Hole 522 (not corrected for compaction).

The presence of 1 to 2 m of nannofossil ooze at 44 to 46 m sub-bottom represents an episode of increased accumulation. Unfortunately, biostratigraphic control in this interval is too poor to allow the calculation of sedimentation rates.

A short-lived episode of intense dissolution in the upper Oligocene sediments at 98 to 106 m sub-bottom is not reflected in the age–depth curve in Figure 7.

## PALEOMAGNETISM

### Sediments

Site 522, which is situated on Anomaly 16, presented an excellent opportunity to obtain a continuous paleomagnetic record for the last 40 m.y.

Because of the problems with rust and overprinting encountered at the previous sites, we decided not to use the long-core spinner. All measurements were obtained on subsamples taken routinely at 20-cm intervals down the sequence. The uncertainties in maintaining a consistent between-core orientation (seen as abrupt changes in the measured declinations from core to core) were so pronounced that it was decided to dispense with the orientation procedure. Unfortunately, at this juncture the maintenance of directional continuity between core sections was also lost. The declination record is thus very fragmentary and does not provide an easily visualized overall record of the geomagnetic polarity. The inclination record was used to define the field polarity.

The Quaternary and upper Pliocene sediments were relatively stable against demagnetization (median destructive fields of order 250 Oe). The viscous overprints (most evident for the reversed samples) were removed in fields of 100 Oe (Core 2) to 200 Oe (Core 6). The magnitude of the normal overprint in Cores 4 to 8 was generally greater than that of the residual primary signal, so obscuring the true polarity record of the natural remanent magnetization (NRM). These results indicate that fine- to medium-grained "magnetite" may be the primary magnetic carrier. The samples from the Oligocene sediments had median destructive fields of order 250 to 300 Oe and minimal overprinting (removed in alternating fields as low as 50 Oe). In all cases the NRM gave the true polarity record. It is believed that the effective magnetic grain size must be lower for these than for the uppermost sediments. These simple stability tests indicate with a high probability that the magnetic record from the Oligocene has been faithfully and well preserved in the sediment. The red clays (Cores 9–14) showed very different magnetic behavior. The record was completely overprinted, 150 to 200 Oe being needed for effective cleaning. The NRM intensities were high (10–20  $\mu\text{G}$ ), compared with approximately 1 to 5  $\mu\text{G}$  for the underlying and overlying sediments, respectively. Median destructive fields of 25 to 50 Oe were typical.

The inclination results, together with the inferred polarity sequence correlated with the time scale of LaBrecque et al. (1977), are summarized in Figure 8. The Oligocene record in particular is of very high quality. The match between the lower Miocene (Anomaly 6B or Chron C-6B; see Hsü, LaBrecque, et al., this vol., for

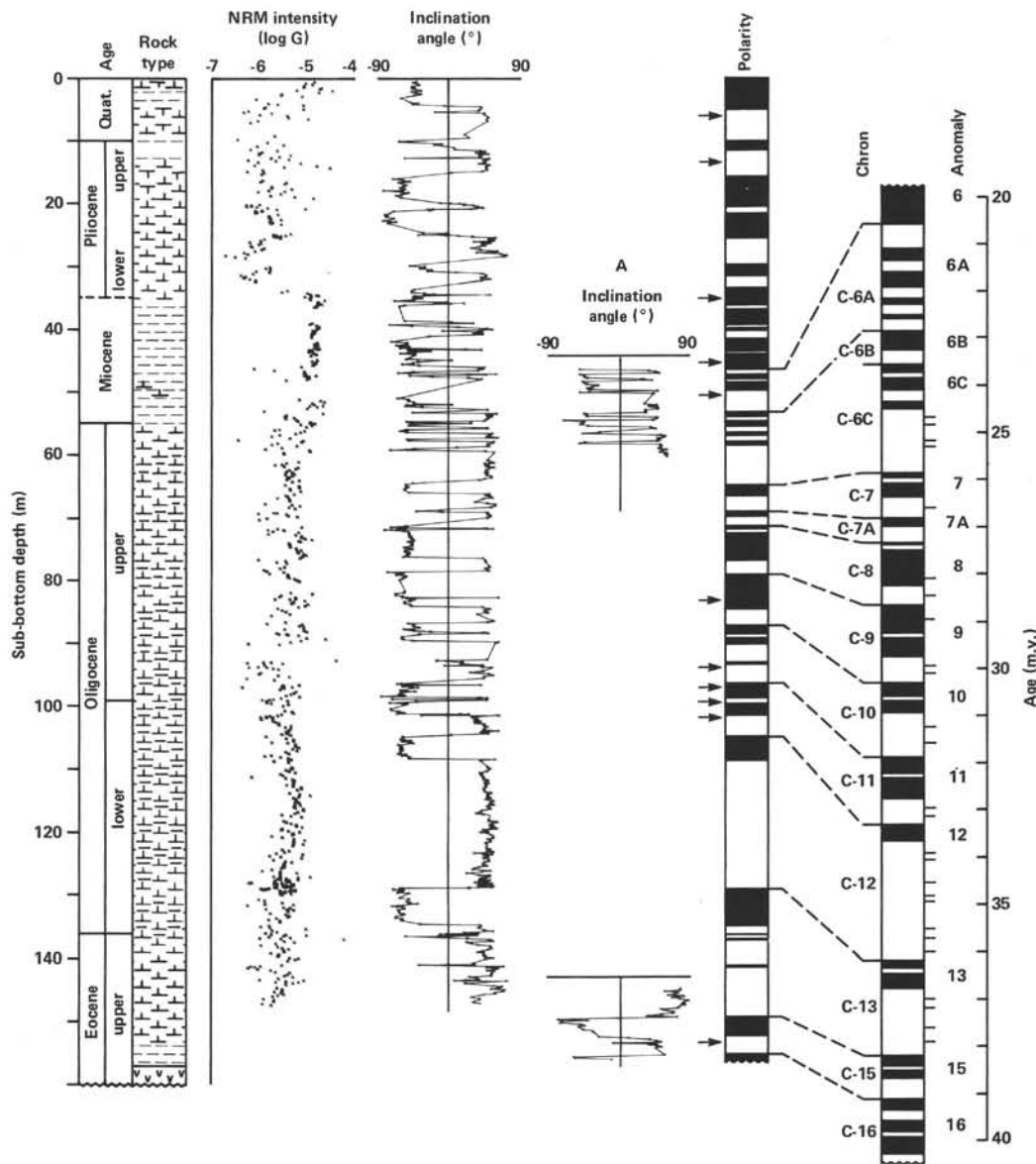


Figure 8. Summary of magnetic polarity stratigraphy at Site 522. Column labeled A refers to results from Hole 522A. Polarity as in Fig. 4. Lithology is defined in Hsü, LaBrecque, et al. (this vol.). Arrows identify the positions of polarity units that are defined by single samples and are therefore tentative (see Tauxe et al., this vol.).

explanation) and the late Eocene (Anomaly 13 or Chron C-13) is excellent; every polarity transition and event was recorded, with the possible exception of the reversed interval in Anomaly 13 (Chron C-13). Possible additional events were also seen in the record (Cores 25, 35, 37).

The Brunhes, Matuyama, Gauss, and the top of the Gilbert epochs were well recorded in Cores 1 to 8. Between the lower Gilbert (Anomaly 3 or Chron C-3) and Anomaly 6 (Chron C-6), the record was either very compressed or incomplete and therefore difficult to interpret. This is a feature we have come to expect with the highly dissolved Miocene sediments. The peculiar magnetic mineralogy of the red clays in this region makes the reliability of the paleomagnetic record even more suspect.

Gaps in the record were filled by correlation to the cores from Hole 522A. These results extend the interpreted range up to Anomaly 5 (Chron C-5) and down to the basement at Anomaly 16 (Chron C-16).

**Igneous Rocks**

The results of the paleomagnetic measurements of basalts recovered from Hole 522B are listed in Table 2. Hole 522B has been placed inside Marine Magnetic Anomaly 16. Anomaly 16 contains two small negative events, and Hole 522B is located on the older transition zone of the younger event. Accordingly, we observe a reversal of remanent magnetization in the drilled basalts. The upper 18 m of basalt have a reversed magnetization polarity (positive inclination means reversed po-

Table 2. Paleomagnetic measurements of basalt at Hole 522B.

Core-Section, interval (in cm), level (in cm), or piece	Natural remanent magnetization			Median destructive force (Oe)	Susceptibility ( $10^{-4}$ G/Oe)	Q-factor
	Intensity ( $10^{-4}$ G)	Inclination ( $^{\circ}$ ) <sup>a</sup>	Stable inclination ( $^{\circ}$ ) <sup>a</sup>			
3-2, 121-123, 2B	19.32	62.5	62	630	5.25	13
3-3, 29-31, 1C	49.37	52.8	52.5	360	7.98	22
3-3, 135-137, 4B	20.49	51.3	52	540	6.65	11
3-4, 42-44, 4	13.85	53.1	55	580	2.24	22
4-1, 4-6, 1A	40.82	48.7	50	140	22.7	6
4-2, 93-95, 3A	25.63	45.5	45	490	3.8	24
4-2, 3-5, 1A	92.9	49.8	46	370	6.09	54
4-1, 76-78, 2	19.77	52.0	52	470	4.20	17
5-1, 28-30, 3B	26.37	48.1	48	560	3.50	27
5-1, 99-101, 7	14.22	50.8	49	540	3.01	17
5-2, 29-31, 2A	72.02	41.9	40	350	3.88	66
5-2, 122-124, 2F	74.88	40.8	43	270	9.17	29
5-3, 55-57, 2C	88.87	31.3	37.5	90	20.93	15
6-1, 33-35, 5	97.29	-31.6	-46	90	23.73	15
6-1, 75-77, 9	47.04	-39.6	-47	140	13.44	12

<sup>a</sup> Positive inclination means reversed polarity on the Southern Hemisphere.

larity on the Southern Hemisphere), and the lower 2 m of basalt have a normal polarity.

The inclination values, both normal and reversed, group tightly around the theoretical field inclination value of  $46^{\circ}$ , as is to be expected at the latitude of the drill site. This means that, in contrast to Site 519, no tilting of the basement has taken place; neither is there any paleomagnetic evidence of a large northward movement of the plate (see Tauxe et al., this vol.).

There is considerable scatter in the NRM intensity values. The mean NRM intensity of the Hole 522B basalts is  $46.8 \times 10^{-4}$  G, as compared with  $15.7 \times 10^{-4}$  G for the Hole 519A basalts. This is surprising, because the Hole 522B basalts are more than twice as old as the Hole 519A basalts.

### PHYSICAL PROPERTIES

The measurements of the physical properties at Site 522 are summarized in Figure 9. The section consisted mainly of foraminifer-nannofossil ooze, with the exceptions of Cores 8 through 14, in which a thick, dissolved interval of Miocene red clay was recovered, and of Core 25, Section 2, a 30-cm-thick layer in which *Braarudosphaera* appeared. The presence of both the red clay interval and the *Braarudosphaera* zone was indicated in the physical property measurements, the former by a drop in velocity and density, the latter by a marked increase in velocity and density. Because the completeness of the section at Site 522 made it especially valuable for detailed biostratigraphic and magnetostratigraphic studies, we decided to minimize gravimetric measurements.

Seven basalt samples were selected for physical property measurements. Unfortunately, two of the samples broke apart while they were being cored for sound velocity specimens (after the thermal conductivity measurements were completed).

Figure 10 shows the variation of the acoustic velocity of the basalts recovered at Sites 519, 520, and 522 versus bulk and gamma-ray attenuation porosity evaluator (GRAPE) density. For all three sites, the velocities measured in the vertical direction form a single cluster. The velocities measured in the horizontal direction, however, form two groups: the Site 522 basalts (open circles)

have comparatively low velocities with very little variation in density, and the Site 519 and 520 basalts have comparatively low densities without the expected decrease in velocity. The presence of cracks approximately oriented in the horizontal plane may explain the distribution of the Site 522 data. The explanation for the velocity-density distribution of the Site 519 and 520 data is less obvious. One cannot use grain orientation as an explanation, because this would be expected to affect velocity strongly but have only a minor effect on density. Elipsoidal vugs oriented with their long axes in the horizontal plane could produce the observed effect. Such an alignment could be the response of the void geometry to the stresses induced during flow of the cooling magma.

Two successful downhole temperature measurements were made in three attempts at Hole 522B. The shallowest two measurements were planned on either side of the dissolution interval because the thermal conductivity values of this interval were approximately 30% lower than those of the overlying and underlying sediments. For the first measurement, sediment was washed down to 28 m sub-bottom, and the heat probe-water sampler was lowered into the hole. The connectors related to the water sampler failed, so no data were recovered. For the next two measurements it was decided to use only the thermal probe. Sediment was washed down to 55 m sub-bottom and readings were taken (Fig. 11). A temperature of about  $4.75^{\circ}\text{C}$  was recorded. A final measurement was made at a depth of 149.8 m sub-bottom, where the instrument stuck (Fig. 11). The probe was extracted and found to be bent. The data scatter for this measurement is thought to be related to whatever perturbations were imposed on the instrument as a result of its being jammed against the coring tool; there was a distinct possibility that the probe was not properly embedded in the sediment. The temperature recorded was about  $6.5^{\circ}\text{C}$ .

The temperature measurement at 55 m sub-bottom was considered the most reliable. The temperature at the mudline is  $2.3^{\circ}\text{C}$ , which yields a thermal gradient of  $45 \text{ deg/km}$ . By using the measured average thermal conductivity at the site ( $1.4 \text{ W/m}^{\circ}\text{K}$ ), we obtained a heat flow of  $63 \text{ mW/m}^2$  ( $1.5 \text{ HFU}$  or heat flow units), a value

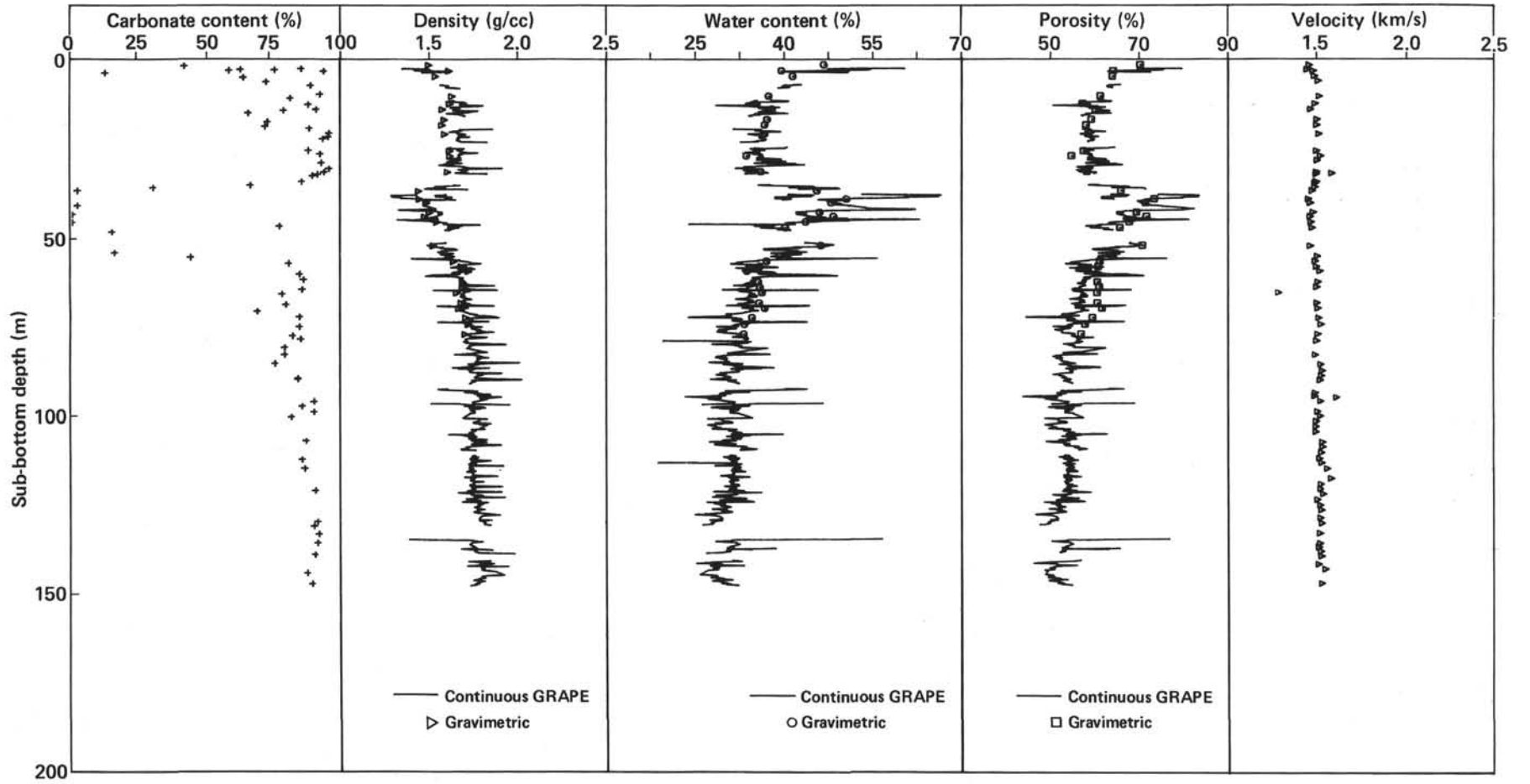


Figure 9. Summary of physical properties, Site 522. Velocity data are for perpendicular beds.

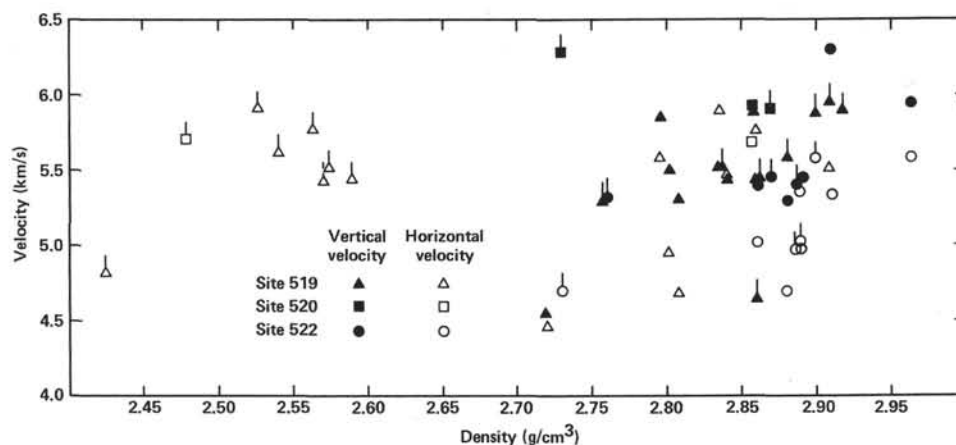


Figure 10. Velocity versus bulk and GRAPE density. GRAPE data are flagged.

that is slightly higher than the average value of 1.1 HFU  $\pm 0.6$  measured from the piston core data of Herman et al. (1977). All the sites yielded thermal conductivities that were considerably higher than most published values (e.g., Lachenbruch and Marshall, 1966; Herman et al., 1977; Horai, 1981). Our measurements of porosity, carbonate content, and water content do suggest that we should expect high thermal conductivities, however (M. Langseth, pers comm., 1983). On the other hand, we also estimated the thermal conductivity from water content using the empirical data of Lachenbruch and Marshall (1966). The average water content of 41.36% yields an estimated conductivity of 1.04 W/m<sup>2</sup>°K and a heat flow of 47.1 mW/m<sup>2</sup> (1.125 HFU). The latter value is more in line with the estimated average regional data of Herman et al. (1977) of 1.1 HFU.

### INORGANIC GEOCHEMISTRY

Chemical analyses of interstitial water squeezed from samples at Site 522 are summarized in Table 3. Except for a slight salinity maximum at about 86 m sub-bottom, no significant downhole gradients were found. Calcium and magnesium concentrations remain fairly constant with increasing depth; they show only slight reversals between 64 and 86 m sub-bottom. The only major lithologic variation in the section, a zone of stiff carbonate-poor clays between 33 and 53 m sub-bottom, appears to have little effect on the interstitial water chemistry.

### GEOPHYSICAL DATA CORRELATION TO DRILLING RESULTS

Site 522 is located over the younger half of Anomaly 16 near the older transition boundary of the last reversed event within Anomaly 16. Seismic data gathered over

the site are displayed in the profile record in Figure 12. The data were gathered by using two (5 and 10 in.<sup>3</sup>) Bolt airguns and bandpass filtering of 80 to 160 cps.

Two sub-bottom reflectors can be distinguished in the seismic data (Fig. 12). A very faint reflector can be discerned at 0.06 to 0.08 s sub-bottom, and a strong reflector appears at 0.18 s sub-bottom (two-way travel times). The first reflector might be correlated to the Miocene dissolution layer encountered at 25 to 55 m sub-bottom; the second is most certainly oceanic basement, which was encountered at 156 m sub-bottom at Hole 522.

Magnetostratigraphic data gathered during the coring of Holes 522 and 522A were in excellent agreement with the seafloor magnetic lineations throughout the Oligocene to Eocene sequence. The magnetic-stratigraphic data were correlated up to Magnetic Chron C-16-N at the bottom of the hole, indicating that the sediments were deposited upon newly formed basement, resulting in a basal sediment age only slightly younger than the basement age. The observation is consistent with similar observations at Sites 519 and 521.

Before Site 522 was approached, the seismic profile system was modified to improve performance. It had been observed that the amplifier levels were difficult to set properly. The Bolt filtering system incorporates a preamplifier prior to a passive filter network. Oscilloscope checks on the signals between the preamplifier and the filter indicated that the seismic signals were saturating (clipping) the preamplifier prior to filtering, which resulted in severe distortion of the seismic signals. Furthermore, the Edo recorders had to be run at maximum gain levels because the output of the Bolt filter was insufficient to drive the Edo recorders otherwise.

### SUMMARY AND CONCLUSIONS

Site 522 is located over the older reversal boundary of the youngest reversed event in Magnetic Anomaly 16. Three holes were drilled at this site. The original hole was cored with the HPC with 92% recovery of the 148-m sedimentary section. A duplicate set of hydraulic piston cores was obtained from the Oligocene/Miocene boundary down to late Eocene basement in Hole 522A; a por-

Table 3. Summary of interstitial water chemistry, Site 522.

Core-Section (interval in cm)	Sub-bottom depth (m)		pH	Alkalinity (meq/l)	Salinity (‰)	Calcium (mmol/l)	Magnesium (mmol/l)	Chlorinity (‰)
	2.9-7.3	63.9-68.5						
2-2, 140-150	2.9-7.3	7.26	2.80	35.5	10.316	52.90	19.78	
7-2, 140-150	63.9-68.5	7.28	2.524	36.6	10.635	51.316	19.07	
22-2, 140-150	85.7-90.1	7.21	2.373	38.2	10.420	52.196	19.27	
31-2, 140-150	121.8-126	7.20	2.292	36.6	10.316	52.360	19.21	

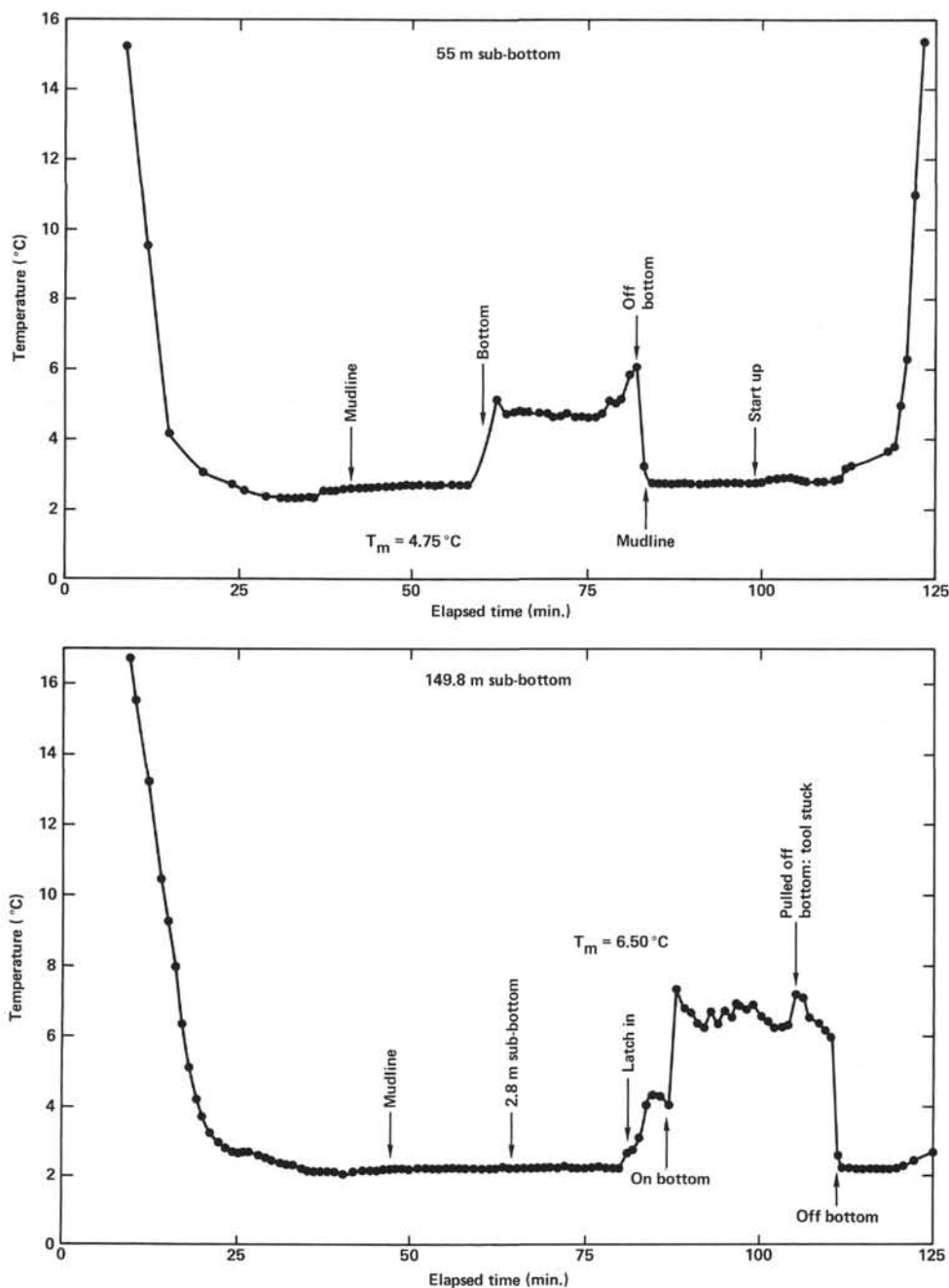


Figure 11. Heat flow probe measurements in Hole 522B.  $T_m$  = equilibrium sub-bottom temperature.

tion of the section missed in Hole 522 was also obtained. The drill string was then tripped and converted to rotary drilling for Hole 522B. Hole 522B was washed down to various levels (approximately 28 m, 55 m, 120 m, and 149.5 m sub-bottom) for heat flow measurements and rotary coring.

#### Biostratigraphy and Magnetostratigraphy

Datums that allow the correlation of biostratigraphic and magnetostratigraphic time scales are called golden spikes. By the same token, Site 522 gave us a yellow brick road. For the first time, a magnetostratigraphic record was obtained for the entire sedimentary sequence from the Quaternary to the upper Eocene. The accom-

plishment underscores the value of the HPC, which permits the establishment of a precision stratigraphy for the study of paleoceanographic and paleomagnetic field history. Most important, we are able to recognize the geomagnetic field reversal pattern from the late Miocene (Chron C-6) to the late Eocene (Chron C-16-N). The magnetic reversal data, in addition to the sedimentological and biostratigraphic observations, indicate that the sedimentary sequence at Site 522 is remarkably free of slumps and unconformities and other resedimentation phenomena. In addition, dissolution is moderate or minor below the Miocene/Oligocene boundary. The sequence here should thus be considered for use as a type section for the magnetostratigraphy of the Oligocene.

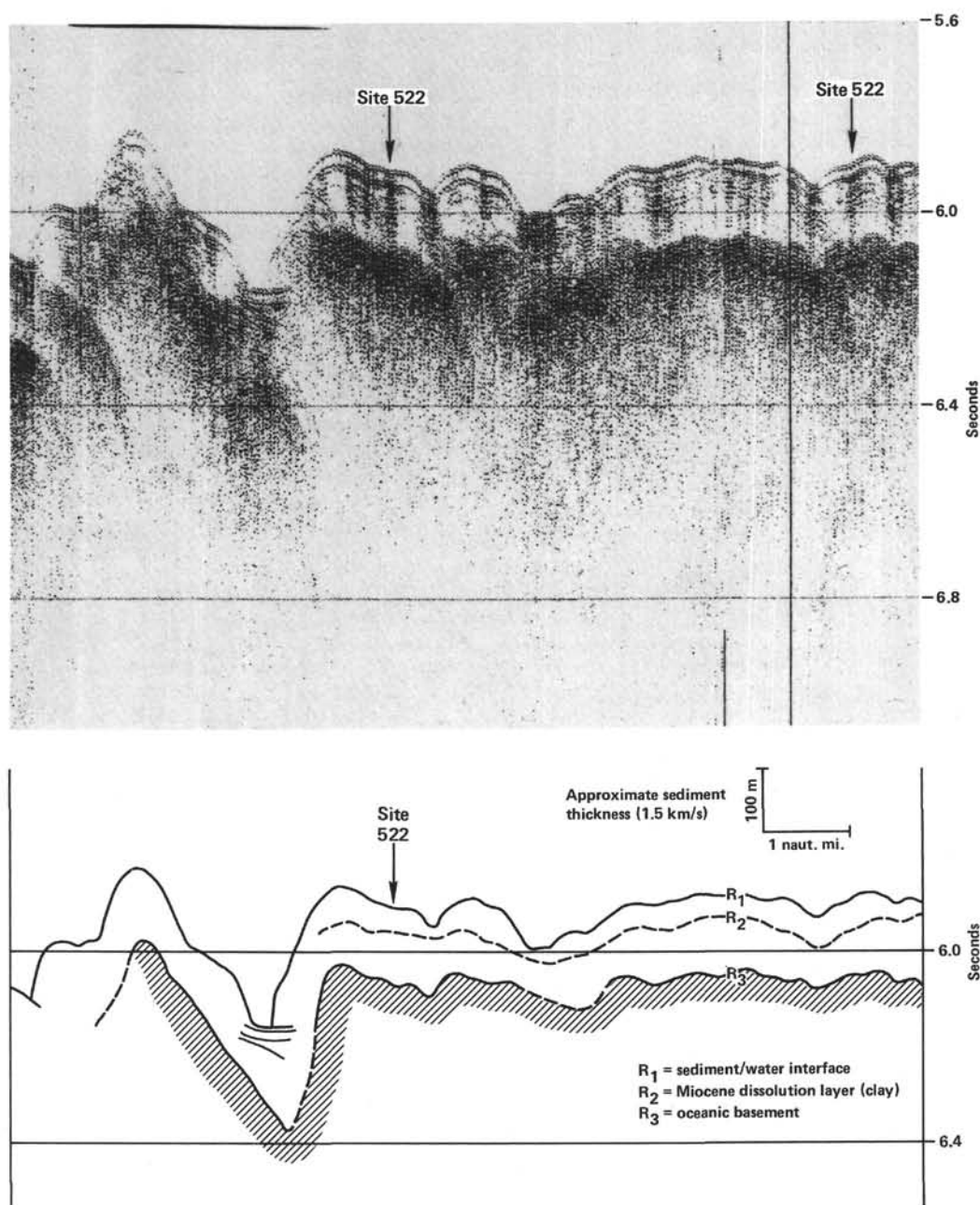


Figure 12. Seismic reflection profile and interpretive line drawing at Site 522.

The Quaternary datum levels are easy to recognize, and the correlation of the biostratigraphic and magnetostratigraphic markers is clear down to the  $C_2$  event of the Gilbert Epoch (Seafloor Anomaly 3; Fig. 13). The highest and lowest occurrences (HOs and LOs) of the nanofossil species are at magnetostratigraphic levels that are similar to their levels at Site 519. It is noteworthy that the HO of *Reticulofenestra pseudoumbilica* here (at a level slightly below the Gauss/Gilbert boundary) is at almost exactly the same level as at Site 519 and that at Site 521 it is considerably lower than reported by Gartner (1973) from his study of Pacific piston cores.

The slow sedimentation rate made the correlation of the Miocene magnetostratigraphic chrons to seafloor anomalies difficult (see Fig. 13). The Miocene/Oligocene boundary, however, is well defined by nanofossils and foraminifers (see Poore et al., this vol.). The boundary falls between Chrons C-6C-2 and C-6B-2 and can be narrowed down to a depth of  $56.3 \pm 0.3$  m sub-bottom in Hole 522A by nanofossil zonation. If the rate of seafloor spreading is assumed to be linear, the age of the boundary is 23.6 Ma. Our boundary is slightly (1 Ma) younger or higher than estimated by Lowrie et al. (in press); it is slightly (1 Ma) older or lower than estimated

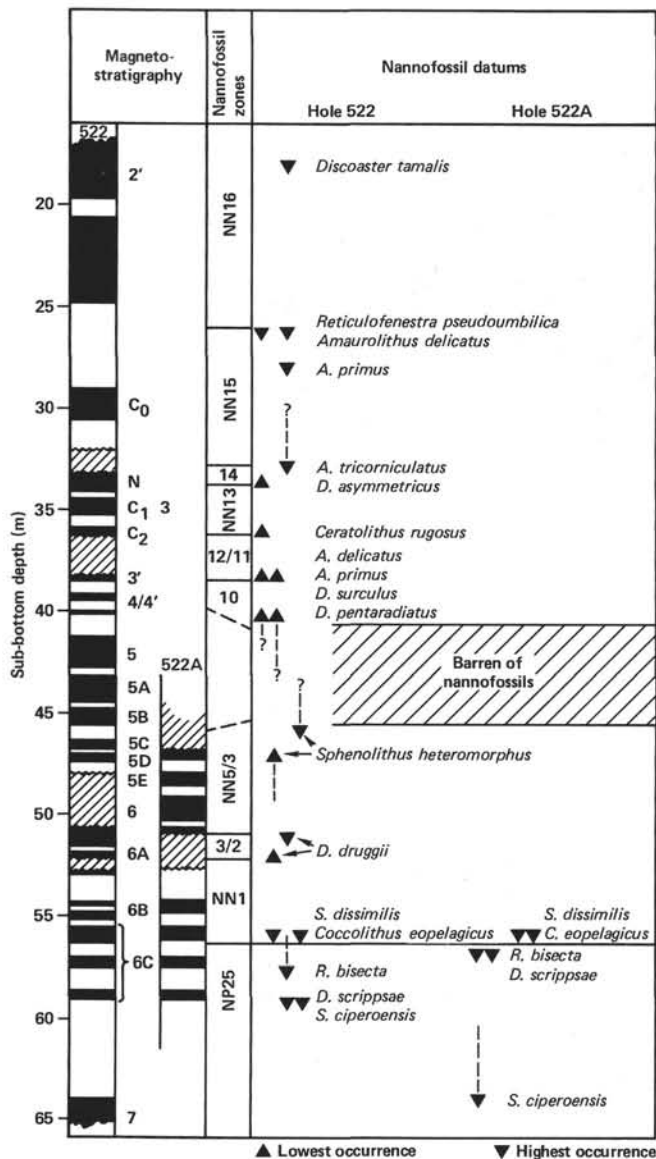


Figure 13. Neogene magnetostratigraphy and biostratigraphy, Site 522. Solid blocks denote intervals of normal polarity, cross-hatched blocks intervals of unknown polarity. Magnetic events are Cochiti (C<sub>0</sub>) and Nunivak (N).

by Bolli, Ryan, et al. (1978). One of us (K.H.) believes that we have the best biostratigraphic and magnetostratigraphic data for the determination of this boundary and recommends that our age for the boundary be adopted.

The interval defined by Nannofossil Zones NN1 and NN5/3 can be correlated with Magnetostratigraphic Chrons C-6C-N to C-5B-R on the basis of the reversal signals, and such a correlation is in general agreement with that of Bolli, Ryan, et al. (1978, p. 14). A 5-m interval above 45.5 m sub-bottom is a red clay barren of nannofossils. The nannofossil assemblage immediately above the barren interval includes the LOs of *Discoaster pentaradiatus* and *D. surculus*. The first appearance datum (FAD) of the former extends down to NN9, and that of the latter extends down to NN10. The LOs of those species above the barren clays are definitely the re-

sult of the truncation of species ranges by dissolution. *D. surculus* is rare, and *D. pentaradiatus* is abundant, and these abundances suggest that the level truncated by dissolution lies closer to the FAD of *D. surculus*, or NN10.

The nannofossil assemblages in the South Atlantic above the HO of *Catinaster coalitus* and below the LO of *D. quinqueramus* include mainly such solution-resistant long-range species as *D. variabilis*, *Coccolithus pelagicus*, *Cyclococcolithus macintyreii*, and so forth (Table 4). A short-range nannofossil, *D. neohamatus* (NN9-11), was found common at Site 16 only. Because of their stratigraphic positions, those assemblages have been zoned as NN11/10, NN10/9, or NN10 at various sites. In our summary for Site 521, we suggest that those sediments be referred to as "NN10" for the sake of convenience. Their age could be correlated either to Chron C-5-N (long-normal Chron 9) or to Chron C-4A-N (Chron 7); we prefer the latter alternative because Chron C-5-N at Site 519 has been correlated to NN8 sediments there. The overlying upper Miocene sediments are thin, and their magnetostratigraphy is not clear.

The correlation of magnetostratigraphic chron with seafloor anomalies is good for the sequence below the Miocene/Oligocene boundary, as discussed in the biostratigraphic summary for this site and in the articles in this volume by Poore et al. and Tauxe et al. The datum levels of the following key species (species useful for zonation) have been determined against a well calibrated Oligocene magnetostratigraphy: HO *R. bisecta*, HO *Cyclargolithus abisectus*, HO *Dictyococcites scrippsae*, HO *Sphenolithus ciproensis*, HO *S. distentus*, HO *S. predistentus*, LO *S. ciproensis*, HO *R. hillae*, HO *R. umbilica*, HO *Cyclococcolithus formosus*, HO *Discoaster saipanensis*, HO *D. barbadiensis*, LO *Globoquadrina dehiscens*, LO *Globigerinoides* sp., LO *Globorotalia kugleri* (s.s.), HO *G. opima*, HO *Globigerina angiporoides*, LO *G. opima*, HO *Globigerina ampliapertura*, HO *Pseudohastigerina* spp., HO *Hantkenina* spp., HO *Globorotalia cerroazulensis*, HO *G. cocoaensis*, and HO *Globigerinatheka* spp. Since the degree of dissolution is moderate or minor at this site, the HOs and LOs are probably very close to, if not the actual, last appearance datums (LADs) and FADs of these species in the South Atlantic. The well calibrated foraminifer datum levels permitted a new zonation of the Oligocene by Poore (this vol.).

Table 4. Abundance of "NN10" nannofossil species.

	Hole 16 NN11/10	Hole 519 NN11/10	Hole 521 NN10	Hole 521A NN10	Hole 522 NN11
<i>Cyclococcolithina leptopora</i>	A	A	A	R	?
<i>C. macintyreii</i>	R	C	A	R	R
<i>Discoaster brouweri</i>	A	A	A	C	R
<i>Coccolithus pelagicus</i>	A	C	A	R	R
<i>D. pentaradiatus</i>	C	C	?	R	A
<i>D. surculus</i>	?	?	C	?	R
<i>D. variabilis</i>	A	A	A	C	A
<i>Reticulofenestra pseudo-umbilica</i> or aff. <i>pseudo-umbilica</i>	C	A	A	R	R
<i>D. neohamatus</i>	C	R	?	R	?

Note: Nannofossils at Holes 16, 519, 521, 522 were examined by S. Percival; those at Hole 521A were examined by A. Salis. A = very abundant or abundant; C = common or frequent; R = rare or very rare; ? = absent or not searched for.

The Eocene/Oligocene boundary, as defined by the HO of the nannofossil species *D. saipanensis* (which is about 2.5 m higher than the HO of *D. barbadiensis* in both sections acquired by HPC at this site), should lie at  $139.6 \pm 0.1$  m sub-bottom. As usual, the Eocene/Oligocene boundary as defined by the HO of the foraminifer species *Globorotalia cerroazulensis* is somewhat higher: near the top of Core 36, at  $137 \pm 1$  m sub-bottom. Both boundaries lie within Chron C-13-R2; they have calibrated ages of 37.6 and 37.1 Ma respectively.

### Calcite Dissolution

The rise of the CCD during the Miocene is impressively shown by Figure 14. The interval barren of nannofossils consists of hololytic red clay, and it is tentatively dated to extend from Chron C-5B-R to Chron C-4A (Chron 8) or from about 15 to 8 Ma. Both the insoluble residue and benthic foraminifer data show a short episode of CCD depression during the time represented by the Nannofossil Zone NN5 at about 15 to 16 Ma. The older and younger Miocene sediments also show signs of severe dissolution (up to 85 and 98% insoluble residue and up to 92 and 99% benthic foraminifers, respectively). By using the tentative chronological correlation shown in Figure 13, we calculated the sedimentation rate of the Miocene intervals to be as shown in Table 5. The sedimentation rates of the insoluble residue during the three Miocene intervals are remarkably similar, and they are also similar to the rates from Sites 519 and 521; the results give us some confidence in our chronological interpretation. The bulk sedimentation rates of more or less 1 m/Ma are typical for the pleistolytic and hololytic sediments of the South Atlantic.

The insoluble residue and benthic foraminifer data suggest subsidiary events of dissolution during the Oligocene and the Pliocene-Quaternary. One, at the bottom of Chron C-11-R (33 Ma), gave rise to sediments with a benthic foraminifer content up to 73% and an insoluble residue content up to 20% (Fig. 14). Other events during the glacial epochs of the late Pliocene resulted in sediments with as much as 75% benthic foraminifers and 35% insoluble residue. Still another may have taken place during the latest Eocene, when the site was still located on the crest of the Mid-Atlantic Ridge. However, the duration of those dissolution events must

have been very brief, so that the influence of the dissolution on sedimentation rate is negligible (see Fig. 15).

We have calculated the rates of accumulation for the various magnetostratigraphic chrons in terms of  $\text{g}/\text{cm}^2/10^3 \text{ yr}$ . As shown by Figure 15, the systematic decrease of the bulk rates during the Oligocene is very impressive. The only deviation is the anomalously high rate during Chron C-8. The somewhat lower insoluble residue content of the sediments deposited during this interval suggests a temporary depression of CCD. However, the benthic foraminifer and foraminifer fragmentation data indicate that the degree of dissolution in those sediments is about the same as in other upper Oligocene sediments.

The rates of insoluble residue accumulation in the various Oligocene chrons are about the same, and they are similar to the average rate for the Pliocene-Quaternary. The rates are, however, more than twice as high as the Miocene rates.

### Paleoceanography

The increase of calcite dissolution in the Oligocene sediments at this site is certainly related to the subsidence shown in Figure 15. However, the effect of the changes in CCD must have been superimposed on changes in depth. The patterns of calcite dissolution during the earliest Miocene and the earliest Pliocene indicate that the CCD first rose and then became depressed sharply during those times. The CCD must have risen above 4000 m about 15 Ma; as we have learned from studies of cores at other sites, it should have reached its highest levels during the late middle Miocene and/or early late Miocene. The CCD did drop below 4200 m about 8 Ma, but the lysocline remained above this depth for a few million years more. The sudden depression of the CCD during the early Pliocene is reflected in the facies change from red clay to nannofossil ooze, a change that must have resulted when the lysocline dropped below 4400 m some 4.5 Ma.

The large shifts of CCD were probably not related to AABW activities. The first increase of *Nuttalides umbo-nifera* during Chron C-10 (30-31 Ma) occurred when the site sank only to about 3100 m. Perhaps the increased vigor of the AABW at that time resulted in the rise of its upper boundary from about 3400 or 3300 m to 3100 m. The shifts in CCD cannot be easily related to worldwide temperature changes either. Detailed studies of Pliocene samples did indicate more dissolution during glacial epochs of more active AABW activities. However, the rise of CCD during the early Miocene is coincident in timing with a warming trend. Again, our observations at this site confirm our tentative conclusion that we must look at the supply side of the equation to understand the shifts in the CCD during the Tertiary. The Oligocene and Pliocene-Quaternary depression of the CCD are probably directly related to oceanic fertility during those epochs and only indirectly related to ocean temperature or worldwide changes in sea level.

The occurrence of the *Braarudosphaera* chalk in the South Atlantic is a most puzzling paleoceanographic problem, and this problem is discussed in a synthesis

Table 5. Miocene sedimentation rate at Site 522.

Datum or interval	Depth (m)	Age (m.y.)	Sedimentation rate (m/m.y.)	
			Interval	Insoluble residue
Chron C-3-N (Event C2)	36	4.5		
Younger Miocene and earliest Pliocene			1.3	0.77
Chron C-4A-R upper and middle Miocene	40.6	8	0.7	0.7
Chron C-5B-R Older Miocene	45.5	15	1.3	0.75
Chron C-6B-R	55.5	23		

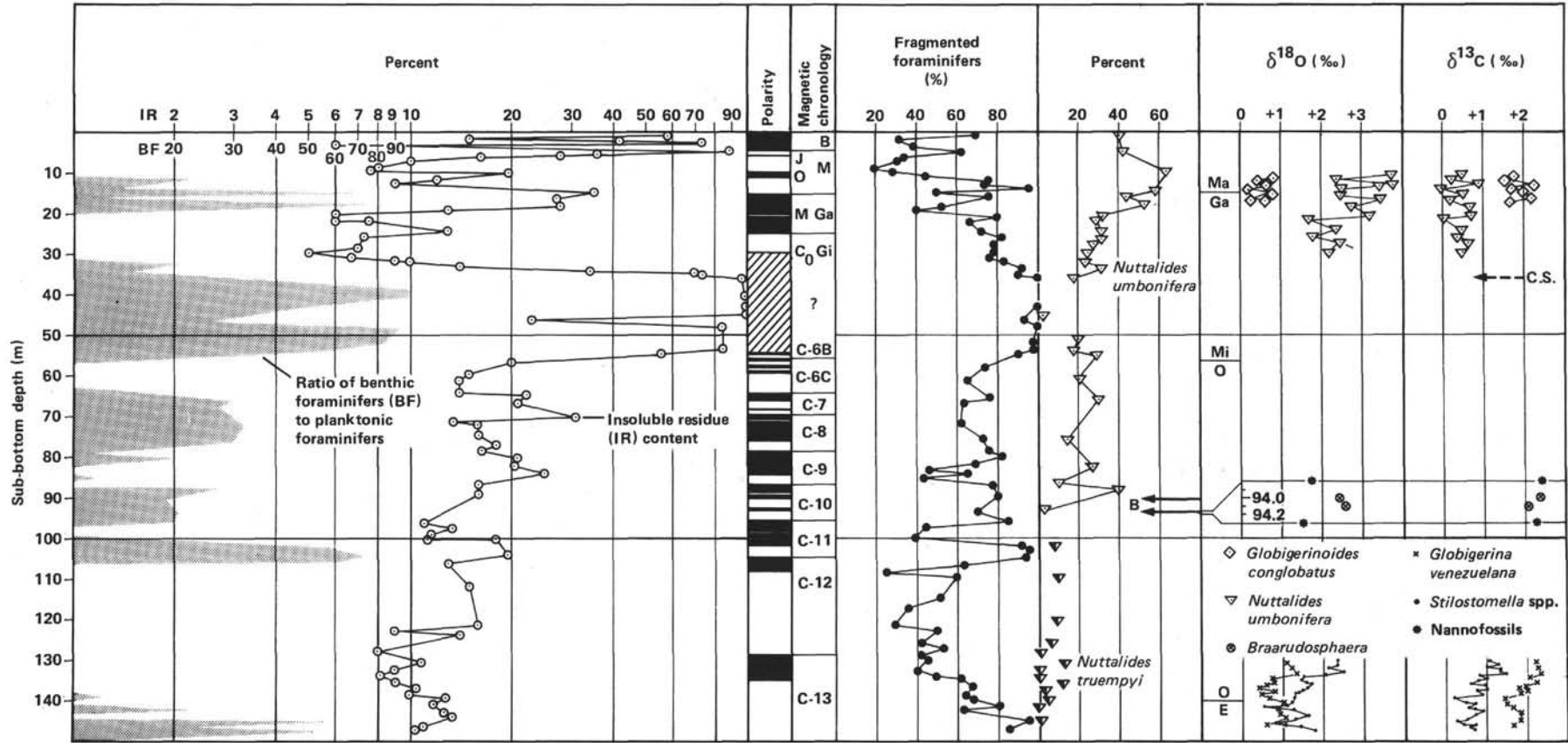


Figure 14. Paleoceanographic data, Hole 522. Polarity as in Fig. 13. Magnetic epochs are Brunhes (B), Matuyama (M), Gauss (Ga), and Gilbert (Gi); magnetic events are Jaramillo (J), Olduvai (O), Mammoth (M), and Cochiti (C<sub>0</sub>).

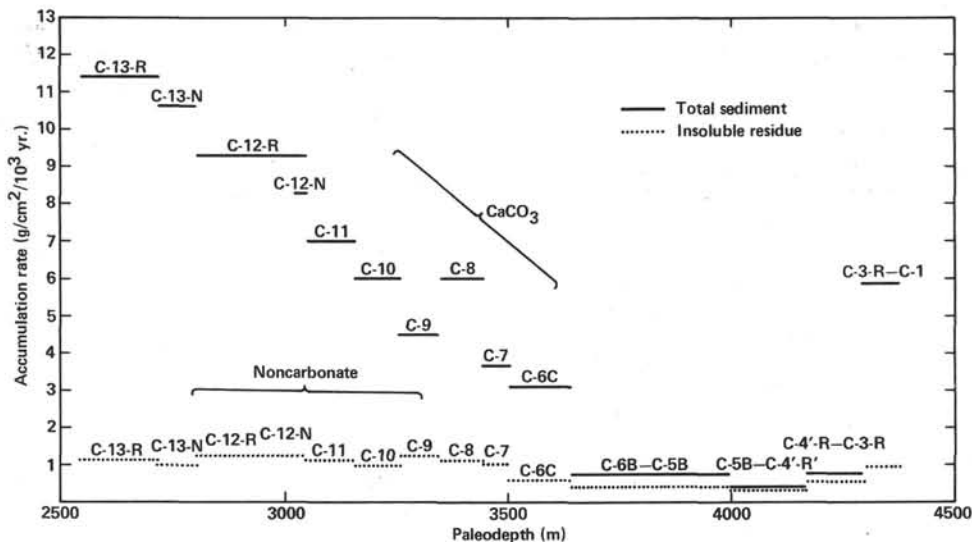


Figure 15. Sedimentation rates, Hole 522.

chapter (Hsü et al., this vol.). More than one chalk layer is present at this site. One 30-cm-thick layer that has been recovered (Core 25; Pl. 3) was deposited during Chron C-10-R2 (~32.5 Ma), the *Globorotalia opima opima* Zone. The chalk consists mainly of pentalites of *Braarudosphaera rosa*, although traces of coccoliths and other nannofossils are present. Comparison of the isotope composition of the *Braarudosphaera* chalk with that of the nannofossil ooze confirms a previous observation by Lloyd and Hsü (1972) that the  $\delta^{18}\text{O}$  of the chalk is similar to that of the middle Oligocene benthic foraminifers and is considerably heavier than that of the planktonic organisms. The two samples at this site give  $\delta^{18}\text{O}$  values of 2.43 and 2.59‰, in contrast to the values of 1.72 and 1.53‰ for the bulk of the nannofossil oozes immediately above and below the chalk. The difference may have resulted from recrystallization in a benthic environment (Lloyd and Hsü, 1972). The carbon-isotope values of all four samples are approximately the same, probably because the partition of carbon isotopes during recrystallization was not temperature sensitive. If the interpretation of recrystallization is correct, the surface and bottom ocean temperatures at this middle-latitude site should have a difference of about 3 or 4°, the same as Boersma and Shackleton (1978) found by analyzing middle Oligocene foraminifer specimens at Site 17; the temperatures should be about 3°C at the bottom and 6° near the surface if no correction is made for the isotopic composition of the seawater.

#### Heat Flow

Three downhole temperature measurements were taken at Site 522. The data indicate that heat flow at Site 522 is 0.3 HFU, much less than that predicted by theoretical models for basement 40 m.y. old.

#### Basalt Basement

Hole 522B penetrated 20 m of basalt. The rock was remarkably unaltered, with samples from several cooling units probably representing pillows and thin flows. The magnetization of the basalts was strong and gave

inclinations that indicated no large northward movement of this site (which is on the African Plate) since the Eocene.

The oldest sediment above the basement belongs to the Nannofossil Zone NP20 (*Sphenolithus pseudoradians*) and to the foraminifer zone *Globorotalia cerroazulensis* s.l. Thus, the basement age extrapolated on the basis of the radiometric dating of paleontological zones (see Odin and Curry, 1981) should be slightly younger than  $37 \pm 1.5$  m.y. On the other hand, the age of the seafloor postulated on the basis of a linear seafloor spreading rate should be 39.2 m.y. The discrepancy is small enough to fall almost within experimental error. On the other hand, this problem is related to the question of the absolute age of the Eocene/Oligocene boundary, so it should not be dismissed lightly.

#### Absolute Ages of Cenozoic Boundaries

The Eocene/Oligocene boundary, as defined by nannofossil zonation, has an age of 37.1 m.y. if we assume (1) a linear rate of seafloor spreading during the Cenozoic and (2) a 66.5-m.y. age for the beginning of the Cenozoic. However, radiometry gives younger ages. W. Glass (pers. comm.) obtained a 34-m.y. age for the Pacific textites found in the sediments immediately below the Eocene/Oligocene boundary defined by radiolaria zonation. Odin and Curry (1981) also indicated that the radiometric age of the base of the Oligocene (base of NP21) should be between 33 and 37 m.y. However, they suggested that the absolute age of the beginning of the Cenozoic may be as young as 63.5 m.y. If we use this minimum age and assume a linear rate of seafloor spreading, the age of the Eocene/Oligocene boundary would be 35.2 m.y. This age would still be a trifle too old to suit Glass but would fall within the range suggested by Odin and Curry. Finally, seafloor spreading rate may not have been absolutely linear. After comparing their time scale with the biostratigraphic dates of DSDP samples, LaBrecque et al. (1977) believed that that assumption might be slightly in error, especially for the Paleogene part of the scale. However, present meth-

ods of determining radiometric ages are not sufficiently accurate to justify basing a magnetostratigraphic scale on a different assumption.

## REFERENCES

- Berger, W. H., and von Rad, U., 1972. Cretaceous and Cenozoic sediments from the Atlantic Ocean. In Hayes, D. E., Pimm, A. C., et al., *Init. Repts. DSDP*, 14: Washington (U.S. Govt. Printing Office), 787-954.
- Boersma, A., and Shackleton, N., 1978. Oxygen and carbon isotope record through the Oligocene, DSDP Site 366, Equatorial Atlantic. In Lancelot, Y., Seibold, E., et al., *Init. Repts. DSDP*, 41: Washington (U.S. Govt. Printing Office), 957-962.
- Bolli, H. M., Ryan, W. B. F., et al., 1978. *Init. Repts. DSDP*, 40: Washington (U.S. Govt. Printing Office).
- , 1975. Oxygen and carbon isotope analyses of Tertiary and Cretaceous microfossils from Shatsky Rise and other sites in the North Pacific Ocean. In Larson, R. L., Moberly, R., et al., *Init. Repts. DSDP*, 32: Washington (U.S. Govt. Printing Office), 509-520.
- Gartner, S., 1973. Absolute chronology of the late Neogene calcareous nannofossil succession in the equatorial Pacific. *Geol. Soc. Am. Bull.*, 24:2021-2033.
- Heirtzler, J. R., Dickson, G. O., Herron, E. M., Pitman, W. C., and LePichon, X., 1968. Marine magnetic anomalies, geomagnetic field reversals, and motions of the ocean floor and continents. *J. Geophys. Res.*, 73:2119-2136.
- Herman, B. M., Langseth, M. G., and Hobart, M. A., 1977. Heat flow in the oceanic crust bounding western Africa. *Tectonophysics*, 41:61-71.
- Horai, K., 1981. Thermal conductivity of sediments and igneous rocks recovered during Deep Sea Drilling Project Leg 60. In Hussong, D. M., Uyeda, S., et al., *Init. Repts. DSDP*, 60: Washington (U.S. Govt. Printing Office), 807-840.
- LaBrecque, J. L., Kent, D. V., and Cande, S. C., 1977. Revised magnetic polarity time scale of Late Cretaceous and Cenozoic time. *Geology*, 5:330-335.
- Lachenbruch, A. H., and Marshall, B. V., 1966. Heat flow through the Arctic Ocean floor—the Canada Basin-Alpha Rise boundary. *J. Geophys. Res.*, 71:1223-1248.
- Lloyd, R. M., and Hsü, K. J., 1972. Stable-isotope investigations of sediments from DSDP III cruise to the South Atlantic. *Sedimentology*, 19:45-58.
- Lowrie, W., Alvarez, W., Napoleone, G., Perch-Nielsen, K., Premoli Silva, I., and Toumarkine, M., in press. Paleogene magnetic stratigraphy in Umbrian pelagic carbonate rocks: the Contessa sections, Gubbio. *Geol. Soc. Am. Bull.*
- Mankinen, E. A., and Dalrymple, G. B., 1979. Revised geomagnetic polarity time scale for interval 0-5 m.y.B.P. *J. Geophys. Res.*, 84:615-626.
- Odin, G. S., and Curry, D., 1981. L'échelle numérique des temps paléogènes en 1981. *C.R. Acad. Sci. Paris, Ser. II*, 293:1003-1006.
- Shackleton, N. J., and Kennett, J. P., 1975. Paleotemperature history of the Cenozoic and the initiation of Antarctic glaciation: oxygen and carbon isotope analyses in DSDP Sites 277, 279, and 281. In Kennett, J. P., Houtz, R. E., et al., *Init. Repts. DSDP*, 29: Washington (U.S. Govt. Printing Office), 743-755.

Date of Initial Receipt: August 12, 1982

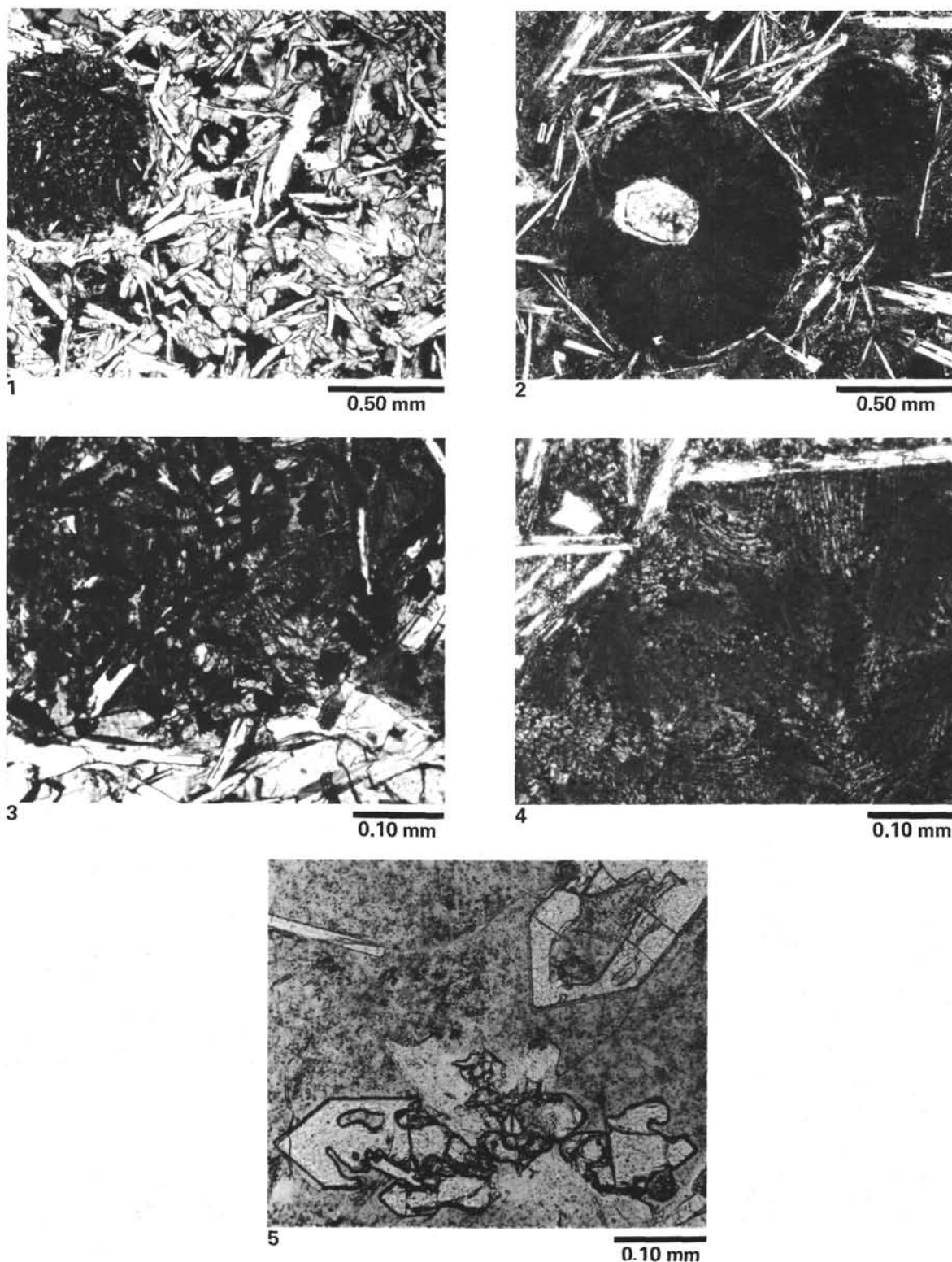


Plate 1. Photomicrographs of igneous rocks, Site 522. 1. Segregation vesicles in seriate, subophitic to intergranular, intersertal basalt. Interior of Unit 5, flow, Sample 522B-4-1, 4-6 cm (Piece 1A). 2. Segregation vesicles of microphyric, plumose dendritic (Zone 5) basalt. Lower part of pillow, Unit 3, Sample 522B-3-3, 135-137 cm (Piece 4B). 3. Detail of segregation vesicle in coarser rock. Abundant ilmenitic and magnetitic opaque grains, sparse plagioclase microlites and dendritic pyroxene matrix. Same sample as in Fig. 1. 4. Detail of segregation vesicle in finer rock. Relatively minor equant opaque grains, abundant dendritic pyroxene and spherulite matrix. Same sample as in Fig. 2. 5. Skeletal (re-sorbed?) olivine in glass. Glass, Zone 1. Lower rim of pillow, Unit 4, Sample 522B-3-3, 138-142 cm (Piece 4C).

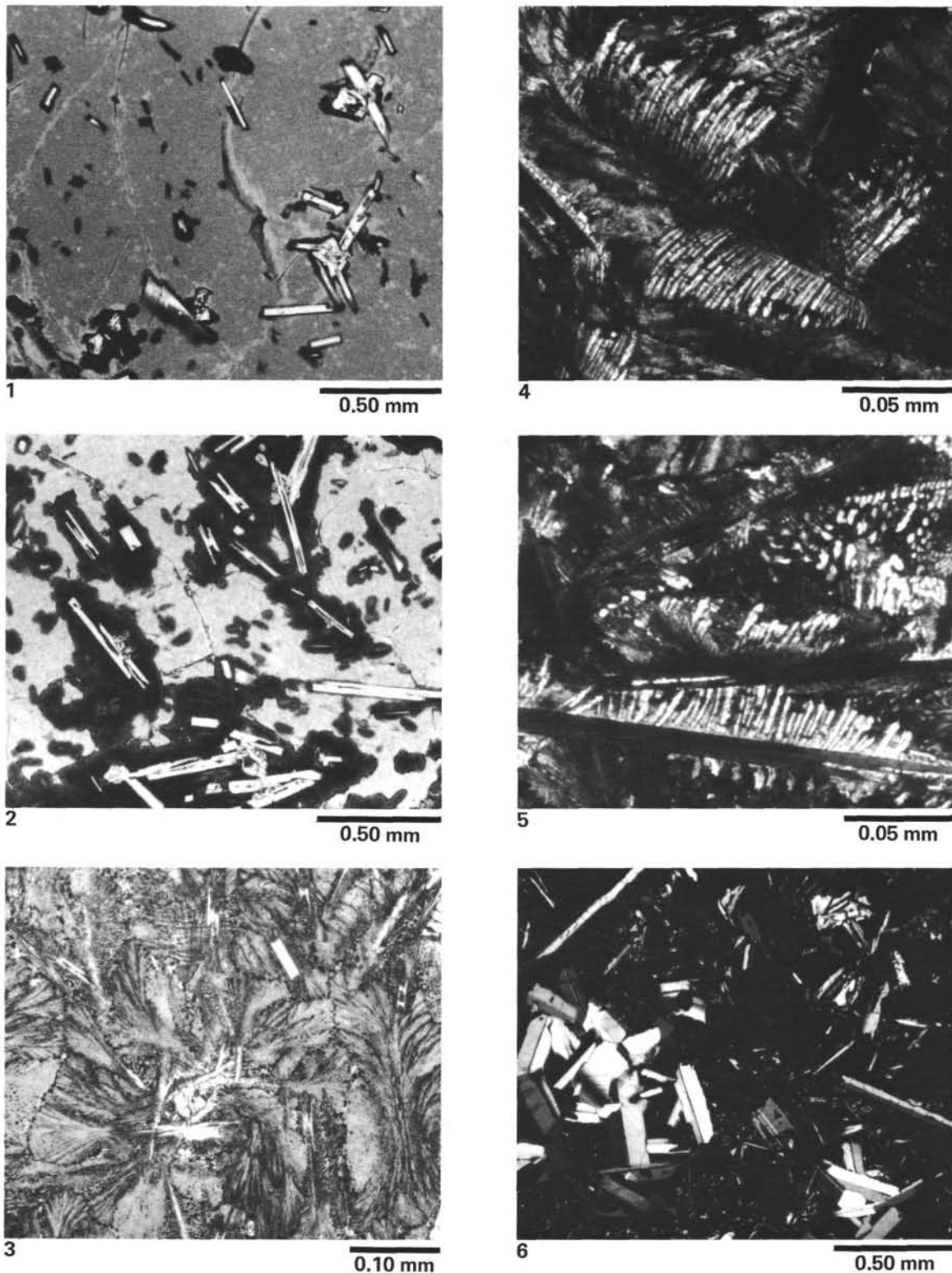
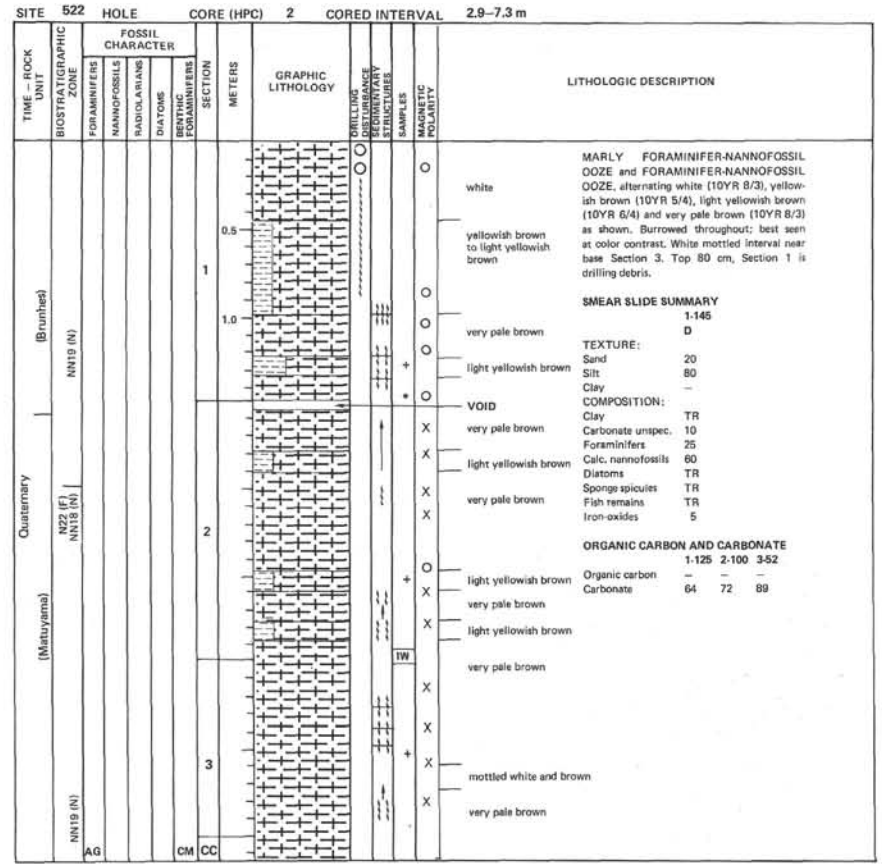
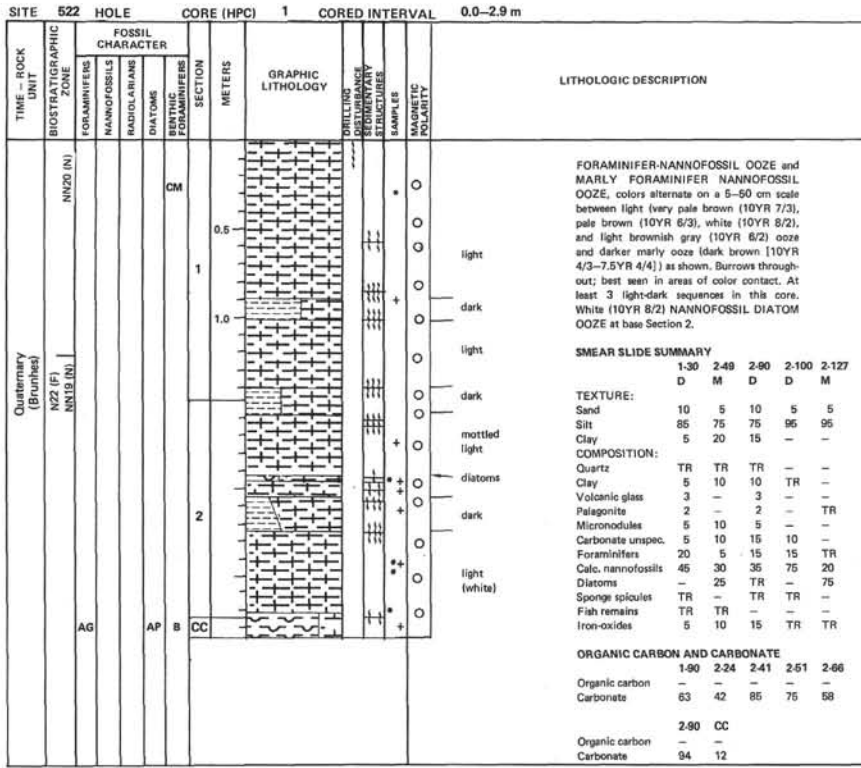


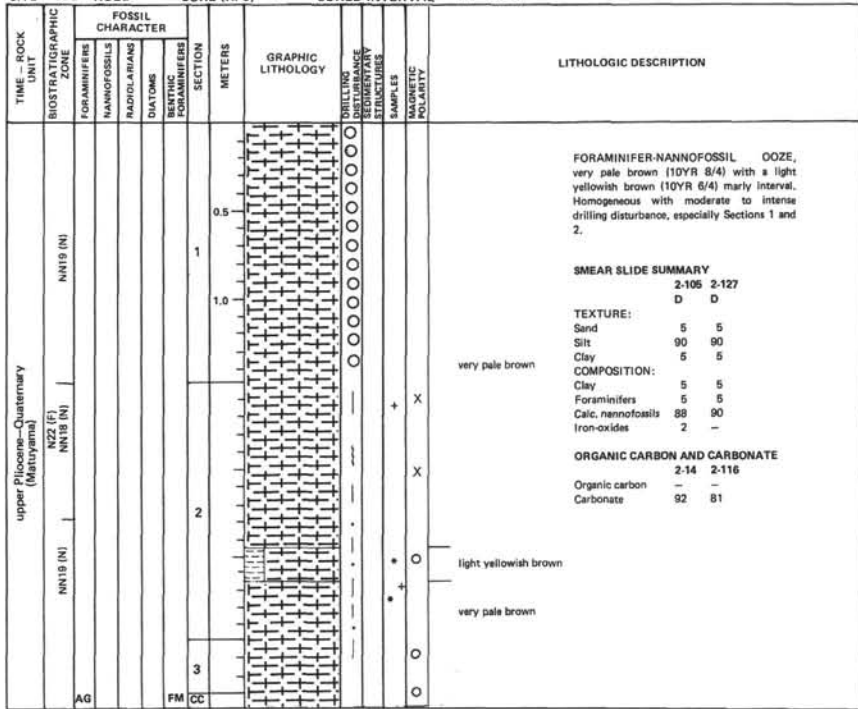
Plate 2. Photomicrographs of igneous rocks, Site 522. 1. Glassy, Zone 1, grading toward glassy spherulitic, Zone 2. Spherulitic rims on second generation plagioclase microphenocrysts. Top of pillow, Unit 4, Sample 522B-3-3, 138-142 cm (Piece 4C). 2. Glassy spherulitic, Zone 2, second generation plagioclase microphenocrysts and spherulites. Same sample as in Figure 1. 3. Sheaf-shaped bow-tie and fan-shaped spherulites, fine quench texture, Zone 4, sheaf-shaped spherulitic. Top of flow, Unit 7, Sample 522B-4-2, 68-71 cm (Piece 2). 4. Plumose dendrites, fine quench texture, Zone 5, plumose dendritic. Top of pillow, Unit 3, Sample 522B-3-3, 76-78 cm (Piece 2D). 5. Comb-shaped dendrites, fine quench texture, Zone 5, plumose dendritic. Same sample as in Fig. 1. 6. First generation (stubby, solid, and glomerocrystic) and second generation (elongate, thin, skeletal, and single) plagioclase microphenocrysts. Interior Unit 7, flow, Sample 522B-4-2, 93-95 cm (Piece 3A). Crossed nichols.



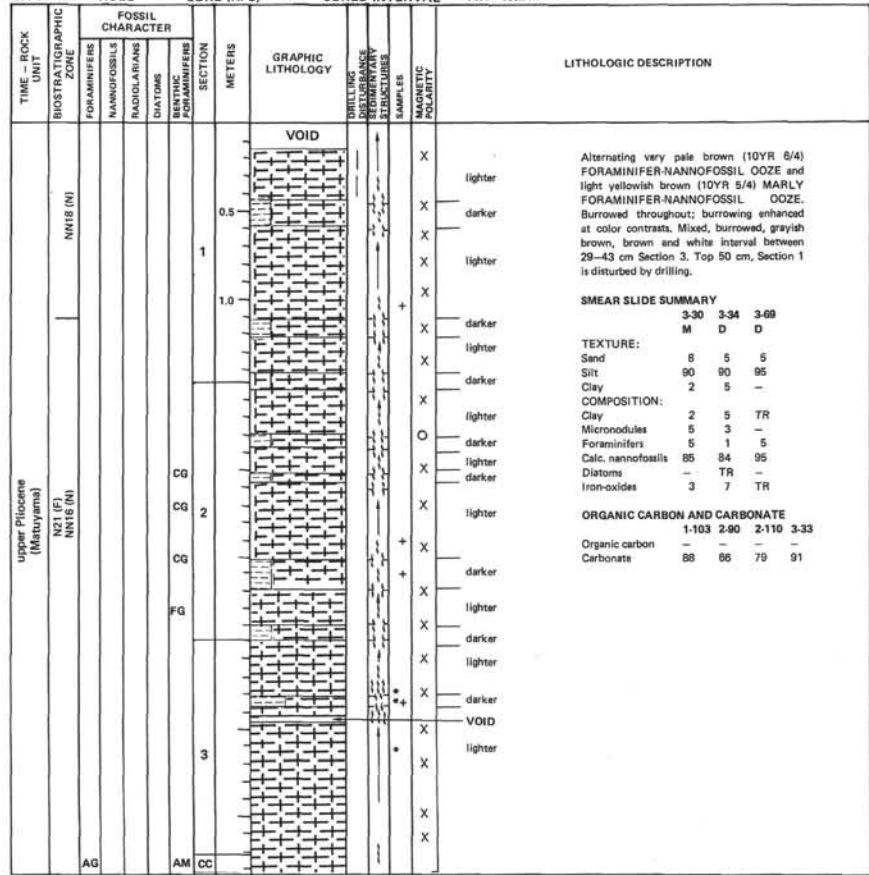
Plate 3. Core photo of *Braarudosphaera* ooze (white layer) intercalated in normal pelagic ooze, Site 522.



SITE 522 HOLE CORE (HPC) 3 CORED INTERVAL 7.3-10.8 m



SITE 522 HOLE CORE (HPC) 4 CORED INTERVAL 10.8-15.2 m









SITE 522 HOLE CORE (HPC) 11 CORED INTERVAL 41.2-44.2 m

TIME - ROCK UNIT	BIOSTRATIGRAPHIC ZONE				SECTION	METERS	GRAPHIC LITHOLOGY	POLLINIFER	SEDIMENTARY STRUCTURES	SAMPLES	MAGNETIC POLARITY	LITHOLOGIC DESCRIPTION
	FORAMNIFERS	NANNOFOSSILS	RADIOLARIANS	DIATOMS								
	Barren (F) Indeterminate (N)				1	0.5 - 1.0						<p>CLAY, dark brown (7.5YR 3/2) to dark reddish brown (5YR 3/2), homogeneous throughout. Top 50-70 cm disturbed by drilling.</p> <p><b>ORGANIC CARBON AND CARBONATE</b>                      1-135                      Organic carbon -                      Carbonate 0</p>
					2							
					CC							

SITE 522 HOLE CORE (HPC) 12 CORED INTERVAL 44.2-48.2 m

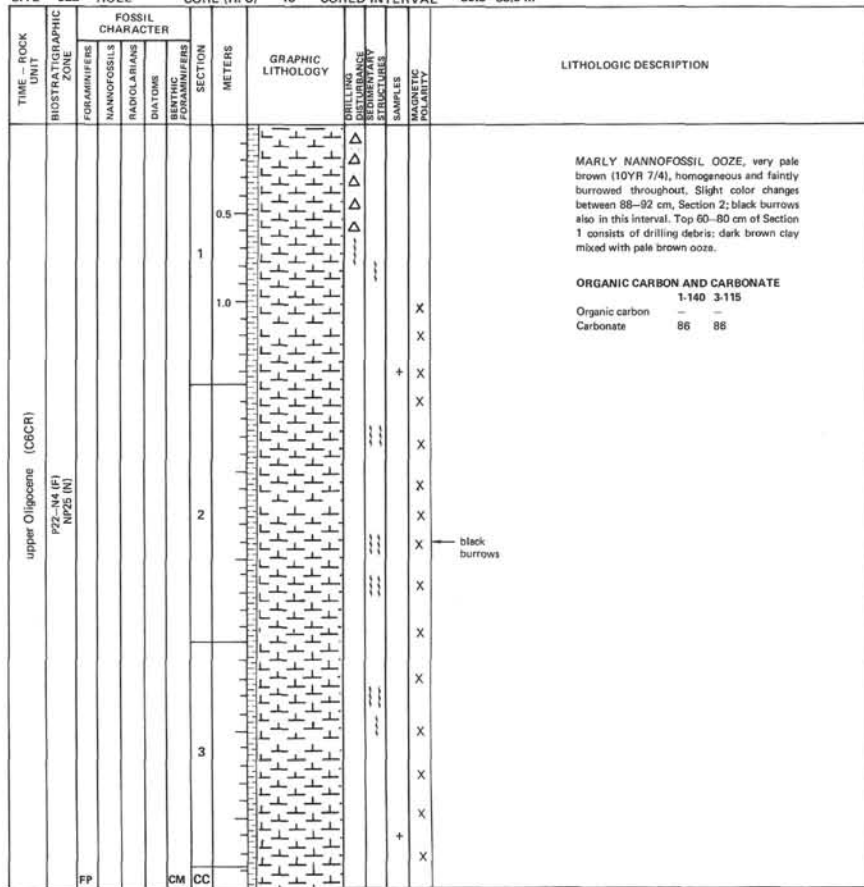
TIME - ROCK UNIT	BIOSTRATIGRAPHIC ZONE				SECTION	METERS	GRAPHIC LITHOLOGY	POLLINIFER	SEDIMENTARY STRUCTURES	SAMPLES	MAGNETIC POLARITY	LITHOLOGIC DESCRIPTION
	FORAMNIFERS	NANNOFOSSILS	RADIOLARIANS	DIATOMS								
	Barren (F) Indeterminate (N)				1	0.5 - 1.0						<p>Dark reddish brown (5YR 3/3) CLAY grading down core to brown (10YR 5/3) and yellowish brown NANNOFOSSIL CLAY and MARLY NANNOFOSSIL DOZE in Section 2, then to dark brown (7.5YR 4/4-5/4) NANNOFOSSIL CLAY in base Section 3. Burrows common especially noticeable where color changes occur. Darker colors match lower carbonate contents. Top 25 cm, Section 1 disturbed.</p> <p><b>SMEAR SLIDE SUMMARY</b>                      1-148 2-117                      D D                      TEXTURE:                      Sand 5 5                      Silt 85 85                      Clay 10 10                      COMPOSITION:                      Quartz TR TR                      Clay 3 10                      Volcanic glass TR 5                      Palagonite TR 5                      Micronodules 5 5                      Carbonate unspec. 5 5                      Calc. nanofossils 85 60                      Diatoms TR TR                      Sponge spicules - TR                      Fish remains TR -                      Iron-oxides 2 10</p> <p><b>ORGANIC CARBON AND CARBONATE</b>                      1-56 2-19 3-26                      Organic carbon - - -                      Carbonate 0 77 15</p>
					2							
					3							
					CC							

SITE 522 HOLE		CORE (HPC) 13		CORED INTERVAL 48.2-50.7 m			
TIME - ROCK UNIT	BIOSTRATIGRAPHIC ZONE	FOSSIL CHARACTER		SECTION	METERS	GRAPHIC LITHOLOGY	LITHOLOGIC DESCRIPTION
		FORAMINIFERS	NANNOFOSSILS				
		RADIOLARIANS	DIATOMS	BIOTIC FORAMINIFERS			
Miocene	NW3-5 (N)			CC			Trace of CLAY in Core-Catcher.

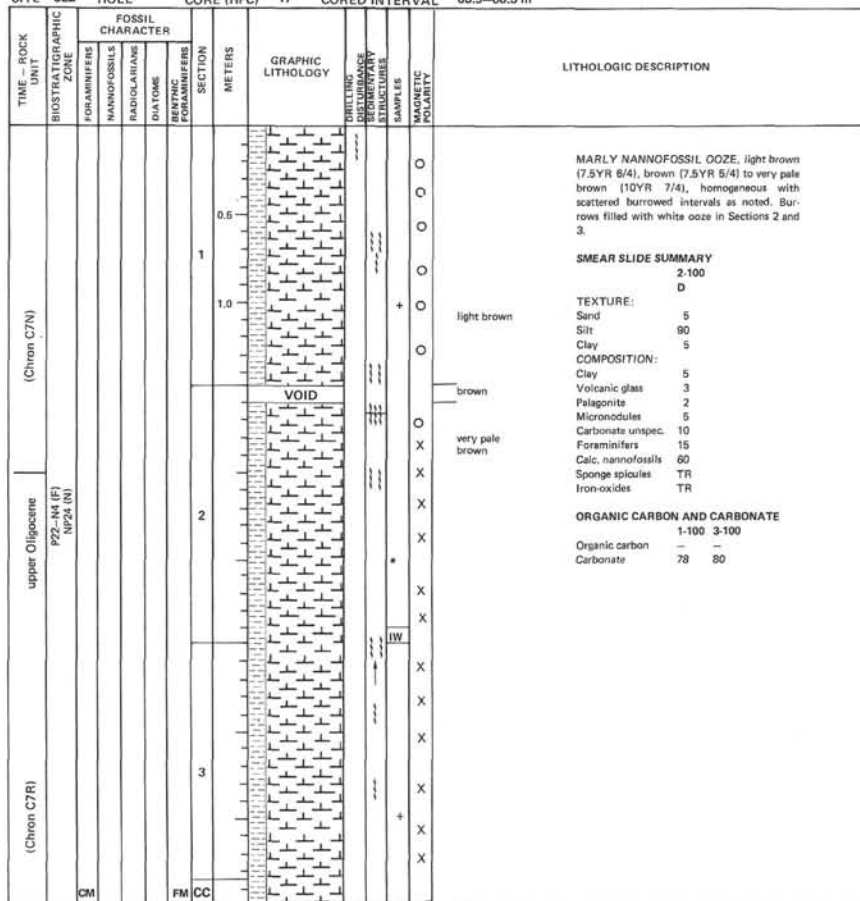
SITE 522 HOLE		CORE (HPC) 14		CORED INTERVAL 50.7-55.1 m			
TIME - ROCK UNIT	BIOSTRATIGRAPHIC ZONE	FOSSIL CHARACTER		SECTION	METERS	GRAPHIC LITHOLOGY	LITHOLOGIC DESCRIPTION
		FORAMINIFERS	NANNOFOSSILS				
		RADIOLARIANS	DIATOMS	BIOTIC FORAMINIFERS			
lower Miocene	NW-8 (F) NW2-3 (N)						CLAY and NANNOFOSSIL CLAY, dark reddish brown (5YR 3/4) to dark brown (7.5YR 3/4) and brown (7.5YR 4/6), homogeneous. Changes to yellowish brown (10YR 5/4), burrowed MARLY NANNOFOSSIL OOZE near base Section 3. Some drilling disturbance in Sections 1 and 2.
							<p><b>SMEAR SLIDE SUMMARY</b></p> <p>1-111 2-127</p> <p>D D</p> <p>TEXTURE:</p> <p>Sand 15 10</p> <p>Silt 55 70</p> <p>Clay 30 20</p> <p>COMPOSITION:</p> <p>Quartz TR TR</p> <p>Clay 25 15</p> <p>Volcanic glass 5 5</p> <p>Palagonite 10 -</p> <p>Micronodules 10 5</p> <p>Zeolite 5 -</p> <p>Carbonate unspec. 10 5</p> <p>Calc. nannofossils 20 55</p> <p>Sponge spicules TR TR</p> <p>Fish remains 5 5</p> <p>Iron-oxides 15 10</p> <p><b>ORGANIC CARBON AND CARBONATE</b></p> <p>2-111 3-90</p> <p>Organic carbon - -</p> <p>Carbonate 16 44</p>
							<p>dark reddish brown</p> <p>brown to dark brown</p> <p>dark reddish brown</p> <p>brown</p> <p>dark reddish brown</p> <p>brown</p> <p>yellowish brown</p>

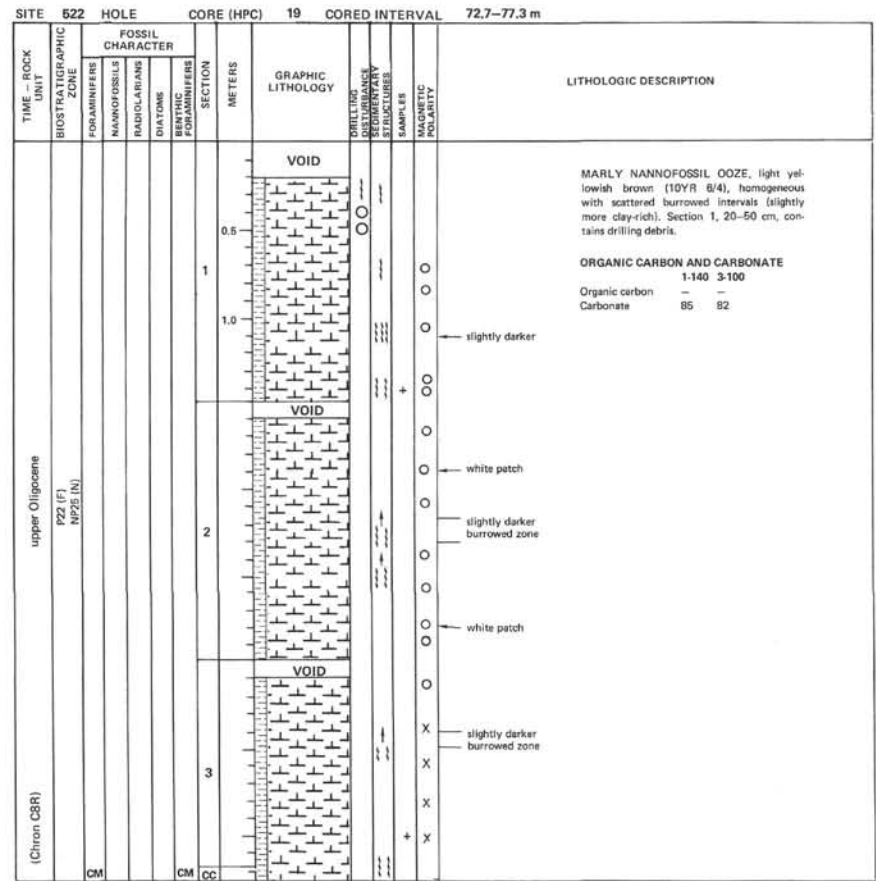
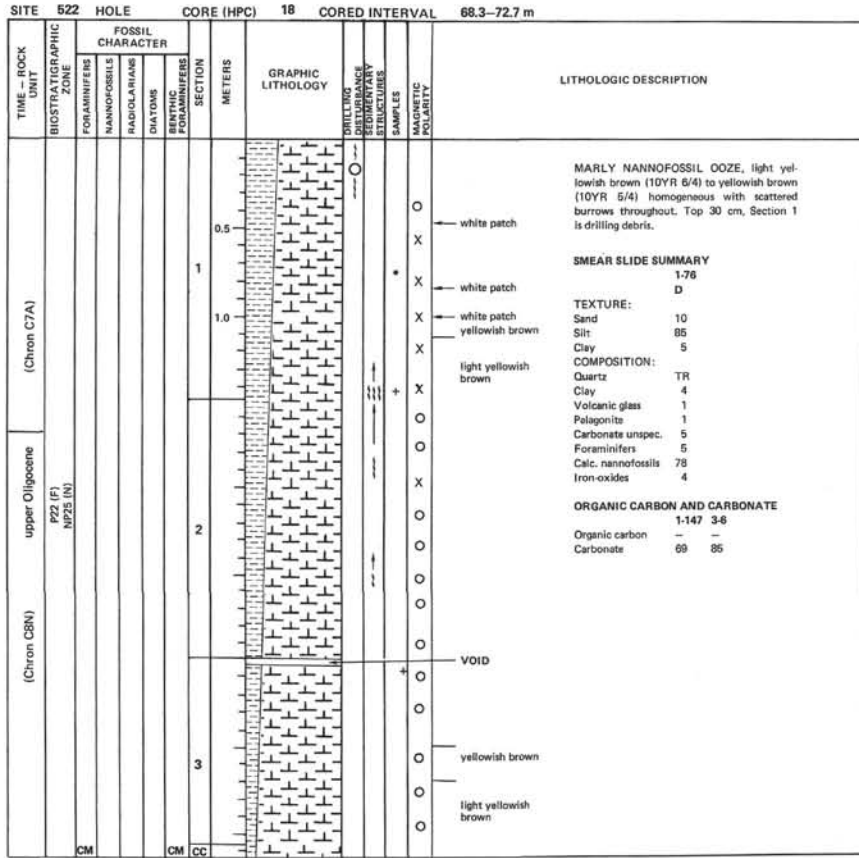
SITE 522 HOLE		CORE (HPC) 15		CORED INTERVAL 55.1-59.5 m			
TIME - ROCK UNIT	BIOSTRATIGRAPHIC ZONE	FOSSIL CHARACTER		SECTION	METERS	GRAPHIC LITHOLOGY	LITHOLOGIC DESCRIPTION
		FORAMINIFERS	NANNOFOSSILS				
		RADIOLARIANS	DIATOMS	BIOTIC FORAMINIFERS			
lower Miocene	NN1 (N)						Light yellowish brown (10YR 6/4) MARLY NANNOFOSSIL OOZE grading down core to very pale brown (10YR 7/4) MARLY NANNOFOSSIL OOZE. Burrows common in Sections 1 and 2. Thin (3 cm) layer of laminated light gray (10YR 7/2) ooze in Section 1. Top 40 cm of core is drilling debris.
							<p><b>SMEAR SLIDE SUMMARY</b></p> <p>1-90 1-126</p> <p>M D</p> <p>TEXTURE:</p> <p>Sand 10 10</p> <p>Silt 75 75</p> <p>Clay 15 15</p> <p>COMPOSITION:</p> <p>Quartz TR TR</p> <p>Clay 10 10</p> <p>Volcanic glass 5 5</p> <p>Palagonite 5 -</p> <p>Micronodules 10 10</p> <p>Carbonate unspec. 10 5</p> <p>Foraminifers 5 5</p> <p>Calc. nannofossils 50 60</p> <p>Sponge spicules TR TR</p> <p>Fish remains TR TR</p> <p>Iron-oxides 5 5</p> <p><b>ORGANIC CARBON AND CARBONATE</b></p> <p>1-126 3-126</p> <p>Organic carbon - -</p> <p>Carbonate 81 85</p>
							<p>light yellowish brown</p> <p>light gray layer</p> <p>light yellowish brown</p> <p>VOID</p> <p>very pale brown</p> <p>brown</p> <p>very pale brown</p>

SITE 522 HOLE CORE (HPC) 16 CORED INTERVAL 59.5-63.9 m



SITE 522 HOLE CORE (HPC) 17 CORED INTERVAL 63.9-68.3 m





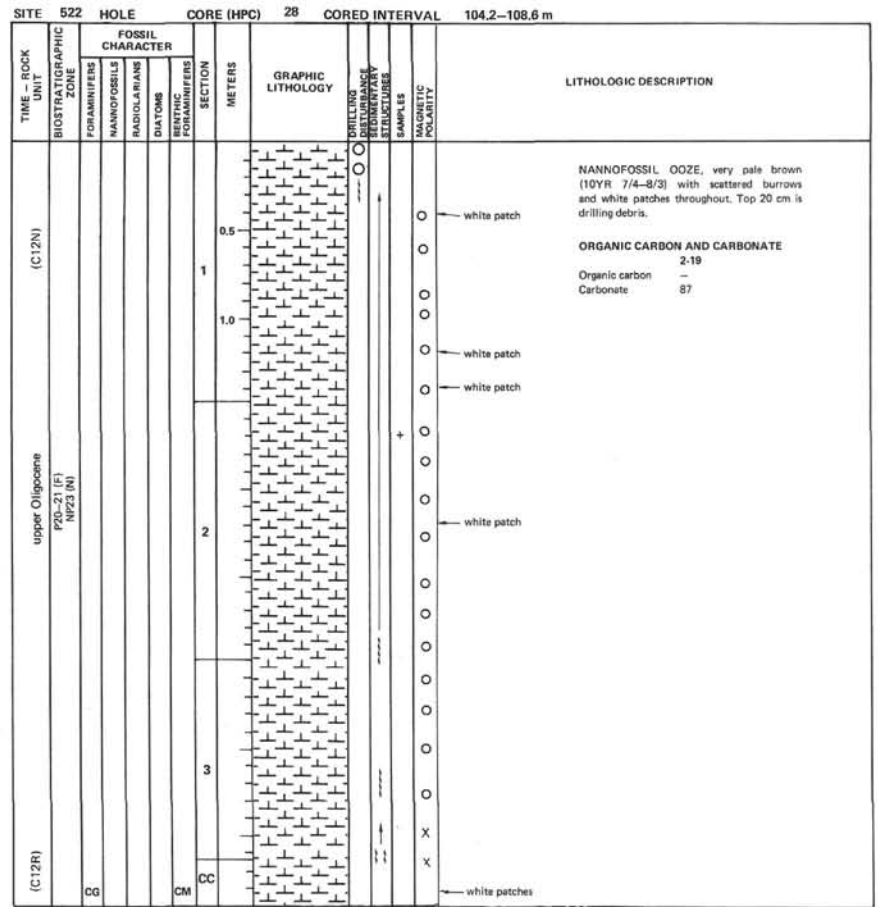
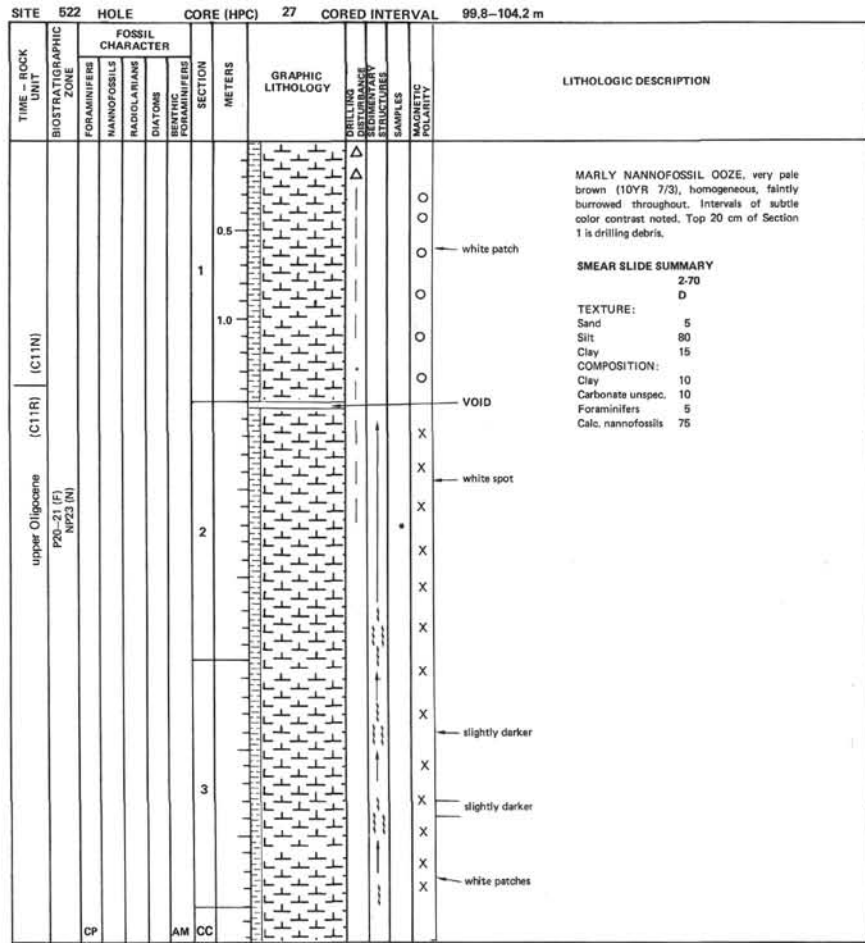


SITE 522		HOLE		CORE (HPC)		22		CORED INTERVAL		85.7-90.1 m		
TIME - ROCK UNIT	BIOSTRATIGRAPHIC ZONE	FOSSIL CHARACTER				SECTION	METERS	GRAPHIC LITHOLOGY	DRILLING DISTURBANCE STRUCTURES	SAMPLES	MAGNETIC POLARITY	LITHOLOGIC DESCRIPTION
		FORAMINIFERS	NANNOFOSSILS	RADIOLARIANS	DIATOMS							
upper Oligocene (Chron C10N)	P20-21 (F) NP23 (N)						0.5	VOID				<p>MARLY NANNOFOSSIL OOZE, light yellowish brown (10YR 6/4), homogeneous with scattered burrows. Several large vertical burrows filled with darker ooze in Section 2, 116-131 cm. Top 30 cm, Section 1 is disturbed.</p> <p><b>SMEAR SLIDE SUMMARY</b> 3-113 D</p> <p><b>TEXTURE:</b> Sand 1 Silt 90 Clay 10</p> <p><b>COMPOSITION:</b> Clay 10 Volcanic glass TR Calc. nannofossils 88 Iron-oxides 2</p> <p><b>ORGANIC CARBON AND CARBONATE</b> 2.137 3-8 Organic carbon - - Carbonate 84 84</p>
							1.0	VOID				
(C10R)	NP23 (N)						2	VOID				<p>white patch</p> <p>large vertical burrows</p> <p>VOID</p>
							3					

SITE 522		HOLE		CORE (HPC)		23		CORED INTERVAL		90.1-91.6 m		
TIME - ROCK UNIT	BIOSTRATIGRAPHIC ZONE	FOSSIL CHARACTER				SECTION	METERS	GRAPHIC LITHOLOGY	DRILLING DISTURBANCE STRUCTURES	SAMPLES	MAGNETIC POLARITY	LITHOLOGIC DESCRIPTION
		FORAMINIFERS	NANNOFOSSILS	RADIOLARIANS	DIATOMS							
upper Oligocene	P20-21 (F) NP23 (N)	CP				FM						<p>Trace of light yellowish brown (10YR 6/4) NANNOFOSSIL OOZE with scattered patches of white (10YR 8/1) NANNOFOSSIL (BRAARUDOSPHAERA) OOZE in Core-Catcher.</p> <p><b>SMEAR SLIDE SUMMARY</b> CC M</p> <p><b>TEXTURE:</b> Sand - Silt 100 Clay -</p> <p><b>COMPOSITION:</b> Carbonate unsp. 96 Calc. nannofossils 5 Iron-oxides TR</p>

SITE 522		HOLE		CORE (HPC)		24		CORED INTERVAL		91.6-91.6 m		
TIME - ROCK UNIT	BIOSTRATIGRAPHIC ZONE	FOSSIL CHARACTER				SECTION	METERS	GRAPHIC LITHOLOGY	DRILLING DISTURBANCE STRUCTURES	SAMPLES	MAGNETIC POLARITY	LITHOLOGIC DESCRIPTION
		FORAMINIFERS	NANNOFOSSILS	RADIOLARIANS	DIATOMS							
Oligocene	NP23 (N)											Trace of MARLY NANNOFOSSIL OOZE in Core-Catcher.













SITE 522 HOLE CORE (HPC) 37 CORED INTERVAL 139.7-143.7 m

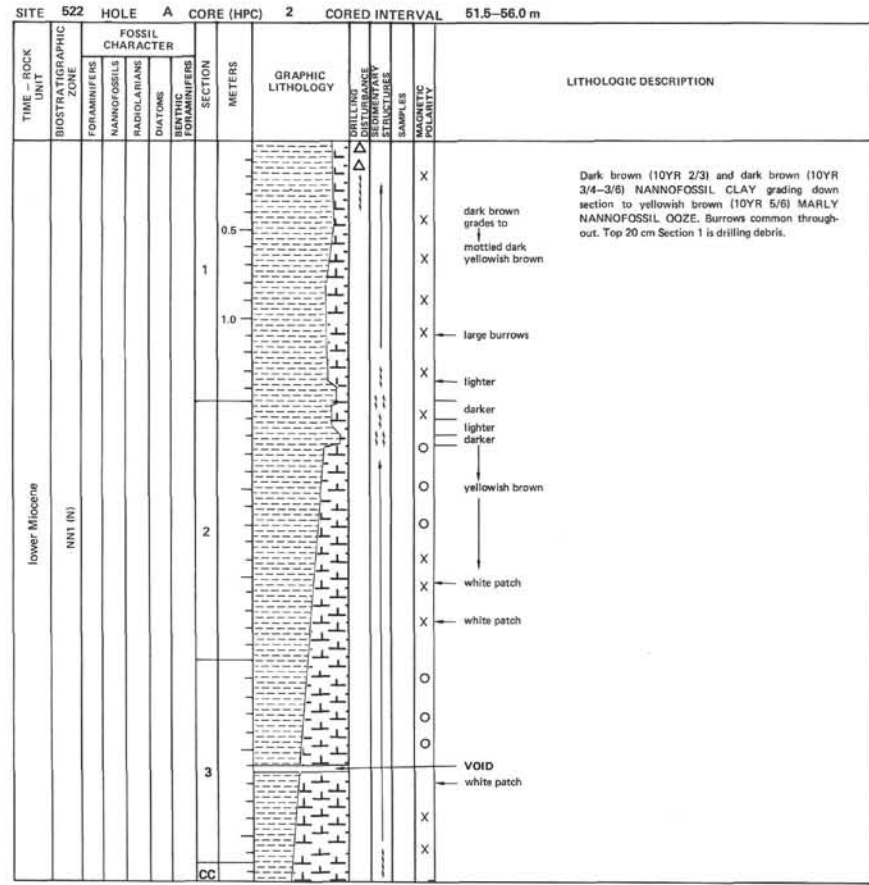
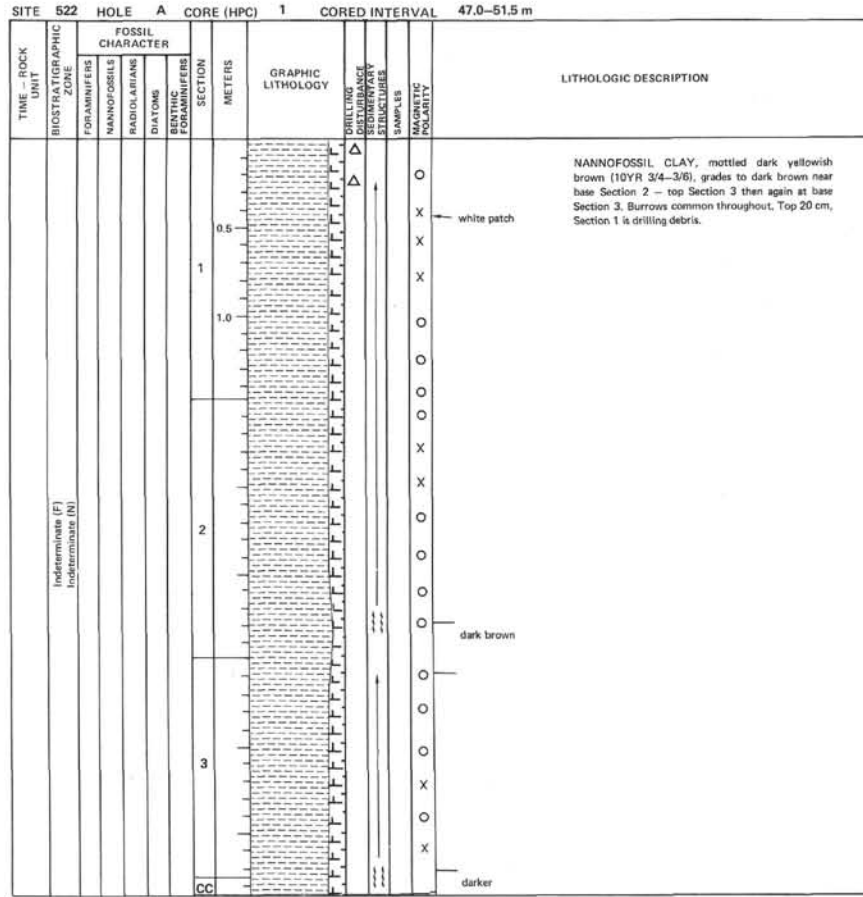
TIME - ROCK UNIT	BIOSTRATIGRAPHIC ZONE	FOSSIL CHARACTER				SECTION	METERS	GRAPHIC LITHOLOGY	DRILLING DISTURBANCE	SEDIMENTARY STRUCTURES	SAMPLES	MAGNETIC POLARITY	LITHOLOGIC DESCRIPTION		
		FORAMINIFERS	NANNOFOSSILS	RADIOLARIANS	DIATOMS										
upper Eocene	P16 (F) NP20 (N)	CG										<p>NANNOFOSSIL OOZE, yellowish brown (10YR 5/4), homogeneous, burrowed throughout. Top 50 cm, Section 1 is drilling debris.</p> <p><b>SMEAR SLIDE SUMMARY</b> 1-135 D</p> <p>TEXTURE: Sand 3 Silt 92 Clay 5</p> <p>COMPOSITION: Clay 5 Micronodules 1 Foraminifers TR Calc. nannofossils 94</p> <p><b>ORGANIC CARBON AND CARBONATE</b> 3-36 Organic carbon - Carbonate 88</p>			
													1	0.5	X
													1.0	X	
2										<p>VOID</p>	<p>white patch</p>				
												2	X		
3										<p>VOID</p>	<p>+</p>				
												3	X		

SITE 522 HOLE CORE (HPC) 38 CORED INTERVAL 143.7-147.7 m

TIME - ROCK UNIT	BIOSTRATIGRAPHIC ZONE	FOSSIL CHARACTER				SECTION	METERS	GRAPHIC LITHOLOGY	DRILLING DISTURBANCE	SEDIMENTARY STRUCTURES	SAMPLES	MAGNETIC POLARITY	LITHOLOGIC DESCRIPTION		
		FORAMINIFERS	NANNOFOSSILS	RADIOLARIANS	DIATOMS										
upper Eocene	P16 (F) NP20 (N)	CG										<p>NANNOFOSSIL OOZE, yellowish brown (10YR 5/4), homogeneous, slightly bioturbated throughout.</p> <p><b>ORGANIC CARBON AND CARBONATE</b> 2-89 Organic carbon - Carbonate 90</p>			
													1	0.5	X
													1.0	X	
2										<p>VOID</p>	<p>+</p>				
												2	X		
3										<p>VOID</p>	<p>+</p>				
												3	X		

SITE 522 HOLE CORE (HPC) 39 CORED INTERVAL 147.7-148.7 m

TIME - ROCK UNIT	BIOSTRATIGRAPHIC ZONE	FOSSIL CHARACTER				SECTION	METERS	GRAPHIC LITHOLOGY	DRILLING DISTURBANCE	SEDIMENTARY STRUCTURES	SAMPLES	MAGNETIC POLARITY	LITHOLOGIC DESCRIPTION
		FORAMINIFERS	NANNOFOSSILS	RADIOLARIANS	DIATOMS								
upper Eocene	NP20 (N)												Trace of yellowish brown (10YR 5/4) NANNOFOSSIL OOZE in Core-Catcher.



SITE 522		HOLE A		CORE (HPC) 3		CORED INTERVAL 56.0-60.5 m					
TIME - ROCK UNIT	BIOSTRATIGRAPHIC ZONE	FOSSIL CHARACTER				METERS	GRAPHIC LITHOLOGY	DRILLING DISTURBANCE UNDESIRABLE STRUCTURE	SAMPLES	MAGNETIC POLARITY	LITHOLOGIC DESCRIPTION
		FORAMINIFERS	NANNOFOSSILS	RADIOLARIANS	DIATOMS						
upper Oligocene	NP25 INJ										
						0.5					
						1					
						1.0					
						2					
						3					
						CC					

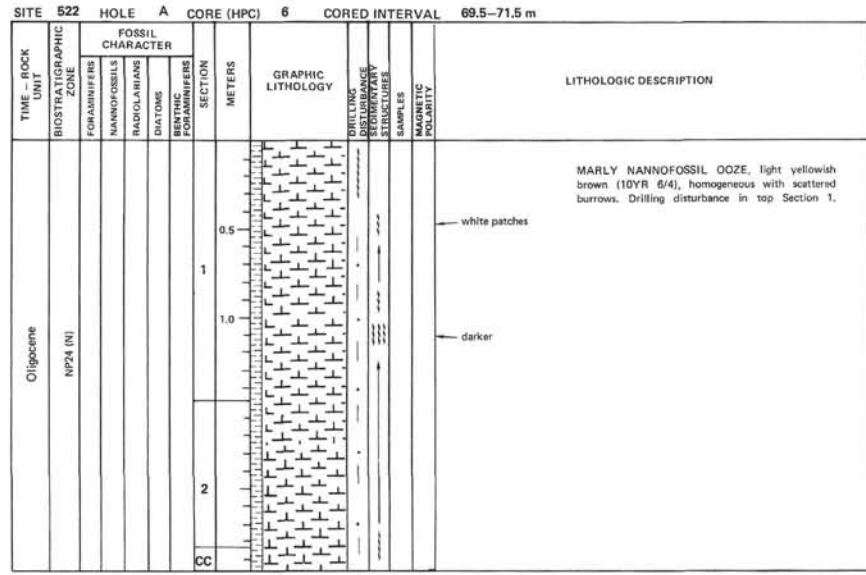
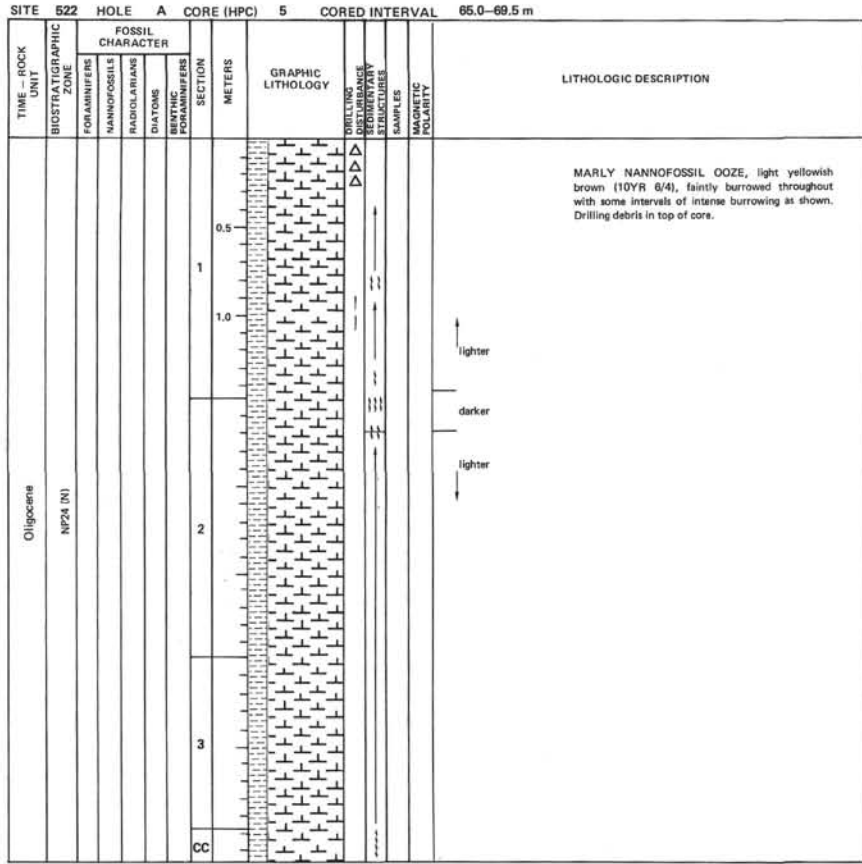
MARLY NANNOFOSSIL OOZE, yellowish brown (10YR 6/4), homogeneous with scattered burrows. Thin very pale brown layer of ooze occurs in Section 1. At 60 cm in Section 2 a semi-circular patch of white ooze rimmed with gray ooze occurs; diameter of patch is approximately 5 cm - possible reduction in top of core as marked.

very pale brown layer

"haloed" reduction patch

SITE 522		HOLE A		CORE (HPC) 4		CORED INTERVAL 60.5-65.0 m					
TIME - ROCK UNIT	BIOSTRATIGRAPHIC ZONE	FOSSIL CHARACTER				METERS	GRAPHIC LITHOLOGY	DRILLING DISTURBANCE UNDESIRABLE STRUCTURE	SAMPLES	MAGNETIC POLARITY	LITHOLOGIC DESCRIPTION
		FORAMINIFERS	NANNOFOSSILS	RADIOLARIANS	DIATOMS						
upper Oligocene	NP25 INJ										
						0.5					
						1					
						1.0					
						2					
						3					
						CC					

MARLY NANNOFOSSIL OOZE, light yellowish brown (10YR 6/4), homogeneous except for minor burrows noted in Section 1. Drilling disturbance throughout most of Section 1.



SITE 522 HOLE A CORE (HPC) 7 CORED INTERVAL 71.5-77.0 m

TIME - ROCK UNIT	BIOSTRATIGRAPHIC ZONE	FOSSIL CHARACTER				SECTION	METERS	GRAPHIC LITHOLOGY	DRILLING DISTURBANCE	CORRECTION STRUCTURE	SAMPLES	MAGNETIC POLARITY	LITHOLOGIC DESCRIPTION
		FORAMINIFERS	NANNOFOSSILS	RADIOLARIANS	DIATOMS								
Oligocene	NP24 (N)						VOID						<p>MARLY NANNOFOSSIL OOZE, light yellowish brown (10YR 6/4) to yellowish brown (10YR 5/6) with dark yellowish brown ooze in intensely burrowed zones. Burrows common throughout. Ooze fairly homogeneous.</p> <p>white patch</p> <p>darker</p> <p>VOID</p>
					1	0.5							
					2	1.0							
					3								
					CC								

SITE 522 HOLE A CORE (HPC) 8 CORED INTERVAL 77.0-80.5 m

TIME - ROCK UNIT	BIOSTRATIGRAPHIC ZONE	FOSSIL CHARACTER				SECTION	METERS	GRAPHIC LITHOLOGY	DRILLING DISTURBANCE	CORRECTION STRUCTURE	SAMPLES	MAGNETIC POLARITY	LITHOLOGIC DESCRIPTION
		FORAMINIFERS	NANNOFOSSILS	RADIOLARIANS	DIATOMS								
Oligocene	NP24 (N)						VOID						<p>MARLY NANNOFOSSIL OOZE, light yellowish brown (10YR 6/4) with burrowed intervals and scattered white patches (burrows?). Drilling deformation in Section 1.</p>
					1	0.5							
					2	1.0							
					CC								

SITE 522		HOLE A		CORE (HPC) 9		CORED INTERVAL 80.5-84.0 m								
TIME - ROCK UNIT	BIOSTRATIGRAPHIC ZONE	FOSSIL CHARACTER			SECTION	METERS	GRAPHIC LITHOLOGY	DRILLING LOG	BIOPOROSITY	STRUCTURES	SAMPLES	MAGNETIC POLARITY	LITHOLOGIC DESCRIPTION	
		FORAMINIFERS	NANNOFOSSILS	RADOLARIANS										DIATOMS
Oligocene	NP24 (N)					0.5							VOID	
						1								MARLY NANNOFOSSIL OOZE, light yellowish brown (10YR 6/4) grading to very pale brown (10YR 7/4) NANNOFOSSIL OOZE in Section 2. Homogeneous with scattered burrows and white patches.
						1.0								
						2								
						3								
						CC								

SITE 522		HOLE A		CORE (HPC) 10		CORED INTERVAL 84.0-87.5 m								
TIME - ROCK UNIT	BIOSTRATIGRAPHIC ZONE	FOSSIL CHARACTER			SECTION	METERS	GRAPHIC LITHOLOGY	DRILLING LOG	BIOPOROSITY	STRUCTURES	SAMPLES	MAGNETIC POLARITY	LITHOLOGIC DESCRIPTION	
		FORAMINIFERS	NANNOFOSSILS	RADOLARIANS										DIATOMS
Oligocene	NP23 (N)					0.5							NANNOFOSSIL OOZE, very pale brown (10YR 7/4) homogeneous, burrowed throughout. Top 40 cm, Section 1 disturbed by drilling.	
						1								SMEAR SLIDE SUMMARY 1-140 D TEXTURE: Sand 5 Silt 90 Clay 5 COMPOSITION: Quartz TR Clay 5 Volcanic glass 3 Palagonite 2 Micronodules TR Carbonate unspec. 15 Foraminifera 10 Calc. nannofossils 65
						1.0								
						2								
						3								
						CC								

SITE 522 HOLE A CORE (HPC) 11 CORED INTERVAL 87.5-89.5 m

TIME - ROCK UNIT	BIOSTRATIGRAPHIC ZONE	FOSSIL CHARACTER				SECTION	METERS	GRAPHIC LITHOLOGY	DRILLING DISTURBANCE	SEDIMENTARY STRUCTURES	SAMPLES	MAGNETIC POLARITY	LITHOLOGIC DESCRIPTION
		FORAMINIFERS	NANNOFOSSILS	RADIOLARIANS	DIATOMS								
Oligocene	Braarudosphaera ooze (N)					1						<p>NANNOFOSSIL OOZE, light yellowish brown (10YR 6/4) to very pale brown (10YR 7/4), burrowed. Significant drilling deformation. Last 4 cm of core is white (10YR 8/1) Braarudosphaera ooze.</p> <p><b>SMEAR SLIDE SUMMARY</b> 2-45 M</p> <p>TEXTURE: Sand 10 Silt 90 Clay -</p> <p>COMPOSITION: Pelagonite TR Micronodules TR Foraminifers 10 Calc. nannofossils 90</p>	
						2							VOID

SITE 522 HOLE A CORE (HPC) 12 CORED INTERVAL 89.5-91.5 m

TIME - ROCK UNIT	BIOSTRATIGRAPHIC ZONE	FOSSIL CHARACTER				SECTION	METERS	GRAPHIC LITHOLOGY	DRILLING DISTURBANCE	SEDIMENTARY STRUCTURES	SAMPLES	MAGNETIC POLARITY	LITHOLOGIC DESCRIPTION
		FORAMINIFERS	NANNOFOSSILS	RADIOLARIANS	DIATOMS								
Misking (N)						1						<p>NANNOFOSSIL OOZE, very pale brown (10YR 7/4), burrowed. White (10YR 8/1) BRAARUDOSPHAERA OOZE in Core-Catcher and between 23-30 cm, Section 1. Drilling debris 0-23 cm of Section 1; intense to slight disturbance below.</p>	
						CC							

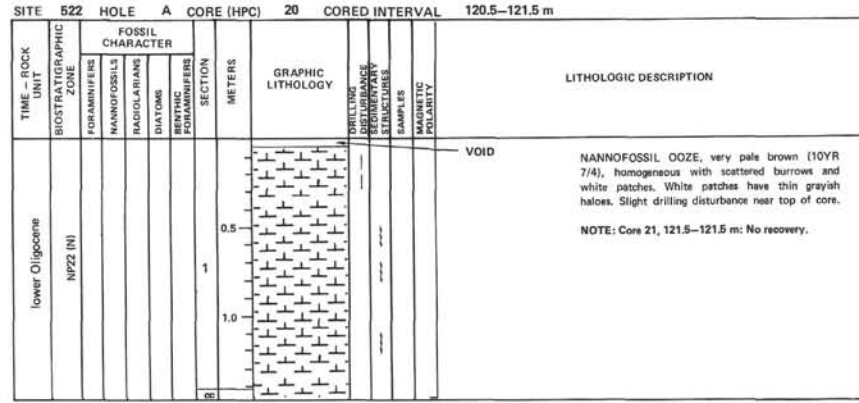
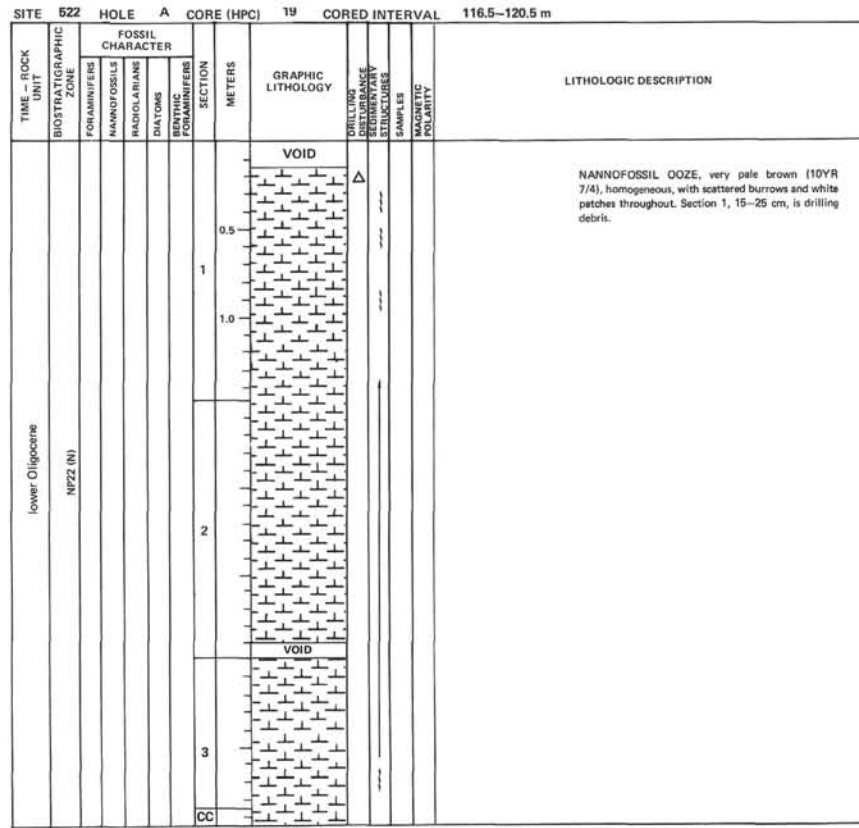
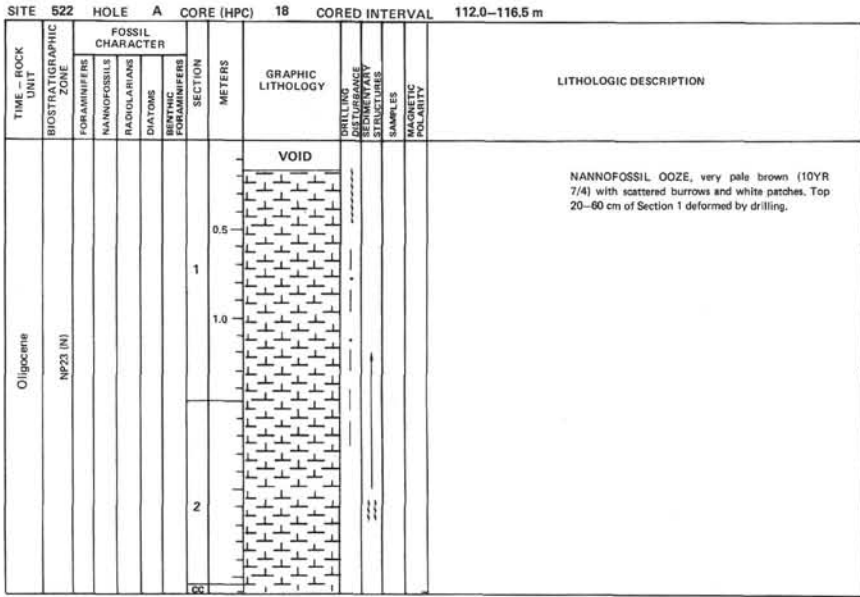
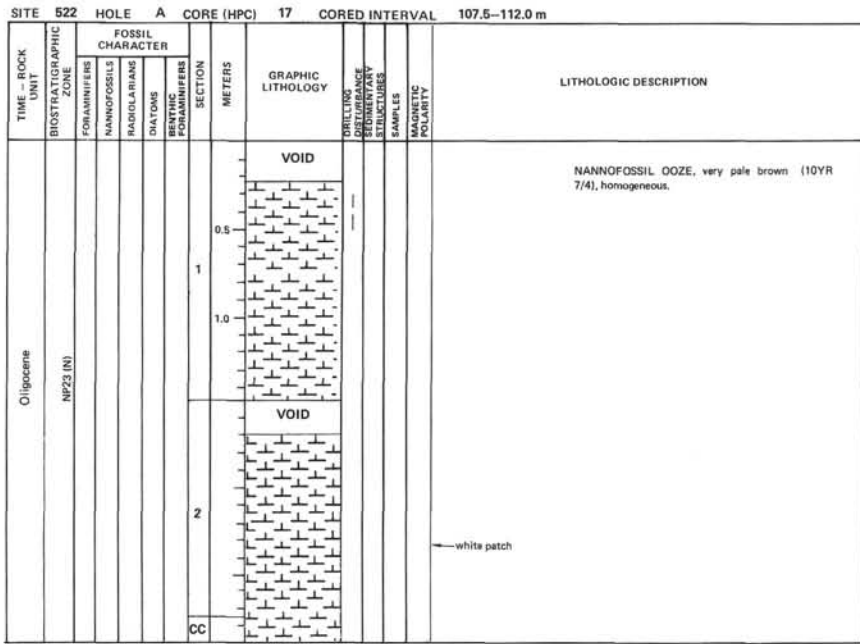
SITE 522 HOLE A CORE (HPC) 13 CORED INTERVAL 91.5-95.5 m

TIME - ROCK UNIT	BIOSTRATIGRAPHIC ZONE	FOSSIL CHARACTER				SECTION	METERS	GRAPHIC LITHOLOGY	DRILLING DISTURBANCE	SEDIMENTARY STRUCTURES	SAMPLES	MAGNETIC POLARITY	LITHOLOGIC DESCRIPTION
		FORAMINIFERS	NANNOFOSSILS	RADIOLARIANS	DIATOMS								
Oligocene	MP23 (N)					1						<p>NANNOFOSSIL OOZE, light yellowish brown (10YR 6/4), homogeneous with some faint burrows. White (10YR 8/1) BRAARUDOSPHAERA OOZE between 90-138 cm has sharp, burrowed contacts with enclosing nannofossil ooze. Top 55 cm, Section 1 is drilling debris.</p>	
						2							Braarudosphaera ooze
						3							VOID
						CC							white patch

SITE 522 HOLE A CORE (HPC) 14 CORED INTERVAL 95.5-100.0 m										
TIME - ROCK UNIT	BIOSTRATIGRAPHIC ZONE	FOSSIL CHARACTER				SECTION	METERS	GRAPHIC LITHOLOGY	DRILLING DISTURBANCE	LITHOLOGIC DESCRIPTION
		FORAMINIFERS	NANNOFOSSILS	RADIOLARIANS	DIATOMS					
Oligocene	NP23 (N)					1			NANNOFOSSIL OOZE, very pale brown (10YR 7/4) homogeneous, sporadic burrows. Top 65 cm of Section 1 is drilling debris.	
						2	VOID			
						3	VOID			
						CC			white patch	

SITE 522 HOLE A CORE (HPC) 15 CORED INTERVAL 100.0-104.5 m										
TIME - ROCK UNIT	BIOSTRATIGRAPHIC ZONE	FOSSIL CHARACTER				SECTION	METERS	GRAPHIC LITHOLOGY	DRILLING DISTURBANCE	LITHOLOGIC DESCRIPTION
		FORAMINIFERS	NANNOFOSSILS	RADIOLARIANS	DIATOMS					
Oligocene	NP23 (N)					1			NANNOFOSSIL OOZE, very pale brown (10YR 7/4) with several slightly darker light yellowish brown (10YR 5/4) intervals. Burrows common. No other sedimentary structures.	
						2	VOID			
						CC				
									very pale brown light yellowish brown very pale brown white patch light yellowish brown very pale brown	

SITE 522 HOLE A CORE (HPC) 16 CORED INTERVAL 104.5-107.5 m										
TIME - ROCK UNIT	BIOSTRATIGRAPHIC ZONE	FOSSIL CHARACTER				SECTION	METERS	GRAPHIC LITHOLOGY	DRILLING DISTURBANCE	LITHOLOGIC DESCRIPTION
		FORAMINIFERS	NANNOFOSSILS	RADIOLARIANS	DIATOMS					
Oligocene	NP23 (N)					1			NANNOFOSSIL OOZE, very pale brown (10YR 7/4), homogeneous.	
						CC				
									white spot white spot	



SITE 522		HOLE A		CORE (HPC) 22		CORED INTERVAL 121.5-125.5 m				
TIME - ROCK UNIT	BIOSTRATIGRAPHIC ZONE	FOSSIL CHARACTER			METERS	GRAPHIC LITHOLOGY	DRILLING DISTURBANCE STRUCTURES	SAMPLES	MAGNETIC POLARITY	LITHOLOGIC DESCRIPTION
		FORAMINIFERS	NANNOFOSSILS	RADIOLARIANS						
lower Oligocene	NP21 (N)									
					0.5	VOID				
					1					
					1.0					
					2					
					3					
					CC					

SITE 522		HOLE A		CORE (HPC) 23		CORED INTERVAL 125.5-129.0 m				
TIME - ROCK UNIT	BIOSTRATIGRAPHIC ZONE	FOSSIL CHARACTER			METERS	GRAPHIC LITHOLOGY	DRILLING DISTURBANCE STRUCTURES	SAMPLES	MAGNETIC POLARITY	LITHOLOGIC DESCRIPTION
		FORAMINIFERS	NANNOFOSSILS	RADIOLARIANS						
lower Oligocene	NP21 (N)									
					0.5	VOID				
					1					
					1.0					
					2					
					3					
					CC					

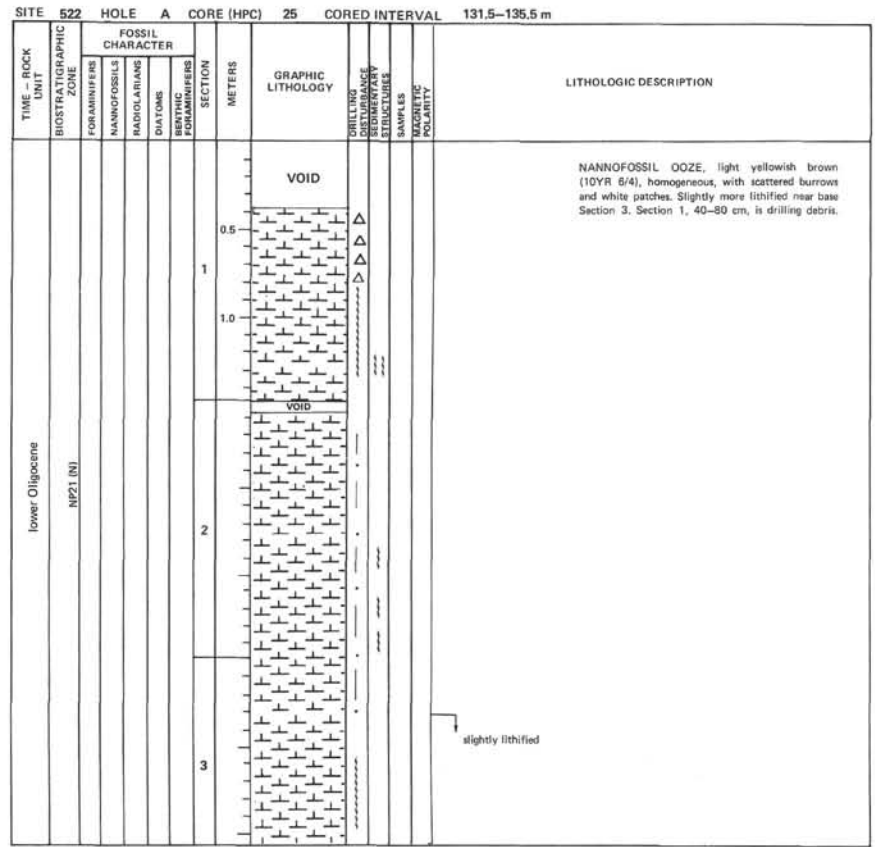
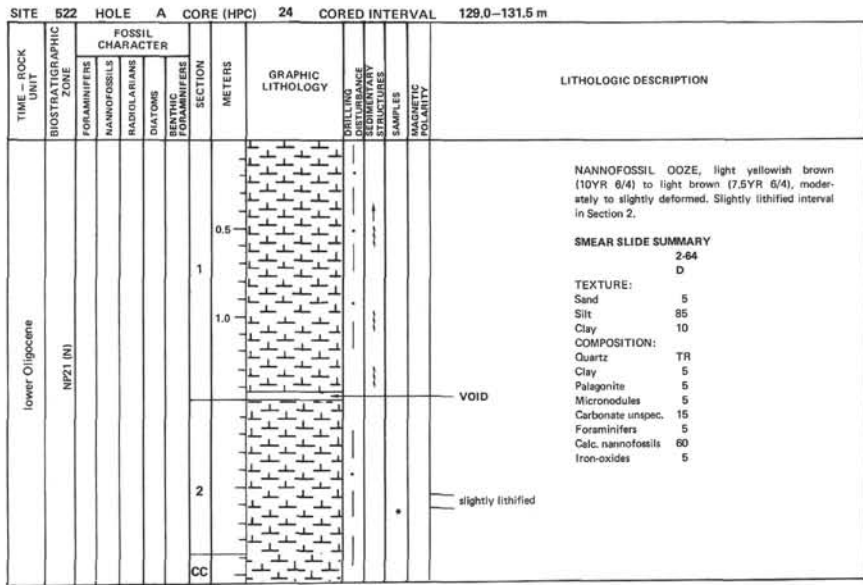
VOID

NANNOFOSSIL OOZE, light yellowish brown (10YR 6/4), homogeneous, with scattered burrows. Drilling debris comprise top 70 cm of Section 1.

**SMEAR SLIDE SUMMARY**  
1-140  
D

TEXTURE:  
Sand 5  
Silt 90  
Clay 5

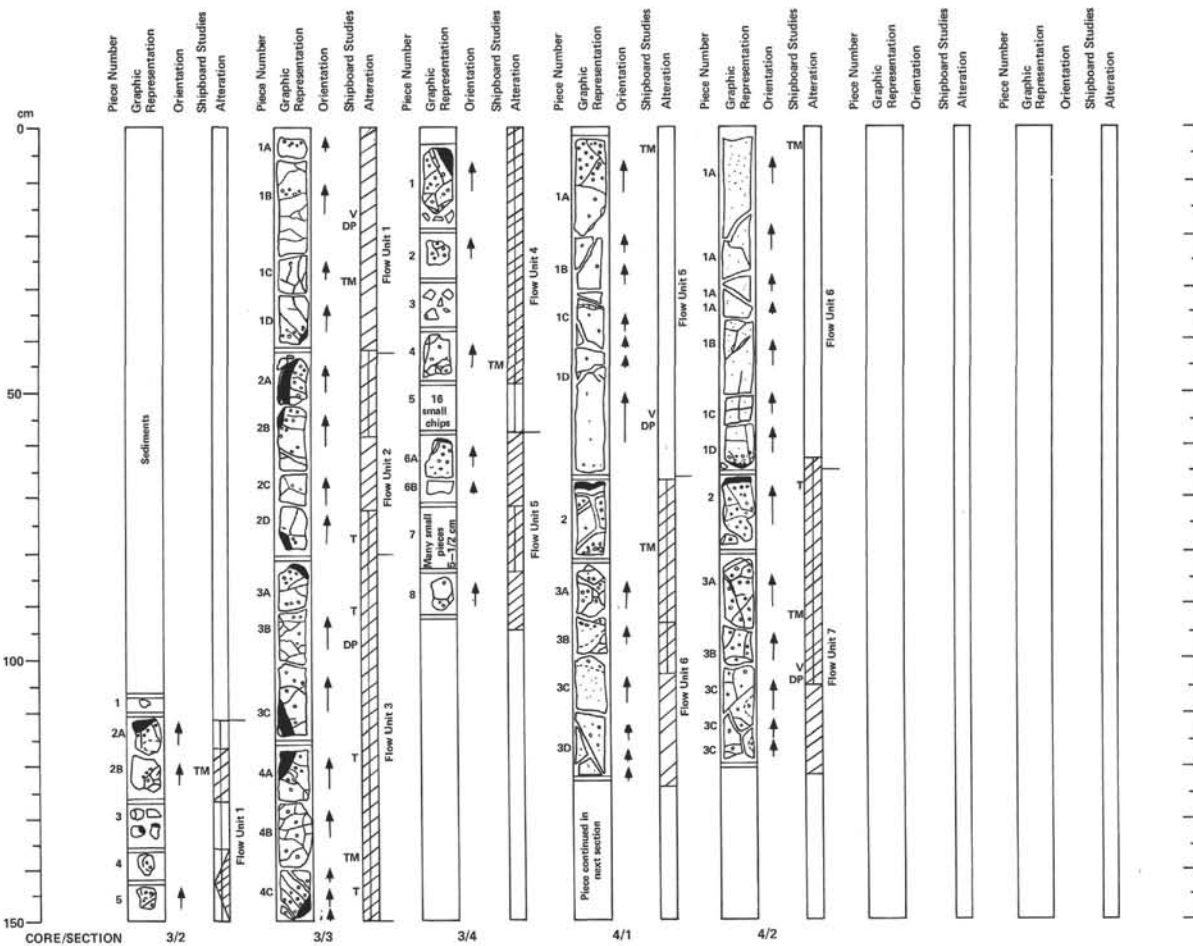
COMPOSITION:  
Quartz TR  
Clay 5  
Micronodules 10  
Carbonate unsp. 10  
Foraminifers 15  
Calc. nannofossils 80  
Fish remains TR











HOLE 522B, CORE 3, SECTIONS 2-4, 151.4-155.3 m

MAJOR ROCK TYPE - BASALT  
MINOR ROCK TYPE - LIMESTONE

Macroscopic Description

**Basalt** - Dark gray, aphyric, very fine-grained to coarse-grained, finely vesicular. Numerous vitreous, black glassy margins (as marked) define boundaries of Flow Units 1-5. Texture coarsens away from glass through vesicular, veined and microbrecciated interval. Matching glassy margins in Pieces 1D, 2A, 2B, 2D, 3A, and 4C, Sec. 3 and in Pieces 3C-4A, Sec. 3 subparallel to core axis suggest individual pillows. Vesicles (as marked) round to irregular up to 2 mm across; often filled with calcite, blue green or dark green smectite, iron oxides or a white amorphous material. Numerous, thin (0.5-2 mm) irregular veins filled with dark green smectite or calcite are often surrounded by brownish, slightly altered basalt. Pieces 3C and 4A, Sec. 3 have 0.5 cm thick layer of clear calcite on the outside of the glass. Fractures common throughout; conjugate fractures oriented ~45° to core axis in Pieces 1-2, Sec. 4. **Limestone** - Piece 1, Sec. 2 is pinkish white limestone with very pale brown calcite coating and with included fragments of vitreous black glass(?) and waxy yellow palagonite(?).

Thin Section Summaries

**Section 2: Piece 2B** is fine-grained, sparsely microphyric, fine quench texture with ~5% plagioclase (0.15-0.8 mm, An<sub>70-80</sub>), ~1% olivine (0.1-0.3 mm, Fo<sub>75-80</sub>) and ~1% clinopyroxene (0.15-0.25 mm)

phenocrysts mostly intergrown in glomerocrystic clusters. Matrix is fine (0.01-0.05 mm) to very fine-grained (<0.01 mm) plagioclase microclots, plumose dendritic clinopyroxene clusters and very fine, fibrous spherulites (probably intergrowths of clinopyroxene with some plagioclase; most are length slow in fiber direction). Opaques are fine to very fine-grained and concentrated between dendrite and spherulite boundaries. Rounded vesicles (2-3%) are calcite-filled; calcite also occurs in irregular patches. Approximate mode: plagioclase 25-35, clinopyroxene 30-40, olivine 1, opaques 10-15, spherulites 20-30, calcite 5-7.

**Section 3: Piece 1C** similar to Piece 2B, Sec. 2 but slightly coarser-grained. Olivine completely altered to yellow brown smectite. Piece 2D includes a glassy margin. Textures are hyaline, microphyric, spherulitic, fine quench and plumose dendritic. Phenocrysts are: 1) 2 generations of plagioclase; first = euhedral, stubby and simply/coarsely twinned crystals, second = subeuhedral-subhedral, skeletal, complexly twinned subradial clusters subophitically intergrown with olivine and clinopyroxene (crystals 0.03-1.2 mm long and zoned - An<sub>66-42</sub>; Cb-Ab twins); 2) olivine, euhedral skeletal with glass inclusions, single grains and subophitic intergrowths with second generation plagioclase (0.05-1.2 mm, Fo<sub>70-80</sub>); 3) clinopyroxene, subophitic intergrowths with second generation plagioclase (0.01-0.18 mm, bow-tie shape common). Five textural zones in fine quench groundmass = glassy, glassy spherulitic, coalesced spherulitic, sheaf-shaped spherulitic and dendritic, and plumose dendritic and spherulitic. Glass pale brown, partly altered to

yellow palagonite along cracks. Olivine fresh in glass but completely altered to brown smectite in crystalline rock. Approximate mode: plagioclase 25-30, clinopyroxene 30-40, olivine 5, spherulites 25-30, opaques 5-10, vesicles filled (calcite, smectite and high relief amorphous material) 1-2. Pieces 3B and 4A-C similar to Pieces 1C and 2B. Segregation vesicles in 3B and 4B filled with very fine-grained clinopyroxene and opaques with plagioclase microclots arranged tangentially. Piece 4C contains Cb-Ab twinning in first generation plagioclase that shows phenocrysts zoned An<sub>80-60</sub>.

**Section 4: Piece 4** is similar to Piece 2B, Section 3 but groundmass and dendritic clinopyroxene less abundant and spherulites more common.

Sample	D	P	V <sub>1</sub>	V <sub>2</sub>	NRM1	NRM2	S. I.
Sec. 2, Piece 2B	-	-	-	-	19,320	82.5	82
Sec. 3, Piece 1B	-	6	5.94	5.59	-	-	-
Sec. 3, Piece 1C	-	-	-	-	49,371	52.8	52.5
Sec. 3, Piece 4B	-	-	-	-	20,499	51.3	52
Sec. 4, Piece 4	-	-	-	-	13,856	53.1	55

HOLE 522B, CORE 4, SECTIONS 1-2, 156.9-159.3 m

MAJOR ROCK TYPE - BASALT

Macroscopic Description

**Basalt** - Dark gray, aphyric with glassy margins marking the boundaries between successive flow units. Flow Unit 5 is a continuation of that in Core 3. Grain size grades from very coarse to fine in lower 15 cm (Piece 1D, Sec. 1). Veins and fractures sparse, latter forming conjugate sets

~45° to core axis. Vesicles near top Sec. 1. Minimal alteration. Flow Unit 6 is texturally and compositionally similar to Unit 5 rocks. Grain size increases away from 2 cm thick glassy rind at top of unit. Piece 3A (Sec. 1) has variable, irregular texture ranging from fine to medium-coarse. Possible flow unit boundary between this piece and overlying Piece 3. Vesicles common, largest near top flow unit. Orange saponite fills some vesicles. Fractures common and bordered by brownish alteration. Fracture surfaces in Pieces 3A-B (Sec. 1) and Pieces 1A-B (Sec. 2) covered with turquoise-colored amorphous(?) material and black coating with fine pyrite crystals. Flow Unit 7 is similar to Unit 6 but slightly less coarse-grained in center. Vesicles and fracture sets common. Moderately altered.

Thin Section Summaries

**Section 1, Piece 1A:** Textures are finely seriate, intersertal to hyalo-ophitic, and intergranular. The rock is coarse- to very coarse-grained with mostly lath-shaped, commonly hollow skeletal, subhedral plagioclase (0.1-1.3 mm, An<sub>61-60</sub>; Cb-Ab twins) subophitically intergrown with clinopyroxene (0.03-0.4 mm, colorless, 2V<sub>1</sub>-60°, some in bow tie shape) and completely altered olivine (0.1-0.5 mm). Clinopyroxene and olivine also are intergranular, olivine euhedral to subhedral and clinopyroxene anhedral. Opaques are minute cubes, octahedral and hexagonal plates (0.005-0.05 mm) concentrated in intersertal patches between the three coarser minerals. Intersertal patches are large (up to 2 mm) and abundant, sometimes interconnecting as to give locally hyalo-ophitic texture. The patches consist of chiefly opaque minerals and saponitic smectite (devitrified glass?), with lesser very fine-grained anhedral clinopyroxene and plagioclase. In the patches, especially where hyalo-ophitic, clinopyroxene-plagioclase clusters have shape and arrangement reminiscent of sheaf growth of spherulites. Vesicles comprise 2-3% of the rock in 3 types: round (~1%, 0.2-0.9 mm), filled diktytaxitic (~1%, 0.3-1.1 mm) and segregation (<1%, 0.5-1.1 mm). Rounded and diktytaxitic vesicles are filled with pale greenish brown ultra fine-grained (0.005 mm or less), fibrous to massive saponitic smectite (moderate to high birefringence). Segregation vesicles are bounded by tangentially aligned plagioclase microclots and filled with very finely granular opaque minerals, clinopyroxene, saponitic smectite and rare plagioclase. Some are only partially filled with this assemblage, having a smaller rounded area filled with the same smectite that fills other vesicles. Olivine is completely altered to pale greenish brown smectite, the same as fills vesicles, but is more coarsely crystalline. Approximate mode: plagioclase 30-40, clinopyroxene 30-40, opaques 10-15, olivine 5-10, altered glass 5-10, vesicles 2-3.

**Section 1, Piece 1D:** Textures are microphyric, seriate, coarse quench transitional to seriate subophitic intersertal. Texture consists of a network of seriate plagioclase (with quench attributes), olivine and finely subophitic clinopyroxene, with fine interstitial opaques. Network is sieve-like with "holes" ranging from rounded segregation vesicles to highly irregular patches containing finely dendritic clinopyroxene, sheafed spherulites, and quench plagioclase with abundant opaques and sparse smectite between the sheaves. Filling of "holes" is all much more fine-grained than the network. Approximate mode: plagioclase 30-40 (0.01-1.2 mm), clinopyroxene 30-40 (0.01-0.25 mm), 1.3-4 (0.05-0.5 mm), vesicles 5-8 (0.02-4.0 mm).

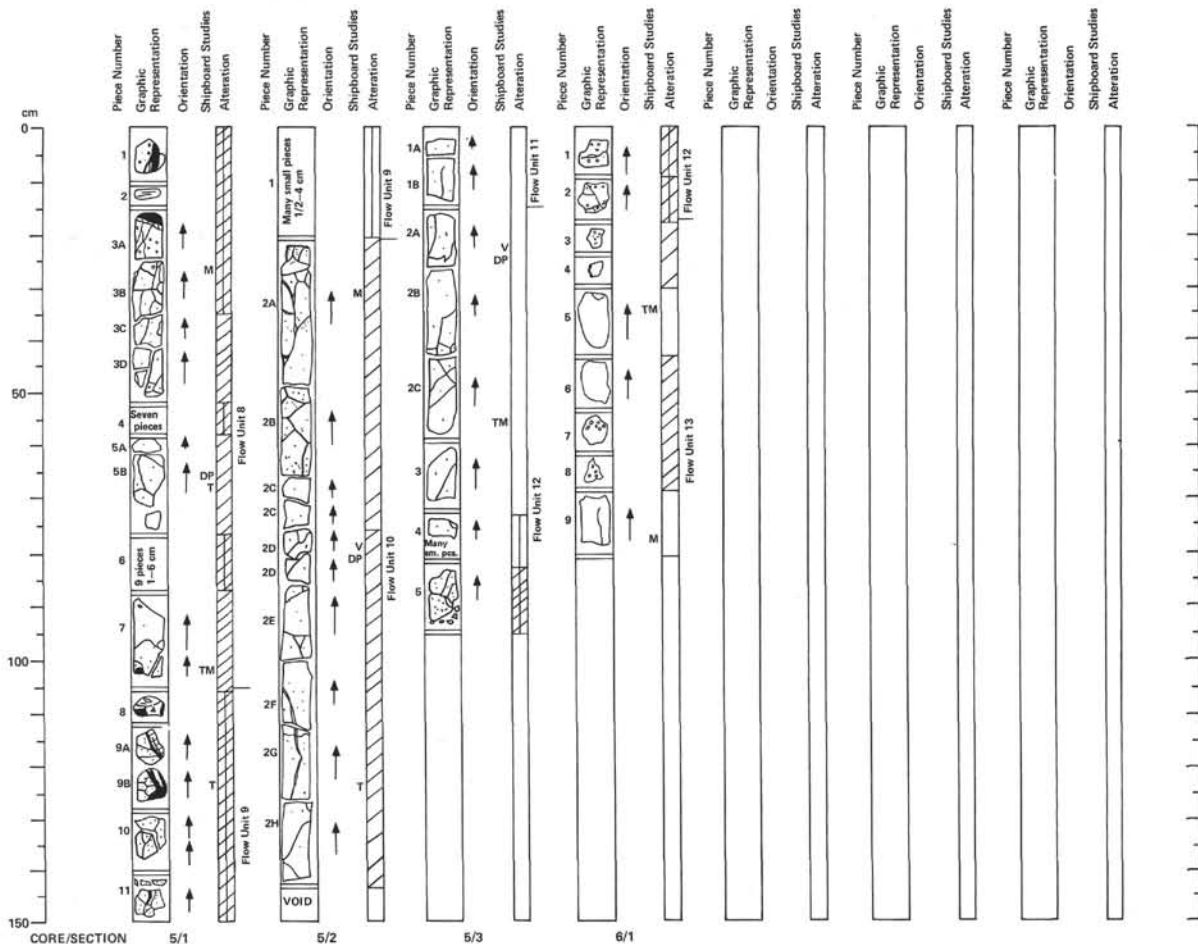
**Section 1, Piece 2:** Textures are hyaline, microphyric spherulitic, quench, plumose dendritic. Rock is same as Core 3, Sec. 3, 76-78 cm Piece 2D, both in textures and mineralogy.

**Section 2, Piece 2:** Textures are microphyric, seriate coarse quench transitional to seriate subophitic intersertal. Similar to Core 4, Sec. 1, 76-78 cm, Piece 2, but more advanced and slightly more coarse-grained with euhedral and subhedral olivine and clinopyroxene patches interspersed with rounded to ellipsoidal crudely radial sheaves of clinopyroxene and plagioclase finely intergrown. The interstices of the network (intersertal patches) are highly irregular and filled with abundant opaque "spars" and cryptocrystalline material. Approximate mode: plagioclase 30-40 (0.04-1.2 mm, An<sub>75-80</sub>), clinopyroxene 30-40 (0.001-0.05 mm), 1.1-2 (0.15-2.0 mm) intersertal smectite 5, vesicles 3-4 (0.08-1.0 mm).

**Section 2, Piece 3A:** Textures are microphyric, seriate, and coarse quench. Sparse first generation (0.5%, 0.12-1.0 mm, An<sub>75</sub>) and second generation (2-3%, 0.16-1.16 mm, An<sub>70-80</sub>) plagioclase microphenocrysts commonly in subradial glomerocrystic clusters, intergrown with subophitic olivine and clinopyroxene. Groundmass consists of seriate very thin quench plagioclase (0.02-0.74 mm long), thickly and crudely plumose dendritic clinopyroxene, and clinopyroxene-plagioclase sheaf-shaped clusters coarsely reminiscent of spherulites in more fine-grained rocks. Opaques (0.003-0.03 mm) are concentrated in intersertal spaces, especially between and around clinopyroxene-plagioclase sheaf clusters. There is a small amount (1-5%) of interstitial smectite (devitrified glass?). Vesicles (0.04-1.2 mm) are both round and highly irregular, ranging from smectite-lined hollow to smectite and calcite-filled. Smectite is yellow in much of slide, but is changed to pale brown to orange-red in more altered part. Approximate mode: plagioclase 30-40, clinopyroxene 40-50, olivine 0.5, opaques 10, altered glass 1-5, vesicles 5.

Shipboard Studies

Sample	D	P	V <sub>1</sub>	V <sub>2</sub>	NRM1	NRM2	S. I.
Sec. 1, Piece 1A	-	-	-	-	40,821	48.7	50
Sec. 1, Piece 1D	2.91	4	8.30	5.34	-	-	-
Sec. 1, Piece 2	-	-	-	-	19,771	52.0	52
Sec. 2, Piece 1A	-	-	-	-	92,911	49.8	46
Sec. 2, Piece 3A	-	-	-	-	25,634	45.5	45
Sec. 2, Piece 3C	2.86	6	5.39	5.02	-	-	-



## HOLE 522B, CORE 5, SECTIONS 1-3, 160.4-168.2 m

## MAJOR ROCK TYPE - BASALT

## Macroscopic Description

**Basalt** - Dark gray, aphyric with glassy rinds (as marked) separating some flow units. Flow Unit 8 is very fine- to medium coarse-grained, moderately finely vesicular. Piece 2 (Sec. 1) is a breccia composed of coarse vein calcite enclosing glass fragments 0.5 cm thick. Pieces 1 and 3A (Sec. 1) have 0.5 cm thick calcite veins associated with glass. Grain size increases through Unit 8. Fractures with dark green clay common. Alteration moderate. Flow Unit 9 has abundant glassy rinds near top, some cut by calcite veins. Glass in contact with microphyric, very fine- to fine-grained vesicular (0.25 mm) basalt, similar to that of Unit 8. Fractures commonly filled with calcite, green clay and sometimes MnO-dendrite coating. Mn-oxide fills center of 3-4 mm calcite vein in Piece 11 (Sec. 1). Flow Unit 10 basalt is similar to Unit 8 and 9. Thin glassy rind at top; texture grades from very fine- to coarse within 10 cm of glass. Lowest piece of unit (Piece 2H, Sec. 1) is very coarse-

grained. Common fractures with smectite filling common in top half, calcite in lower half of unit. Slightly altered with 1 cm zone of moderate alteration parallel to fractures. Flow Unit 11 aphyric basalt same as overlying units. No glass, but texture grades from fine- to medium coarse-grained within 2-3 cm of top. Finely vesicular (0.25 mm) with green smectite filling fractures. Rock appears fresh. Flow Unit 12 is same as overlying basalt. Calcite fills shallow depressions; clay-filled fractures common. Very fine-grained at top grades downward irregularly to medium-grained. Piece 4 (Sec. 3) is badly altered. Vesicles slightly larger (0.5 mm) than overlying basalt.

## Thin Section Summaries

**Section 1, Piece 5B:** Textures are microphyric, seriate, coarse quench, and intersertal. Textures and mineralogy quite similar to Core 4, Sec. 2, 93-95 cm Piece 3A except:

- 1.) This rock is slightly more coarse-grained and groundmass plagioclase is thicker.
- 2.) Intersertal patches containing green smectite and very fine-grained opaques are distinct.

3.) Several segregation vesicles (0.08-0.6 mm) are present.

4.) Vesicles are finer (0.08-0.4 compared with 0.04-1.2) and less abundant (1-2% against ~5%).

**Section 1, Piece 7:** Sparsely microphyric, coarse quench quite similar to Core 4, Sec. 2, 93-95 cm Piece 3A, except as follows:

- 1.) First and second generation plagioclase microphenocrysts and associate olivine and clinopyroxene are less abundant (total 2-3% compare with 7-10%) and slightly more fine-grained.
- 2.) Plagioclase is more even-grained and abundant in groundmass (30-40% against 25-30%).
- 3.) Because of 1) and 2) rock is not seriate.
- 4.) Olivine may be present as tiny (0.01-0.03 mm) altered grains in groundmass.
- 5.) Section cut by thin (0.02-0.06 mm) palagonite-filled fracture, palagonite retains spherulitic texture.
- 6.) Vesicles filled with yellow smectite.
- 7.) Segregation vesicles present.
- 8.) Interstitial yellow smectite relatively abundant (10-15%).

**Section 1, Piece 9A:** Textures are hyaline, microphyric, spherulitic, fine quench, and plumose dendritic. The rock is the same mineralogically and texturally as Core 3, Sec. 3, 76-78 cm Piece 2D. It grades into moderately coarse quench at 2.5 cm from zone 4.

**Section 2, Piece 2F:** Finely seriate, intersertal to hyalophitic, subophitic, and intergranular. Same rock type and texture as Core 4, Sec. 1, 4-6 cm, Piece 4A. Differences are:

- 1.) There is a coarse, highly irregular and discontinuous calcite patch or thick veinlet.
- 2.) Smectite in vesicles is more coarsely crystalline and colored bright green to slightly yellowish green.
- 3.) Some vesicles filled with dark orange-red fibrous, or scaly material, around calcite patch (oxidized smectite?).

Plagioclase composition is normal. Second generation microphenocrysts or coarse groundmass grains show strong zoning ( $An_{77-30}$ ,  $Ca-Ab$  twins) and typical composition at most cores ( $An_{77-30}$ ,  $Ca-Ab$  twins).

**Section 3, Piece 2C:** Subophitic, intersertal to hyalophitic, very sparsely microphyric. Similar textures and same mineralogy as Core 4, Sec. 1, 4-6 cm Piece 1A. Differences are:

- 1.) This rock is more fine-grained (average texture is medium- to coarse-grained and never reaches very coarse-grained.)
  - 2.) Microphenocrysts are distinct first generation plagioclase (<1%, 0.1-0.45 mm, zoned  $An_{70-62}$ ,  $Ca-Ab$  twins).
- Groundmass plagioclase composition is typical ( $An_{63}$ ,  $Ca-Ab$  twins). Vesicles are identical to those of Core 4, Sec. 1, 4-6 cm Piece 1A.

## Shipboard Studies

Sample	D	P	V <sub>i</sub>	V <sub>g</sub>	NRM1	NRM2	S. I.
Sec. 1, Piece 3B	-	-	-	-	26.370	48.1	48
Sec. 1, Piece 5B	3.06	2.9	-	-	-	-	-
Sec. 1, Piece 7	-	-	-	-	14.220	50.8	49
Sec. 2, Piece 2A	-	-	-	-	72.024	41.9	40
Sec. 2, Piece 2D	2.89	5.4	5.45	4.98	-	-	-
Sec. 3, Piece 2A	2.88	6.0	5.29	5.47	-	-	-
Sec. 3, Piece 2C	-	-	-	-	88.876	31.3	37.5

## HOLE 522B, CORE 6, SECTION 1, 167.4-168.2 m

## MAJOR ROCK TYPE - BASALT

## Macroscopic Description

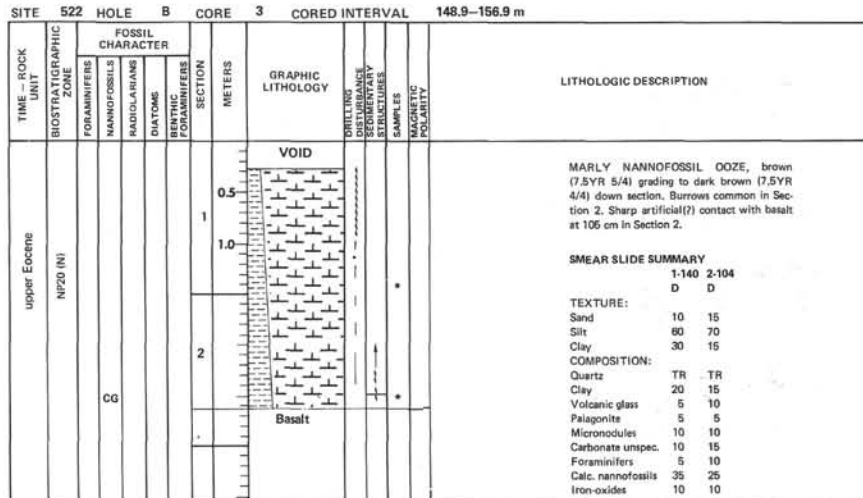
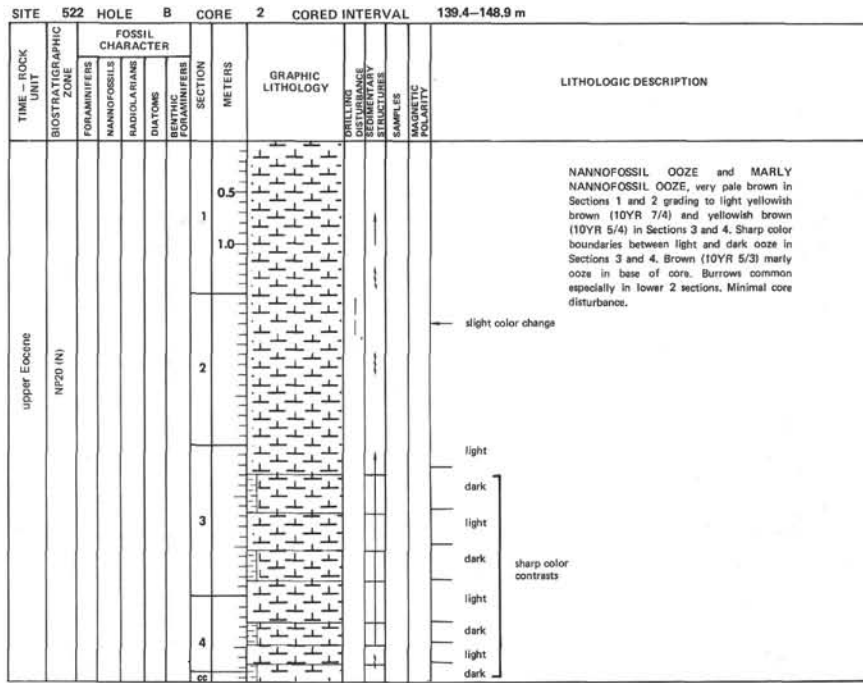
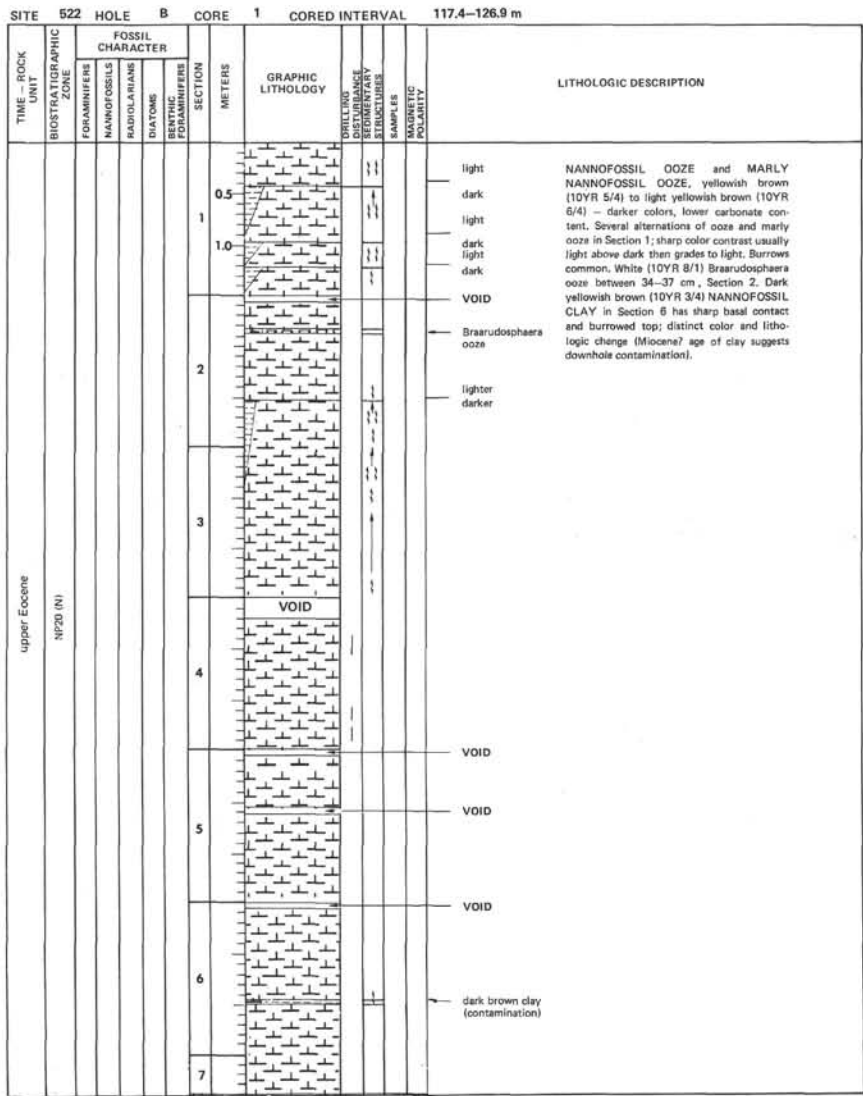
**Basalt** - Dark gray, aphyric with glassy margin (as marked) separating flow units. Flow Unit 12 (continued from Core 5, Sec. 3) is slightly more vesicular (5%, ~0.5-1 mm) than Piece 5 (Sec. 3) of previous core. Piece 2 is very fine-grained grading to 3 mm glassy rind. Otherwise identical to Core 5, Sec. 3. Flow Unit 13 basalt is similar to overlying basalt. Glassy margin on back side of Piece 4, Piece 3 is fine- to medium-grained and quite vesicular (10%, 0.25-1 mm). Pieces 5-9 are medium- to coarse-even grained and fresh. Piece 7 has 2 cm vesicular zone; vesicles have highly irregular shapes and line with greenish blue clay; some contain tiny clusters of euhedral chalcocopyrite or pyrite. Pieces 8-9 similar, but have mostly pyrite filling some round, irregular vesicles.

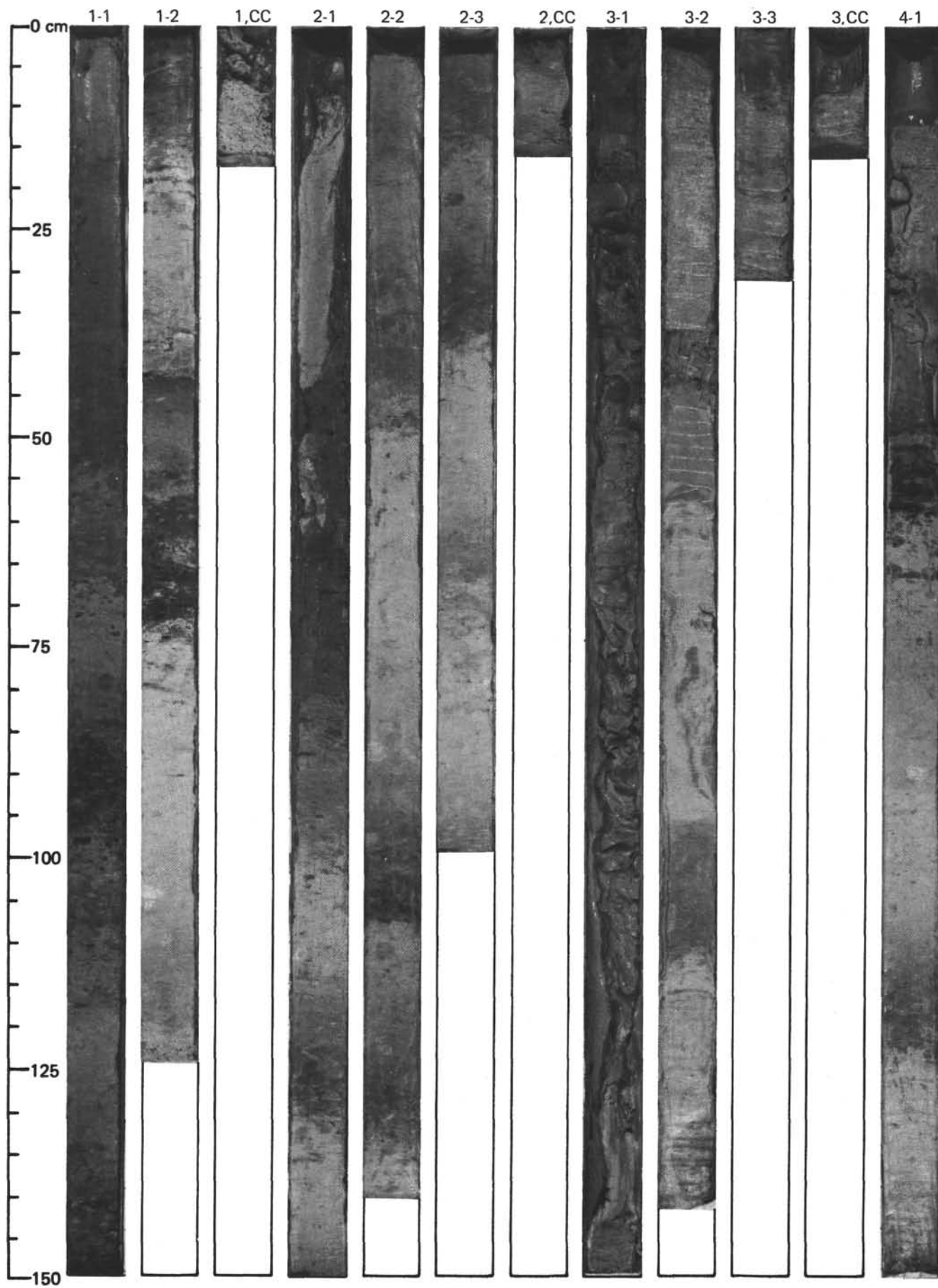
## Thin Section Summary

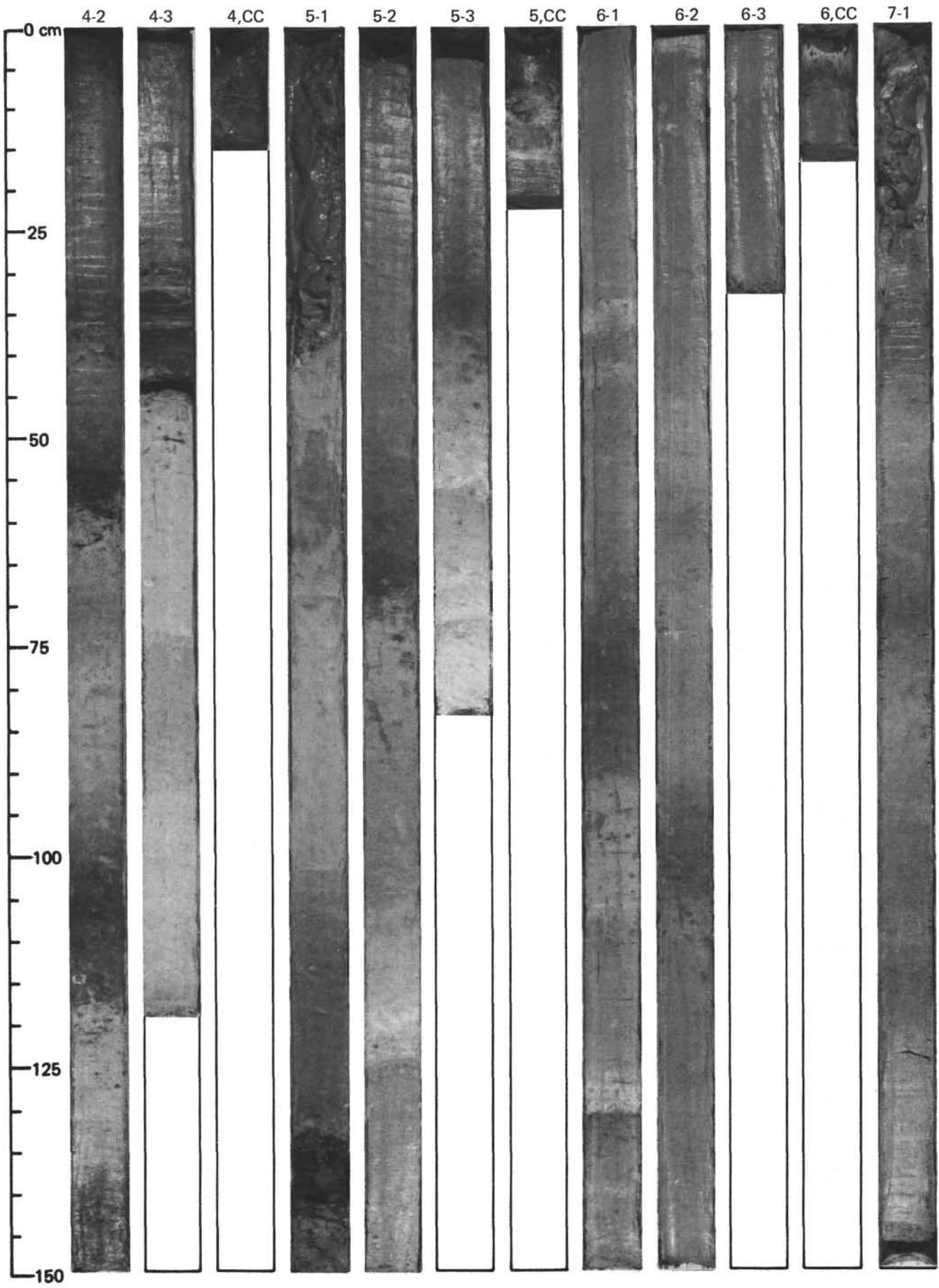
**Section 1, Piece 5:** Finely seriate, microphyric, intersertal to hyalophitic, subophitic and intergranular. Essentially the same textures and mineralogy as Core 4, Sec. 1, 4-6 cm Piece 1A except that all phases other than microphenocrysts are more fine-grained (fine- to coarse-grained, not reaching very coarse-grained). First generation microphenocrysts are typical in morphology, size and composition ( $An_{70-80}$ ), as are coarser groundmass grains ( $An_{62-36}$ ).

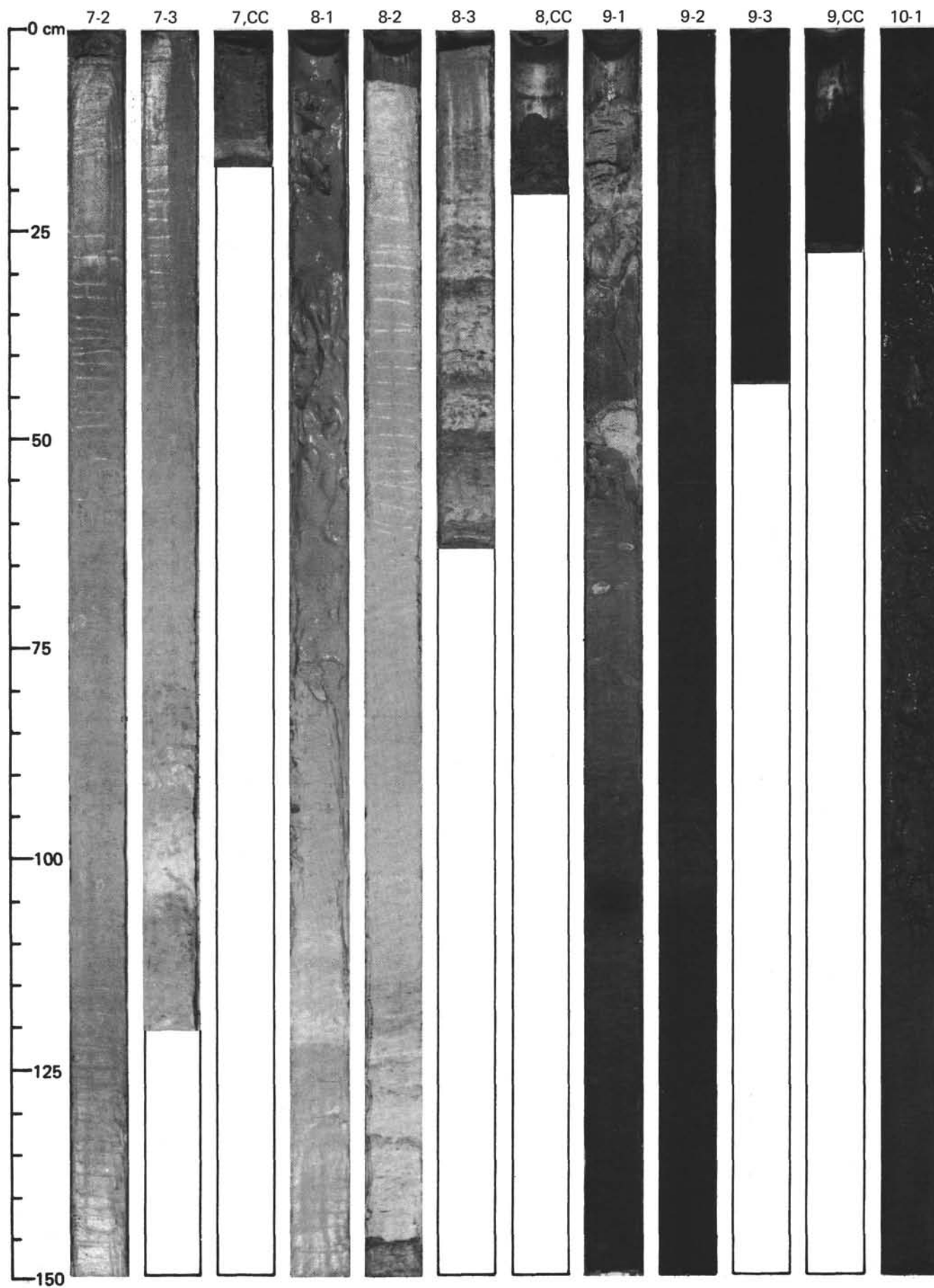
## Shipboard Studies

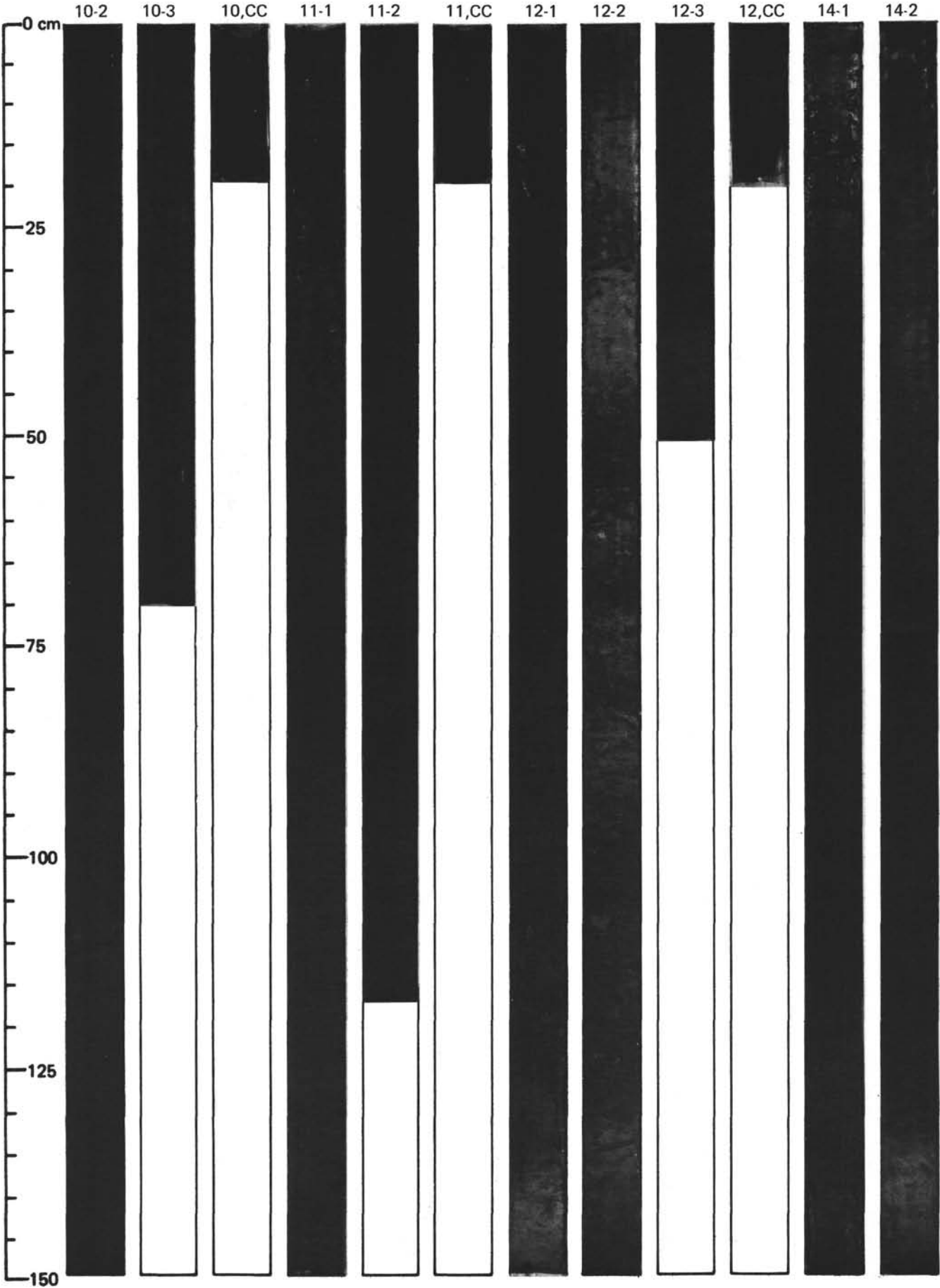
Sample	D	P	V <sub>i</sub>	V <sub>g</sub>	NRM1	NRM2	S. I.
Sec. 1, Piece 5	-	-	-	-	97.295	-31.6	-46
Sec. 1, Piece 9	-	-	-	-	47.045	-39.6	-47

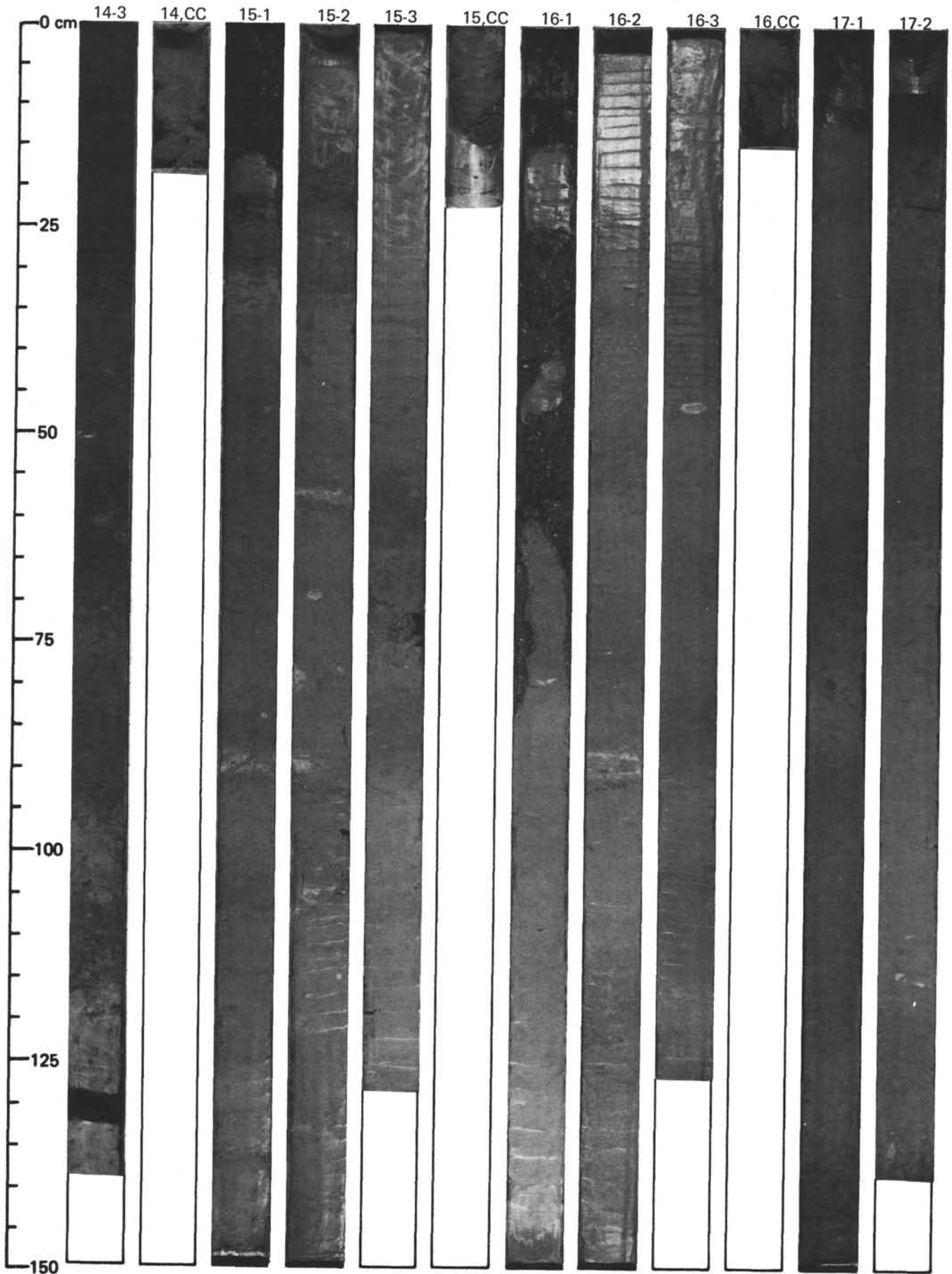


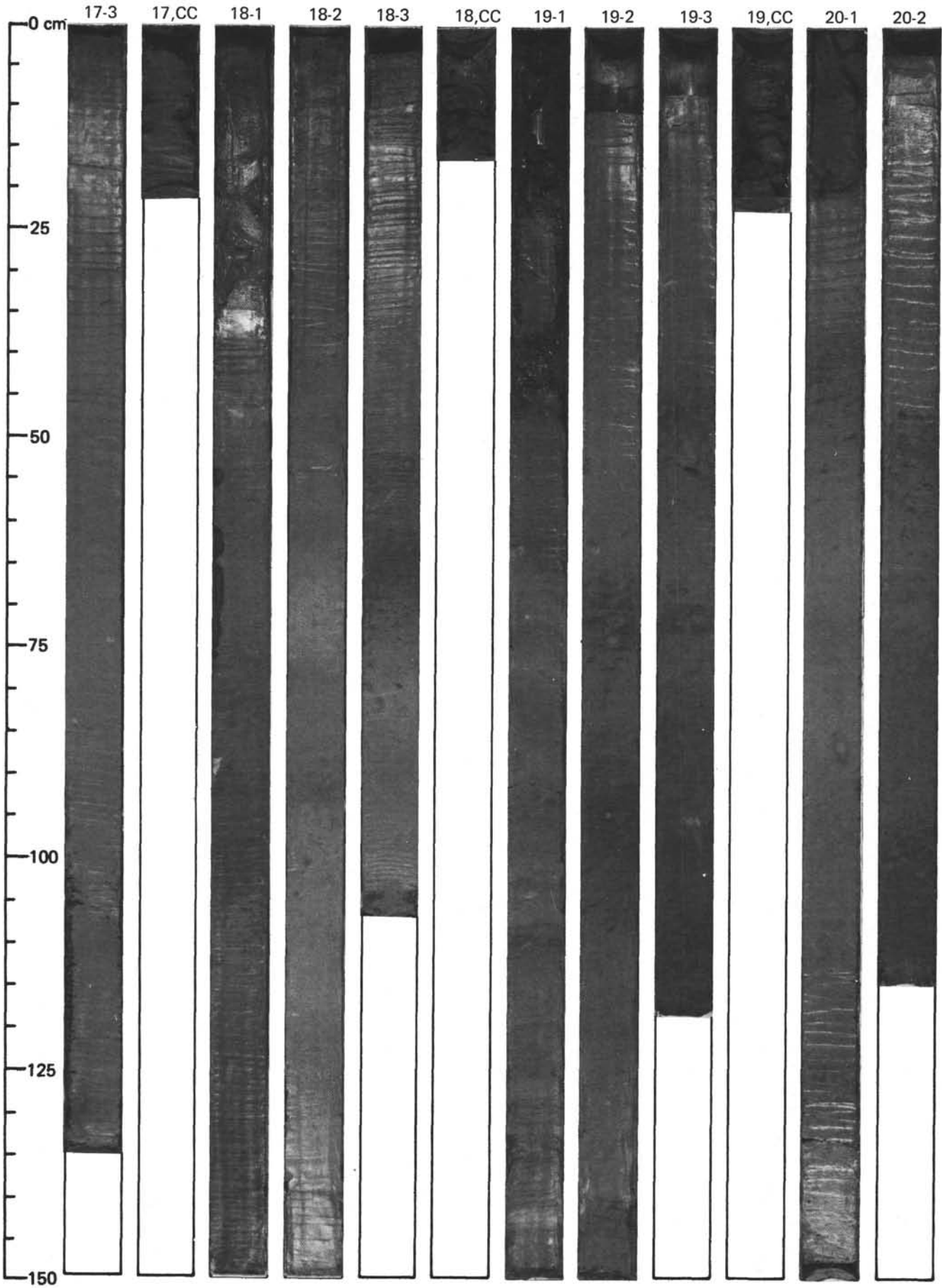


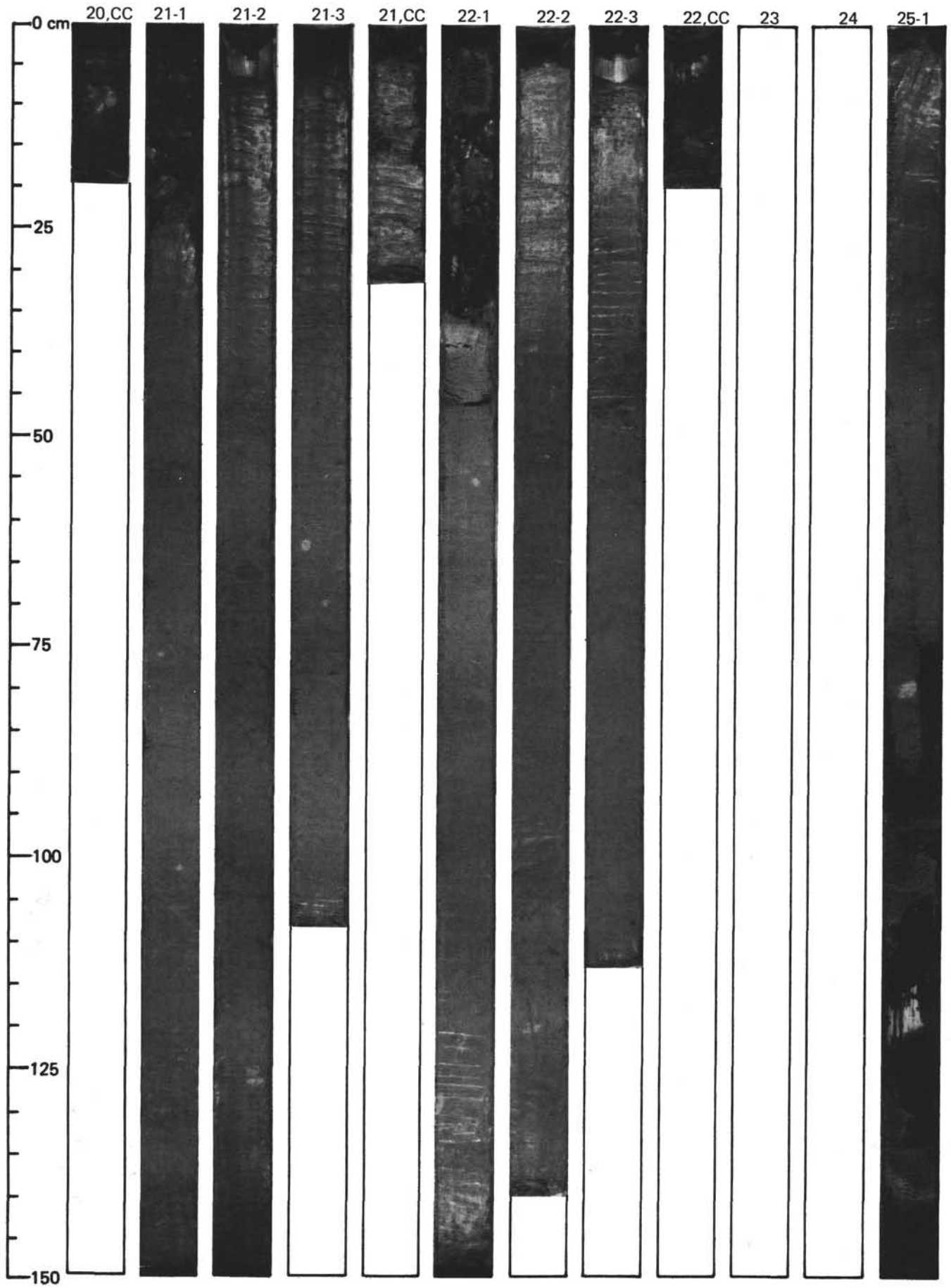


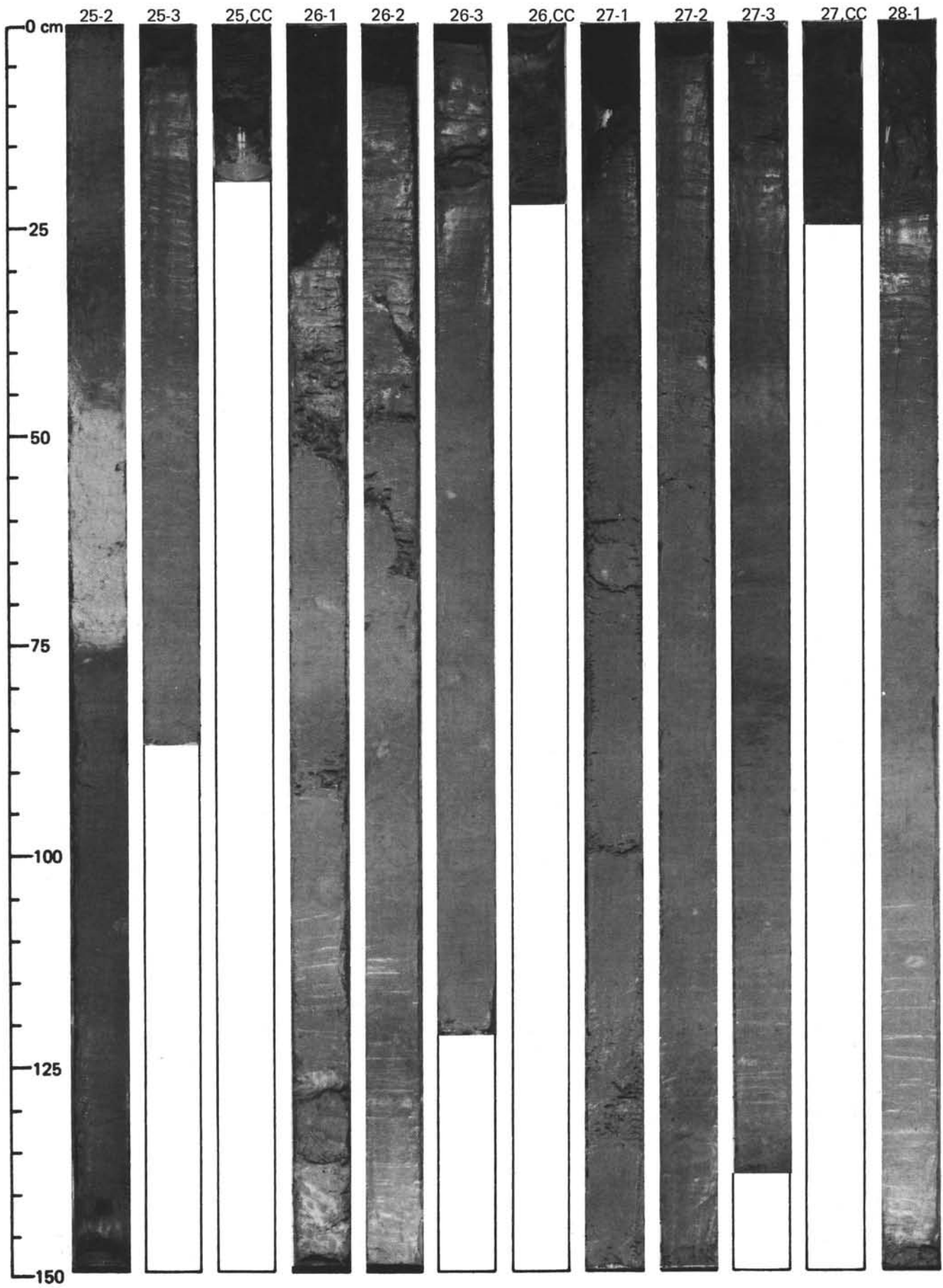


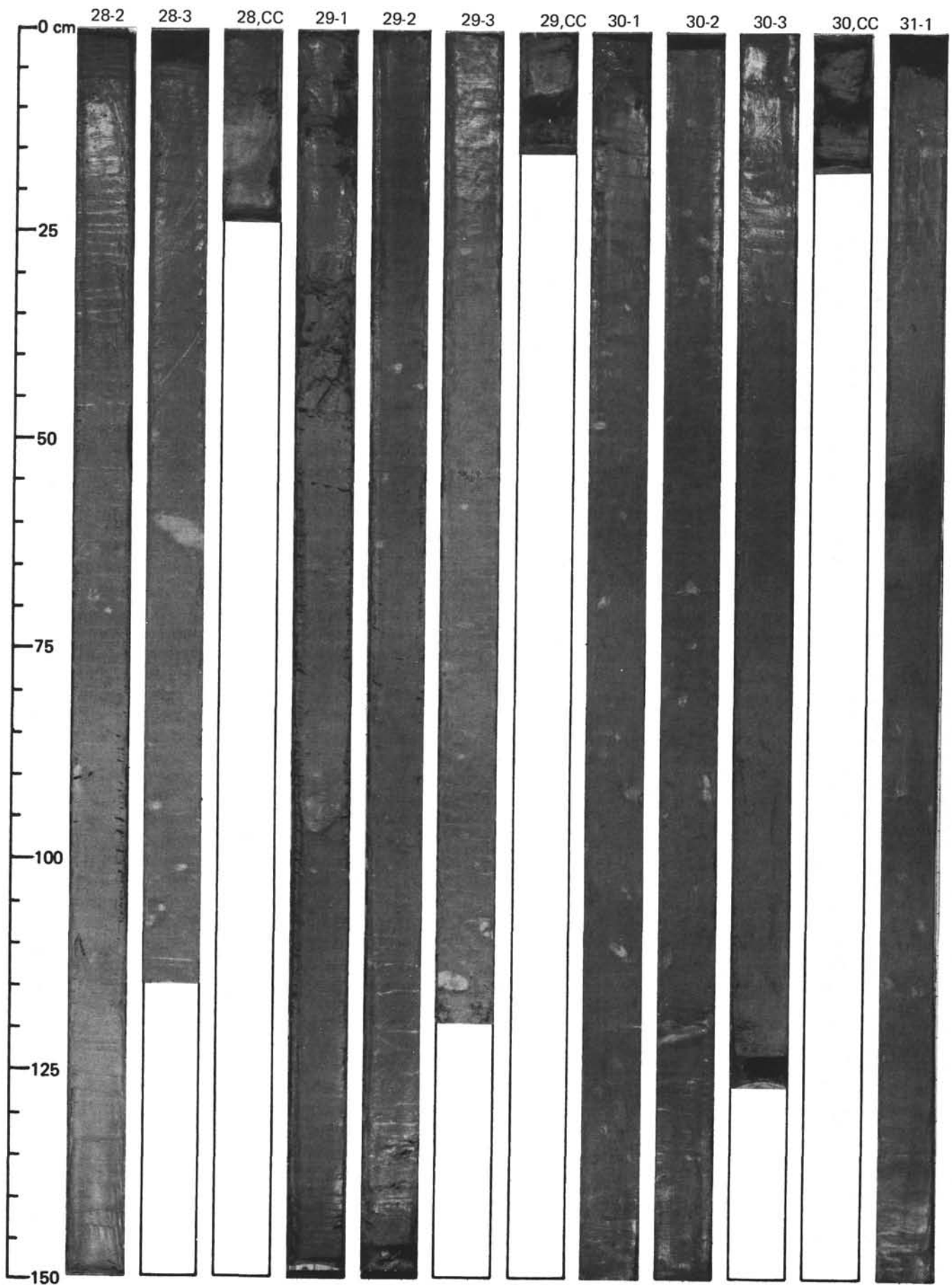


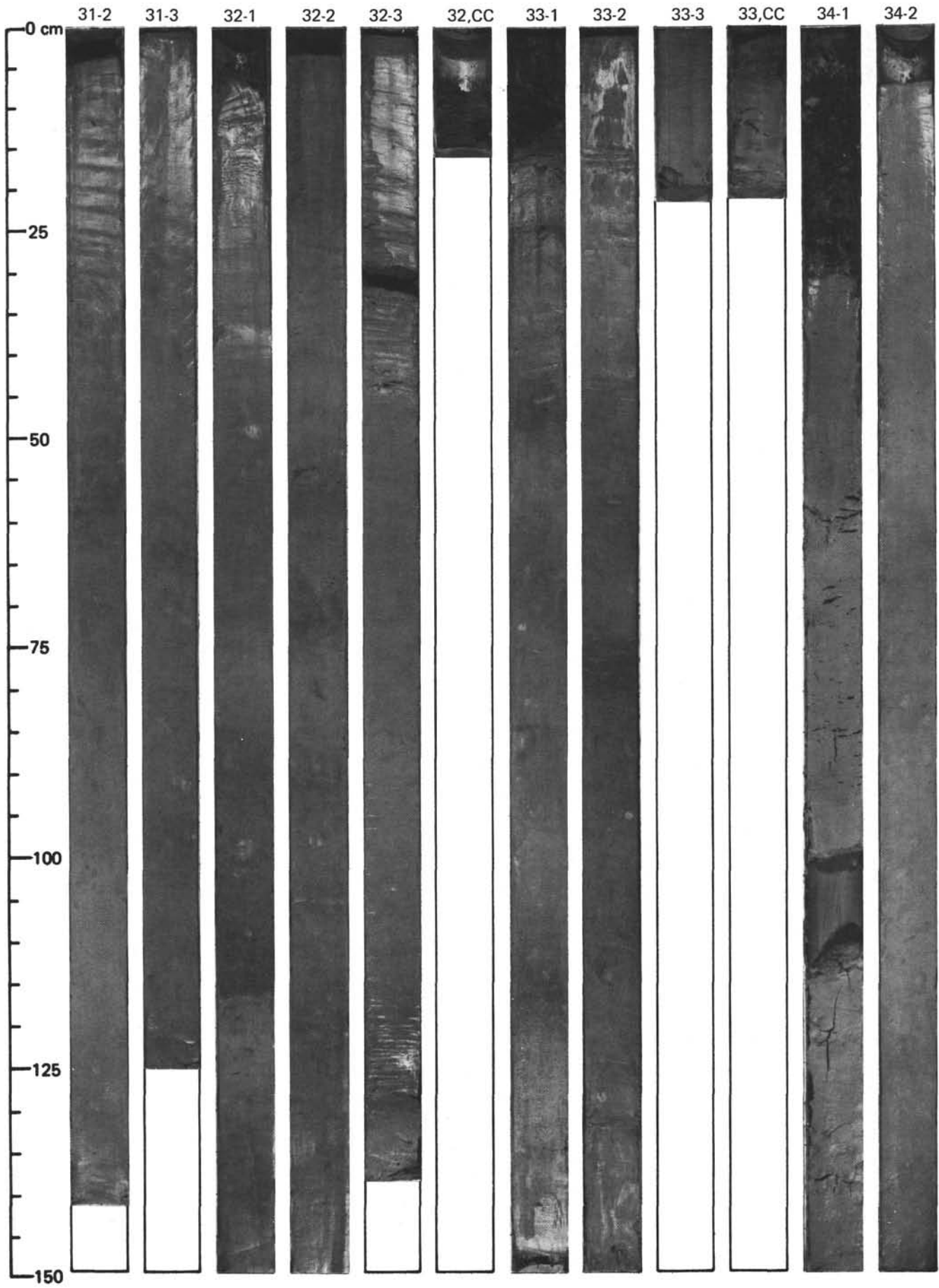


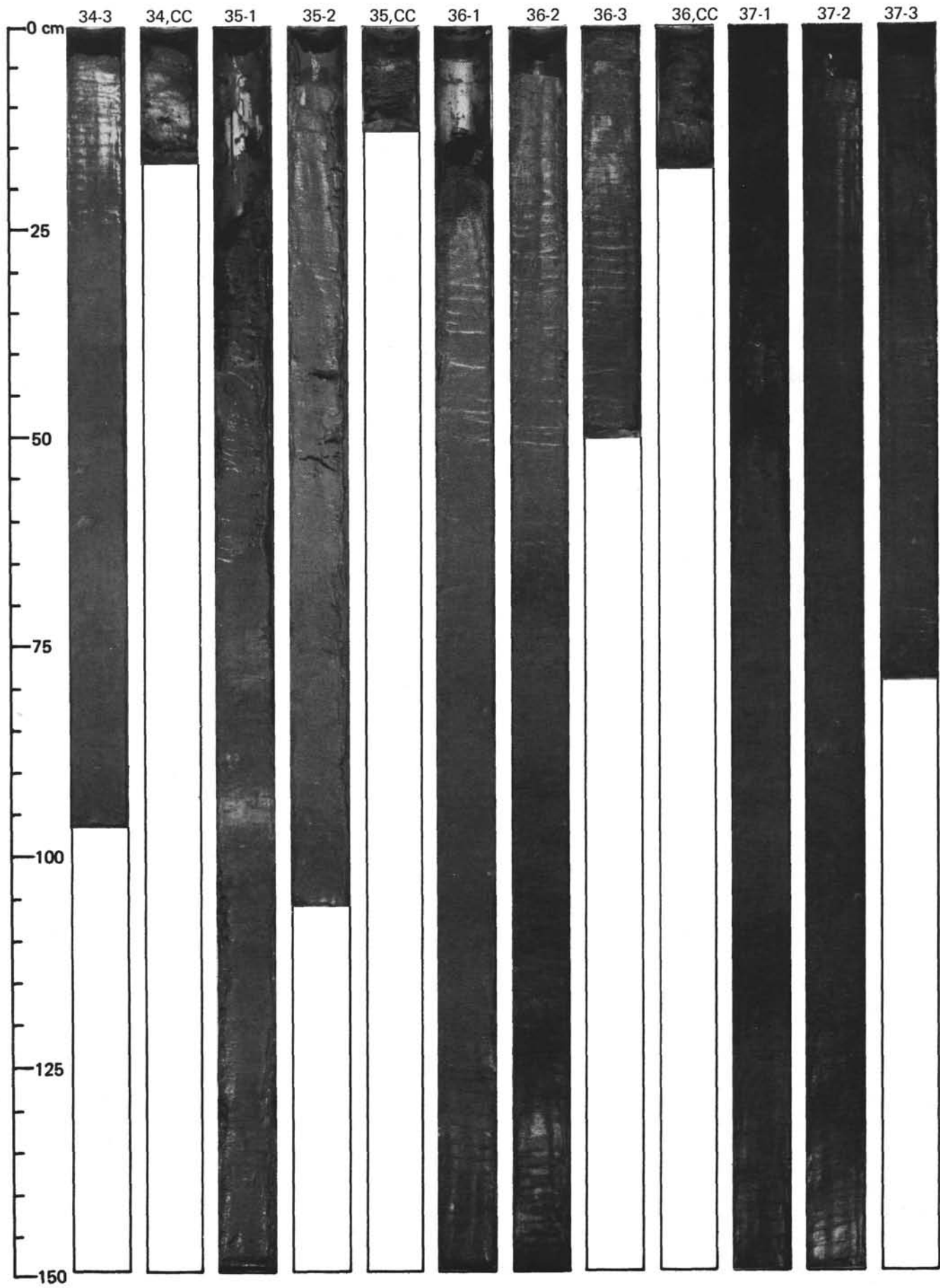


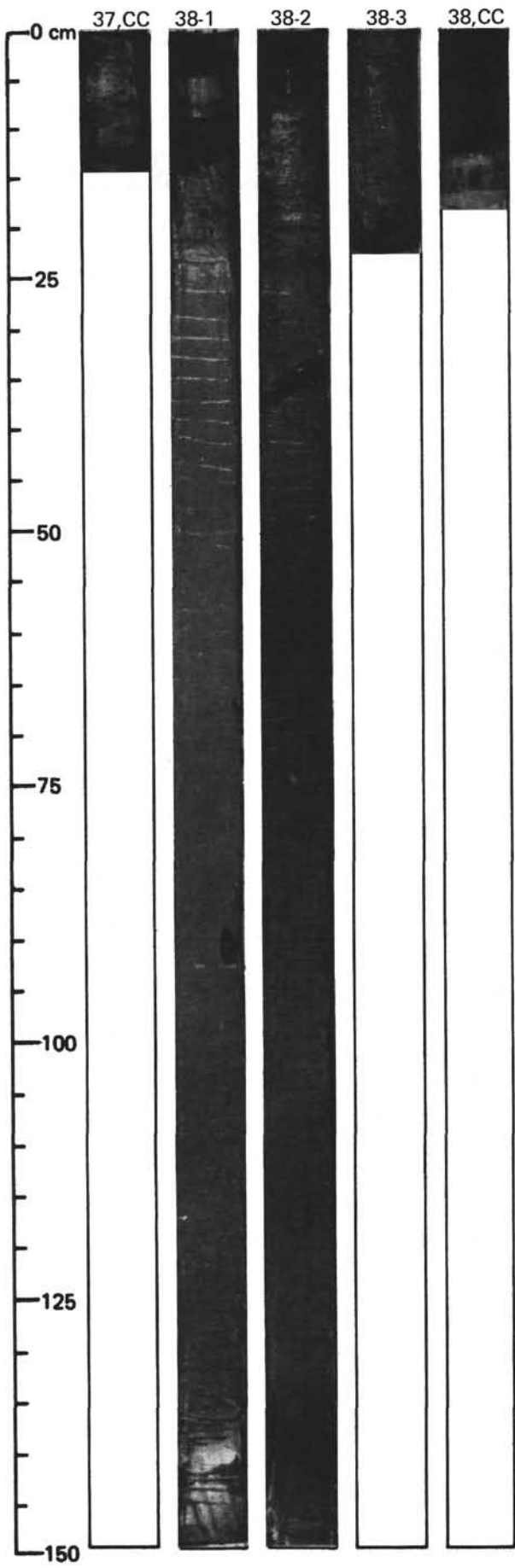


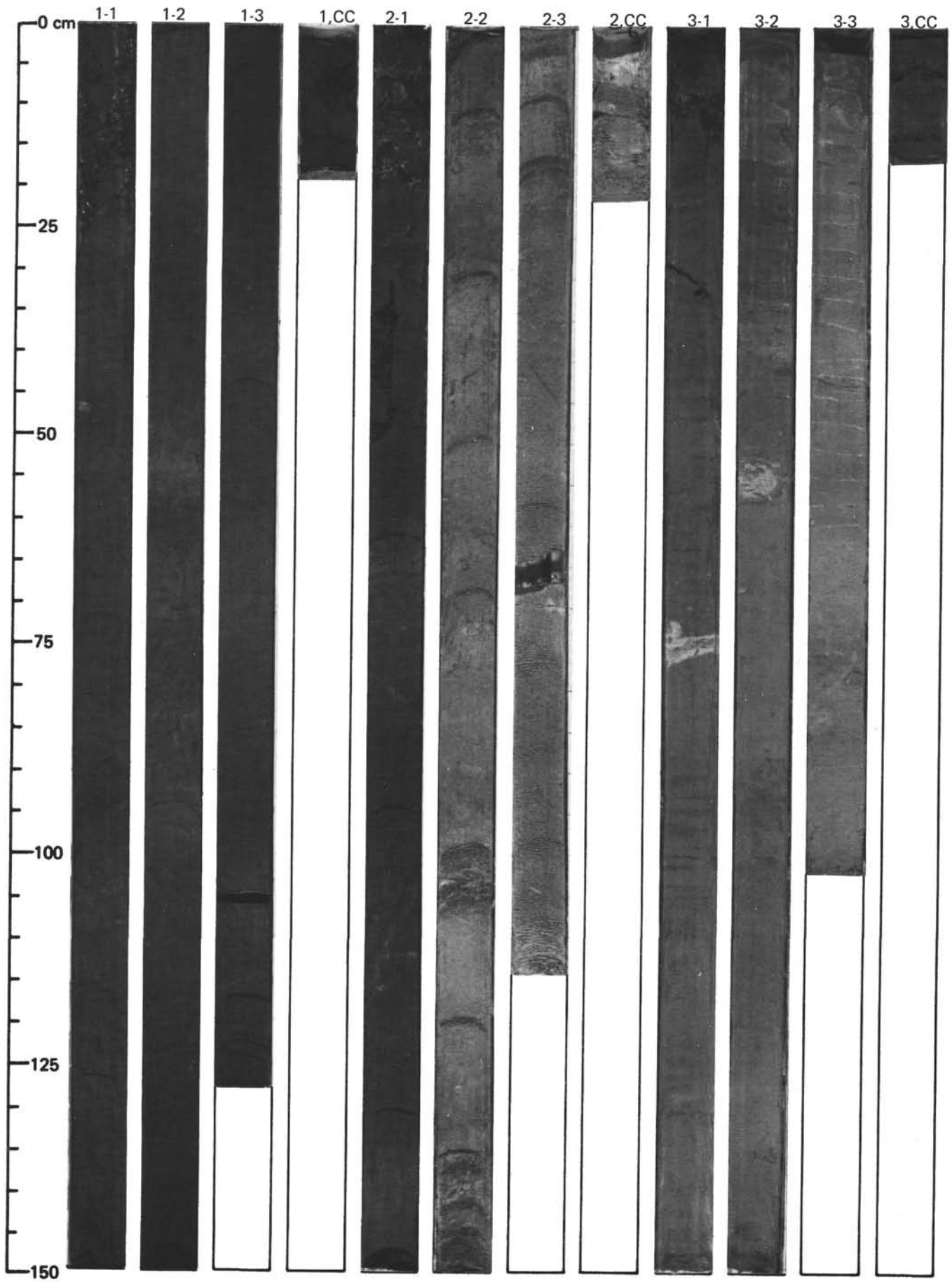


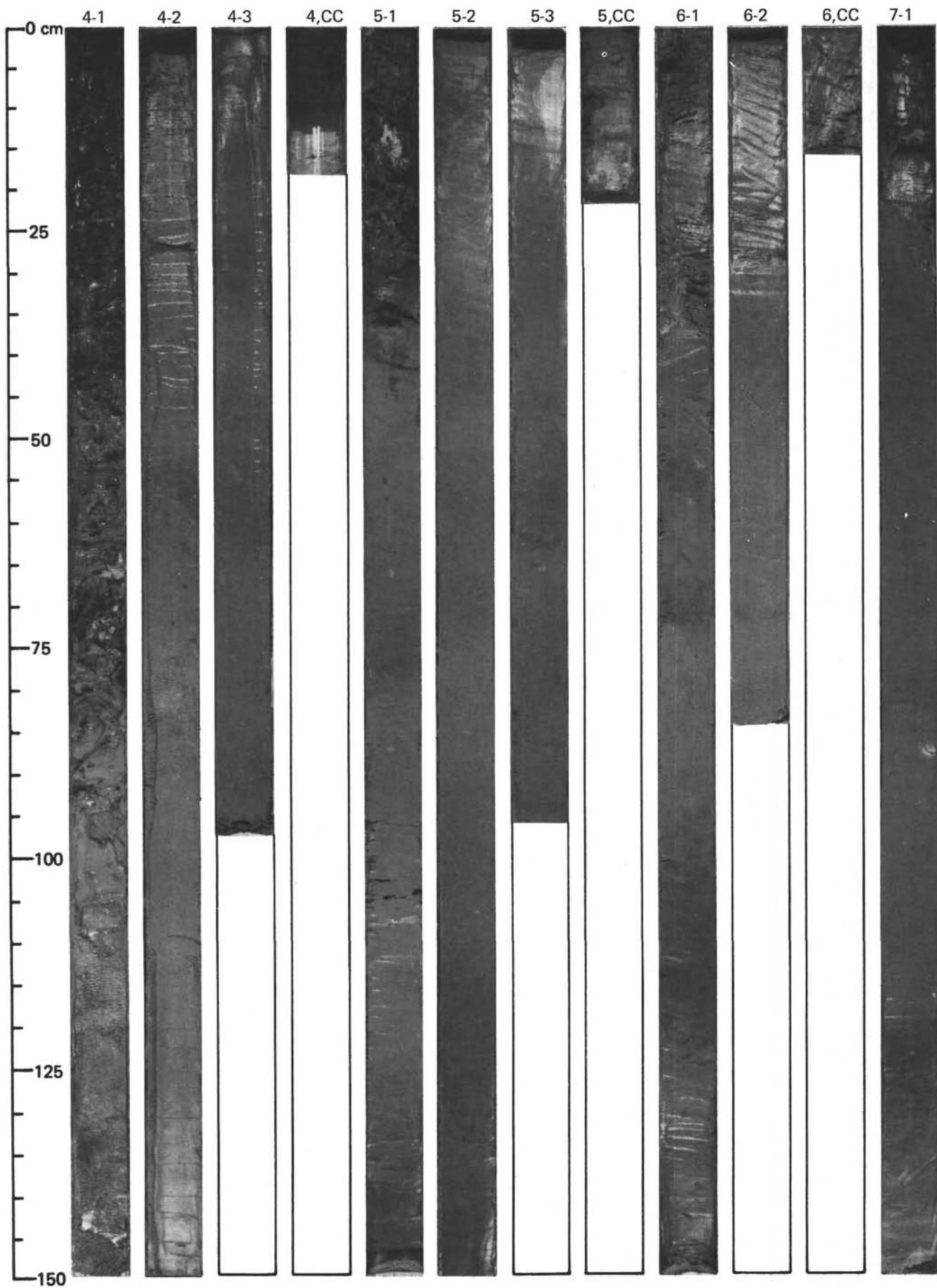




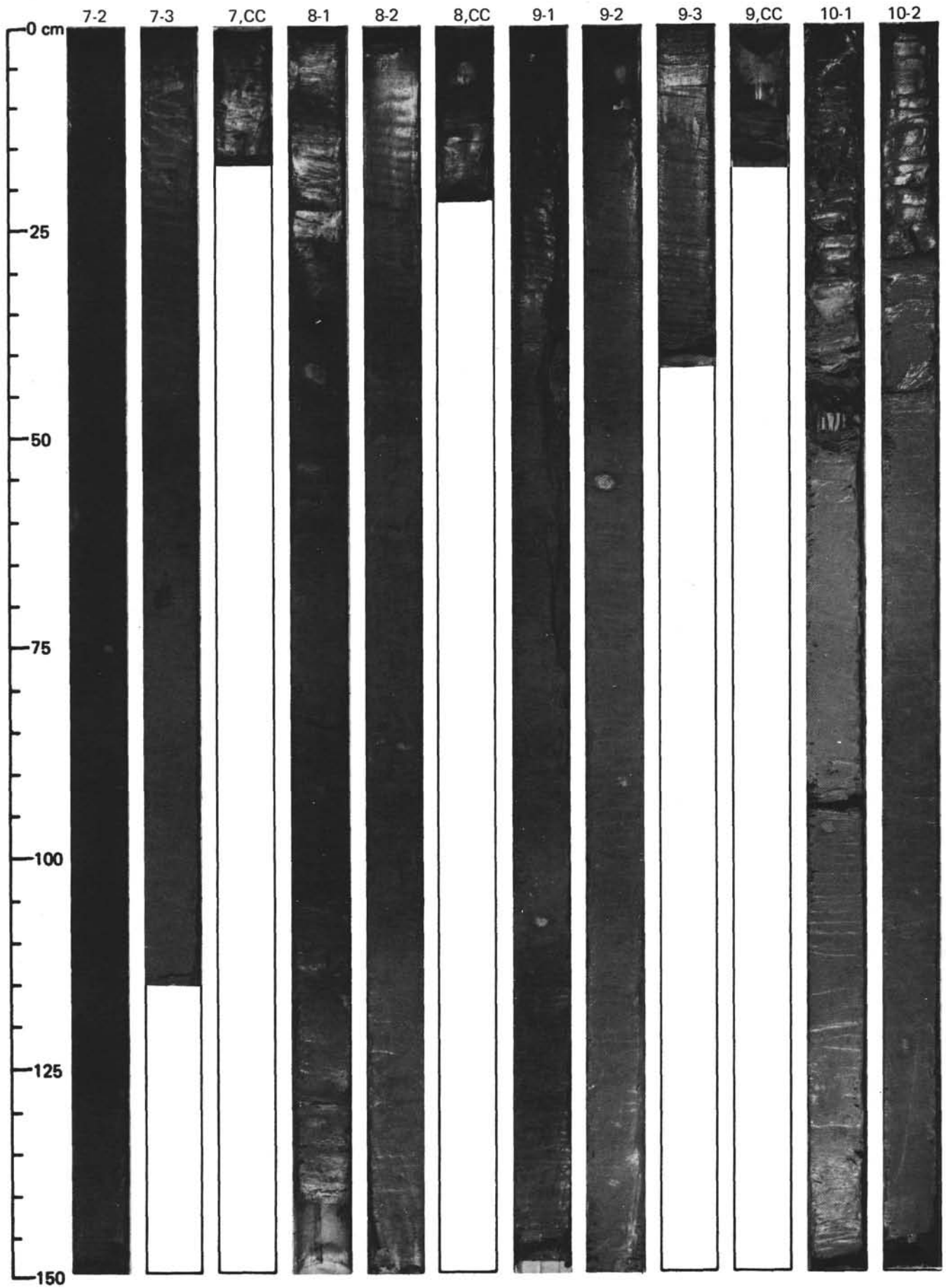


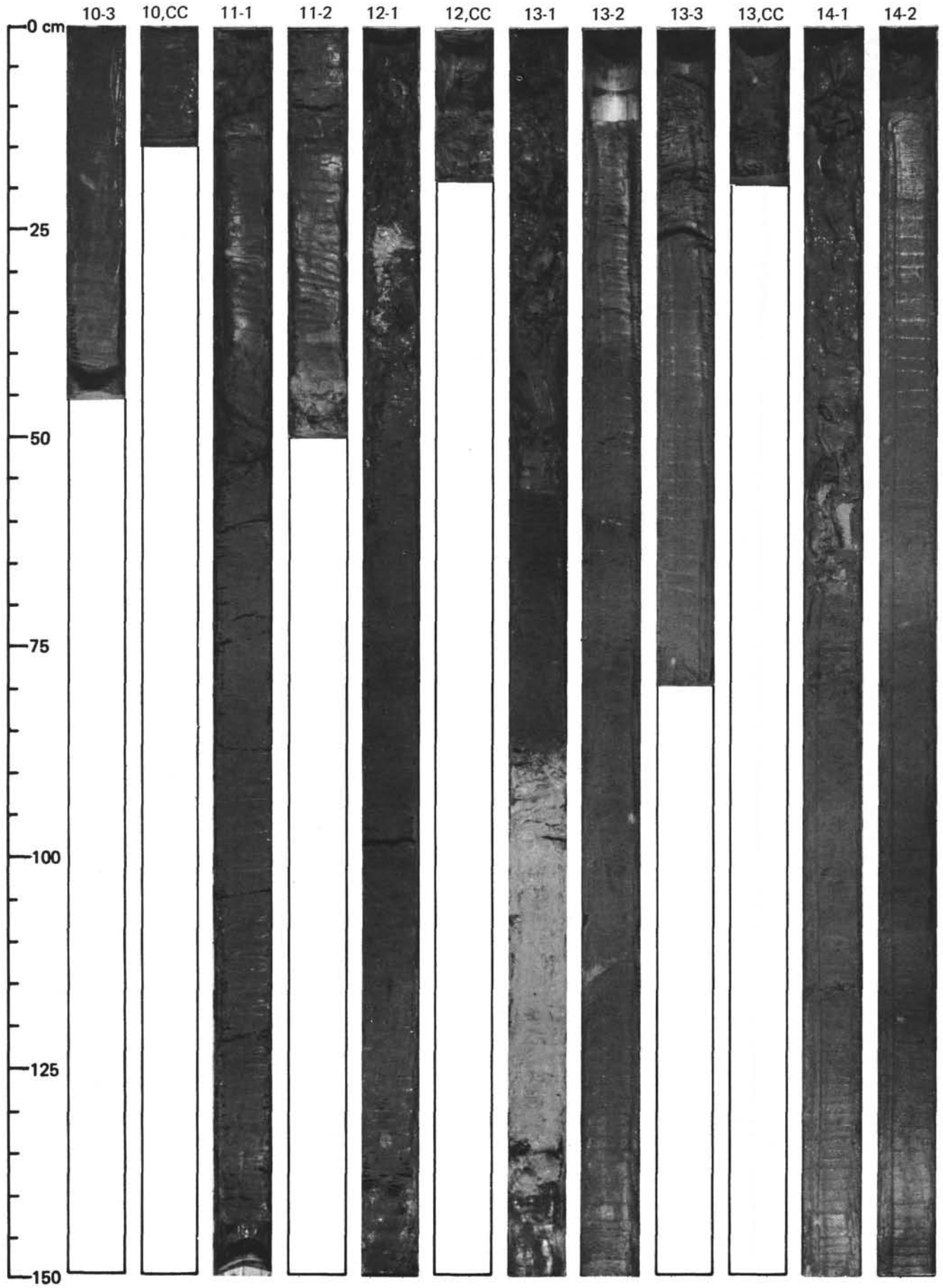


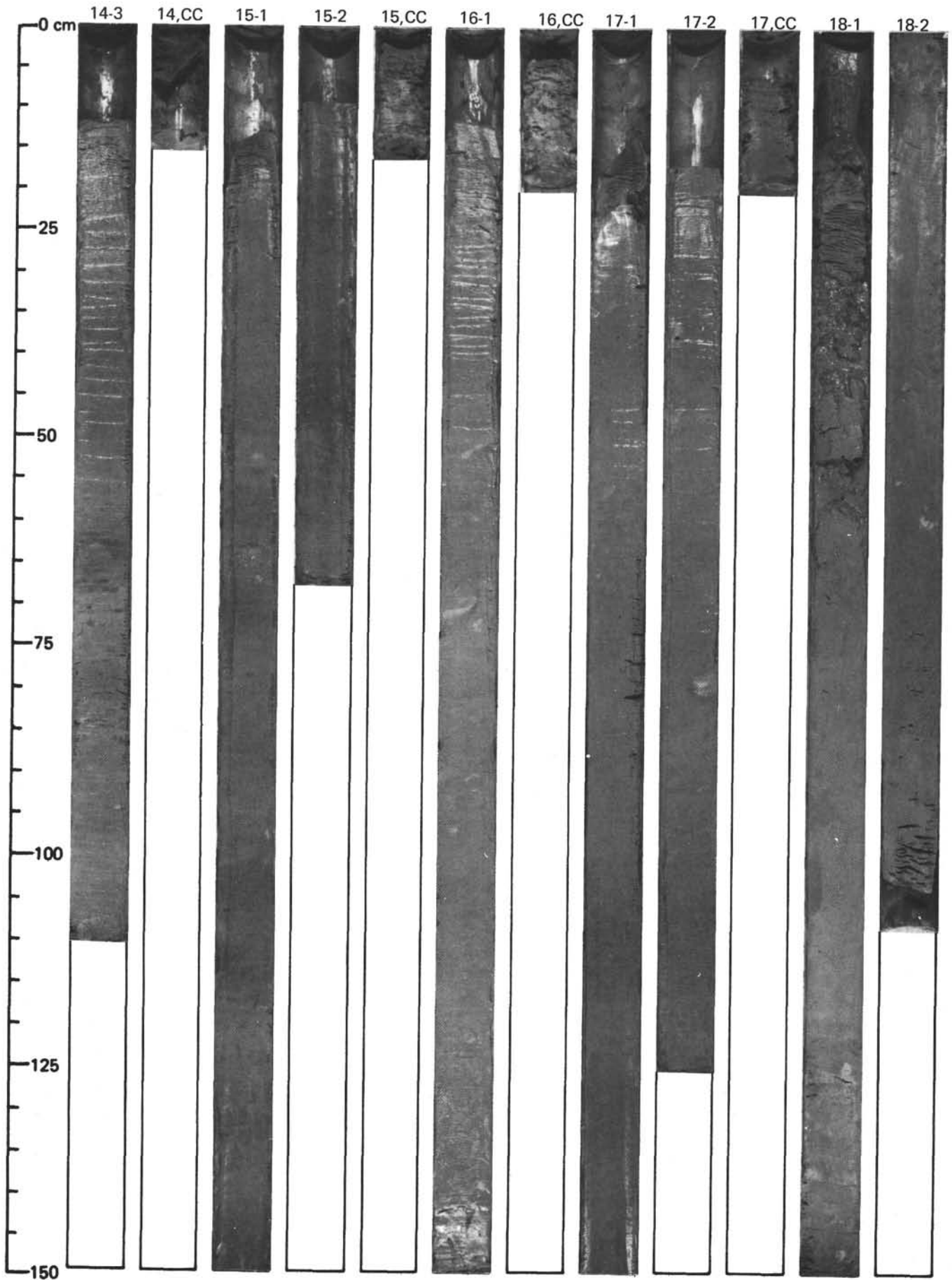


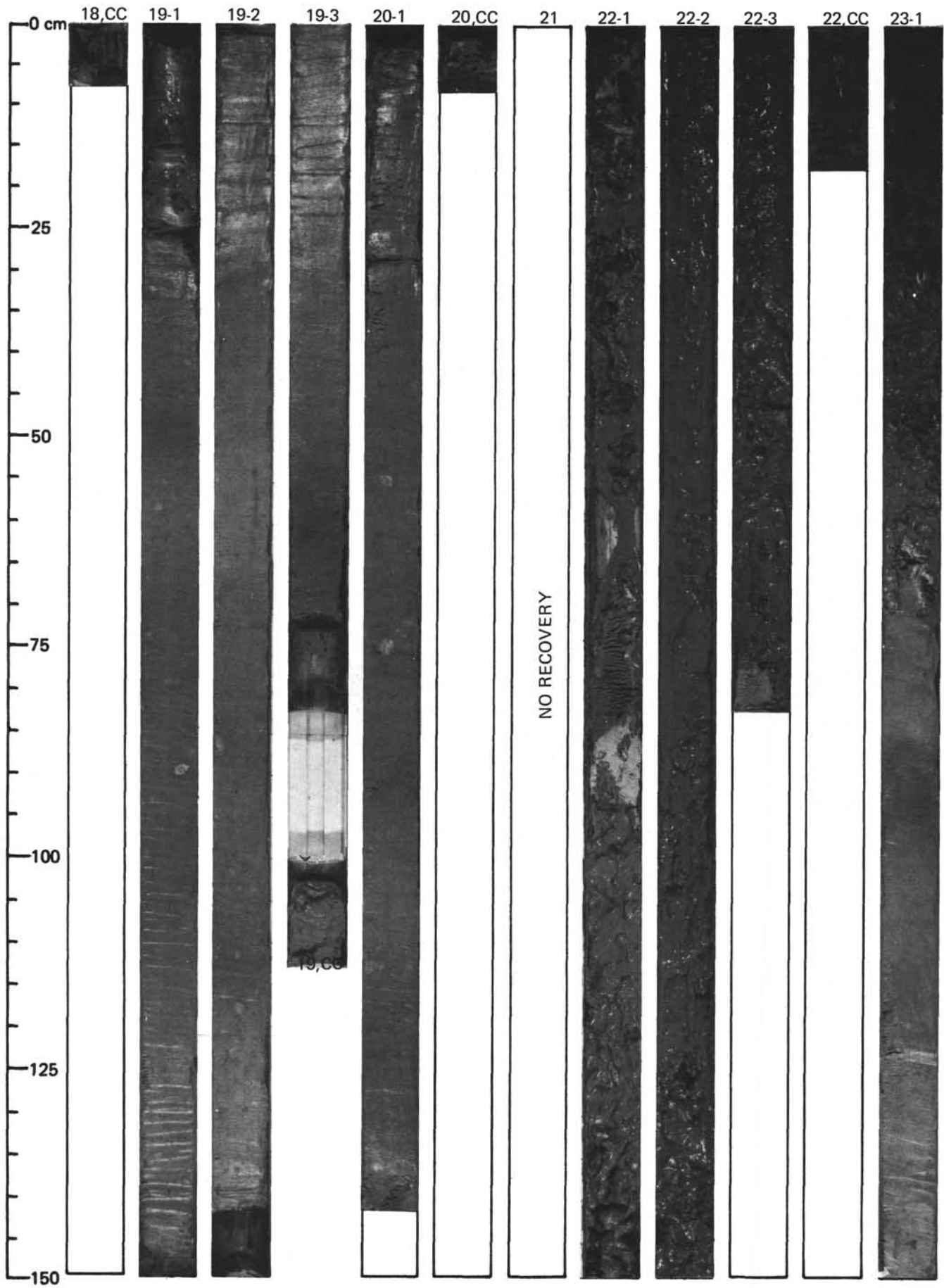


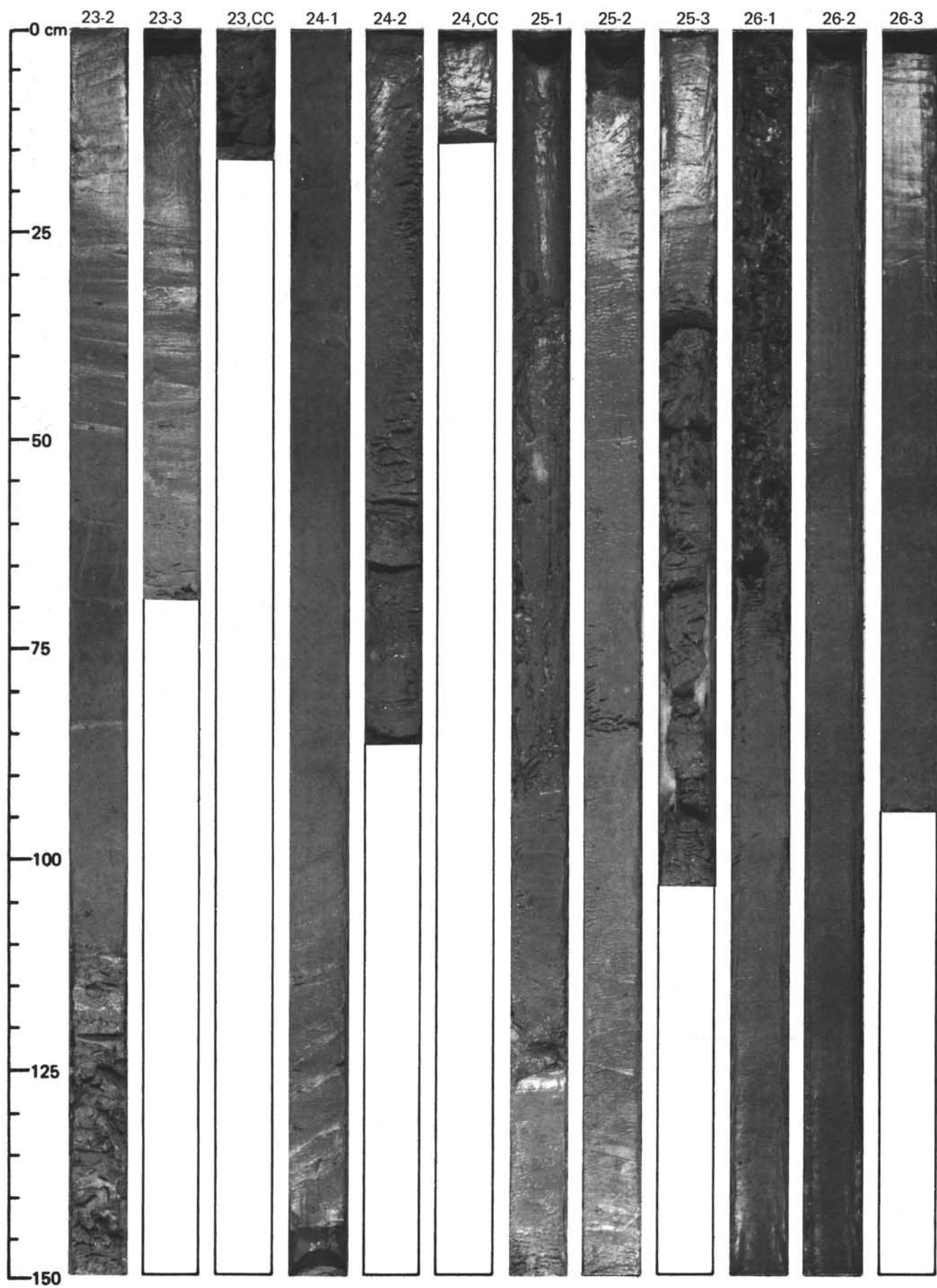
SITE 522 (HOLE 522A)

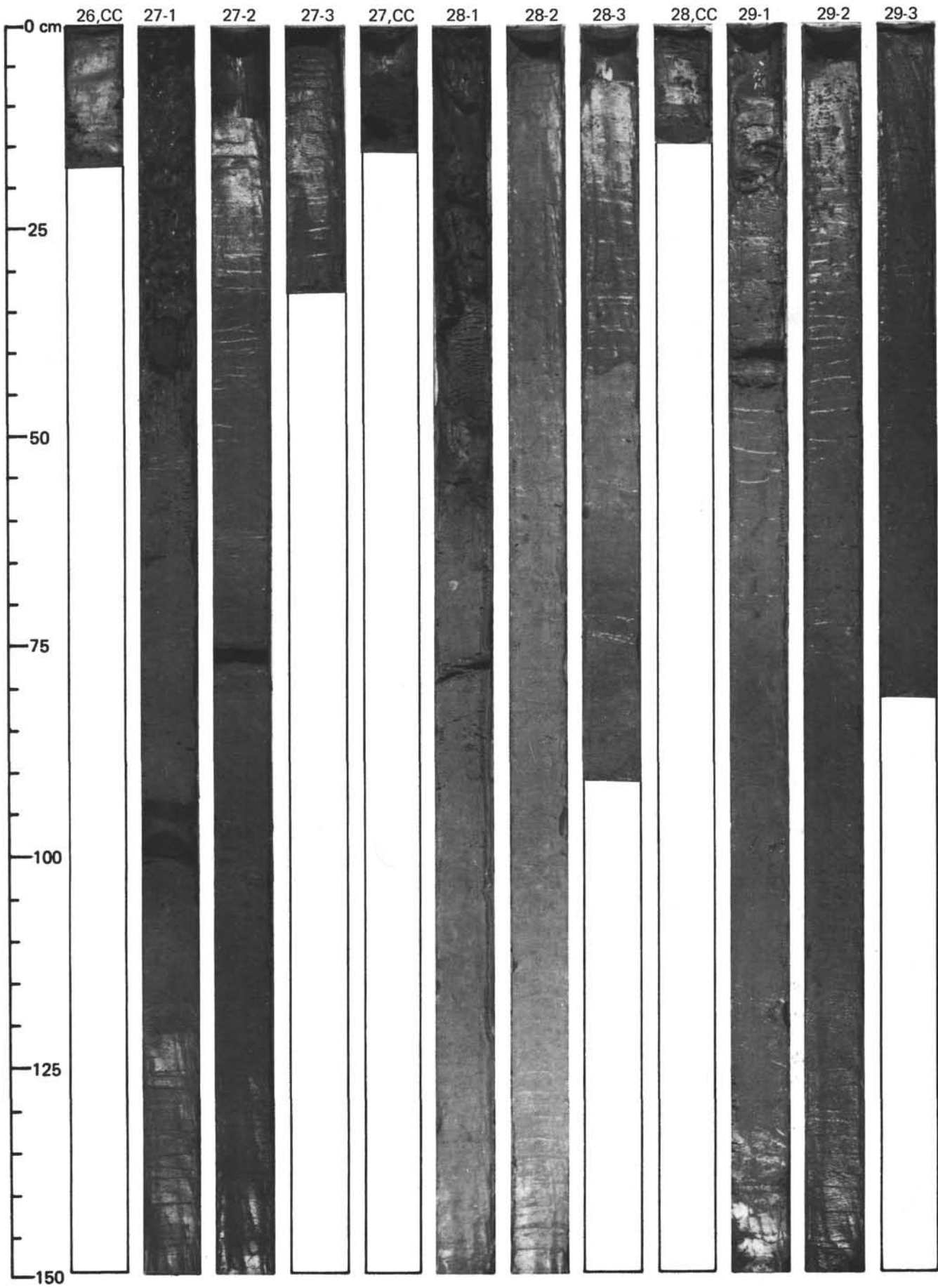




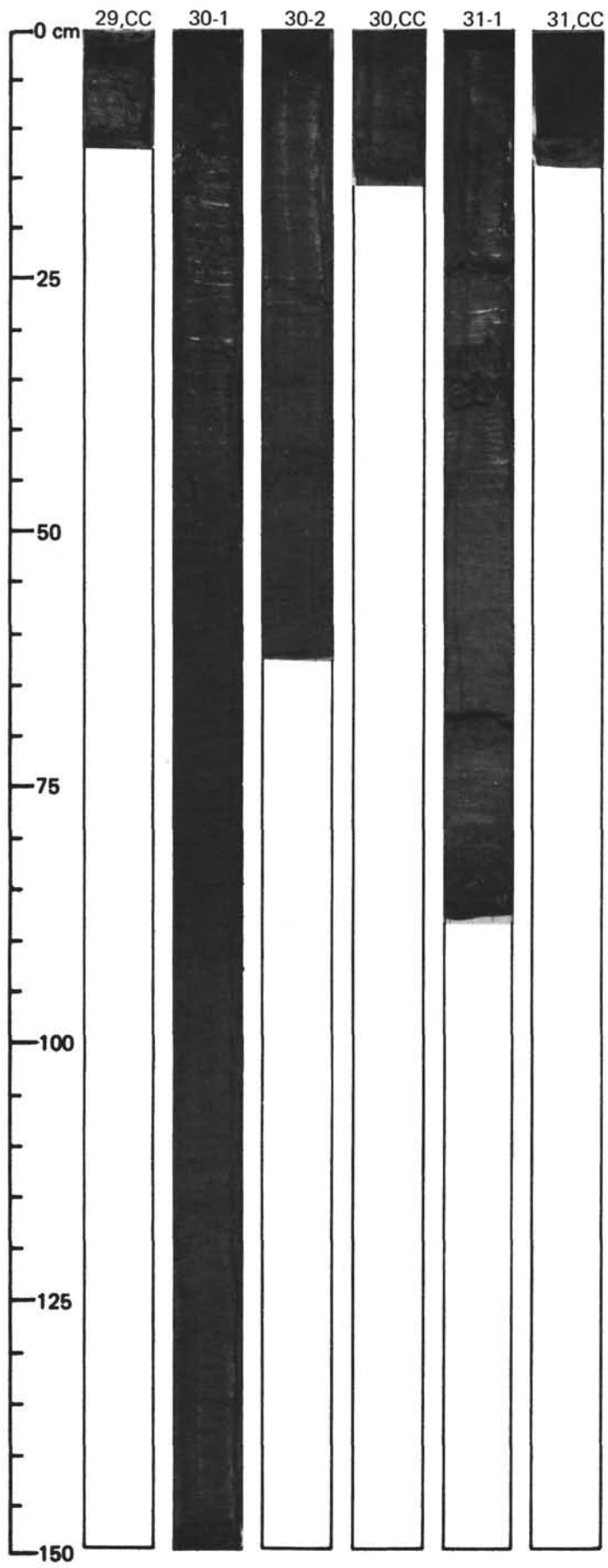


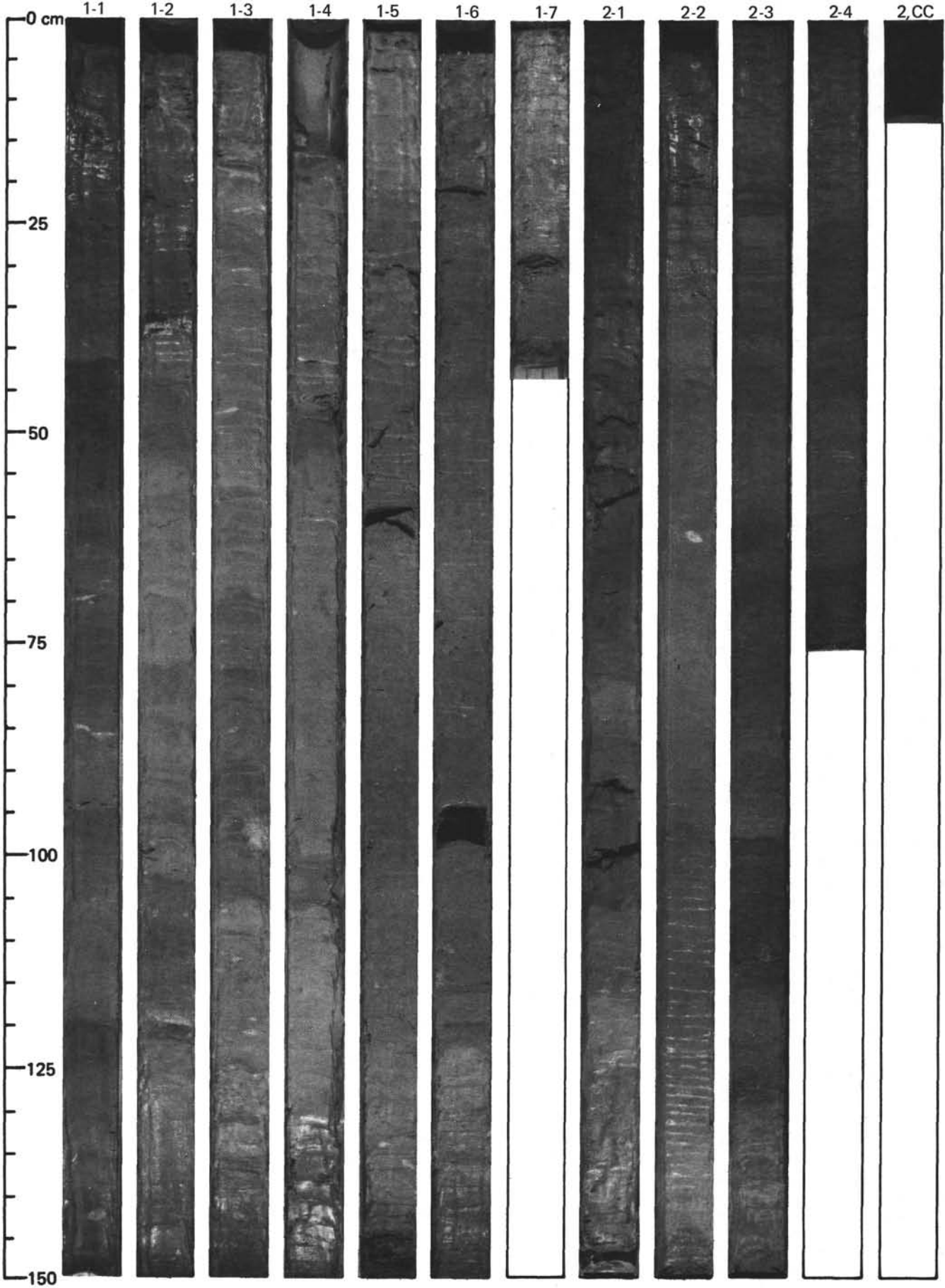






SITE 522 (HOLE 522A)





SITE 522 (HOLE 522B)

